A VOLTAMMETRIC STUDY OF SOME HETEROCYCLIC MERCAPTANS.

Brian Lynch B.Sc.

Candidate for the degree of Master of Science at N.I.H.E. Dublin.

Supervisor: Dr. Malcolm R. Smyth, School of Chemical Science.

Declaration: I declare that this thesis is based on my own work.

Signed: 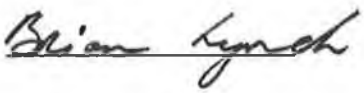

September 1988

Acknowledgements

I would like to thank Prof. Albert Pratt for providing the research facilities and my supervisor Dr. Malcolm Smyth for his guidance throughout this project. Olin Chemicals in Swords for allowing me examine their plant process.

A special thanks to my collegues in the 'Arctic' research laboratory, Walter, John, Tony and Evin for their friendly disposition. Michelle for her help with the spectroscopic measurements, and finally the technical staff for all their assistance.

Dedication

I dedicate this thesis to my family.

'It was a lover and his lass,
with a hey and a ho, and a hey nonino,
that o'er the green cornfield did pass....'

W. Shakespeare from 'As you like it'

TABLE OF CONTENTS

ABSTRACT

A Voltammetric Study of some Heterocyclic Mercaptans
by Brian Lynch

The four mercaptans studied were 2-mercaptopyridine (2MP), 2-mercaptopyridine-N-oxide (2MP-O), 2-mercaptopyrimidine (2MPr), and 2-mercapto-4-methylpyrimidine.HCl (2MmPr). The pK_a values of each compound were determined by both an ultraviolet spectroscopic method and a polarographic method. The pK_a values calculated by each technique were in good agreement. The reversibilty of each compound's electrode reaction was assessed from their sampled direct current (DC) polarograms, and it was found that each reaction was quasi-reversible in nature.

The electrocapillary (EC) curves of 2MP and 2MP-O indicated that the product of their corresponding electrode reactions (a mercury thiolate salt) was adsorbed at the electrode surface. In cyclic voltammetric (CV) analysis, the oxidation peak current was controlled by diffusion of the mercaptan to the electrode. However, as the concentration was increased, an adsorption controlled oxidation peak was also present in the recorded CV's. The CV's displayed the characteristics of weak thiolate adsorption at the electrode surface, and also the film formation was dependent on the time the potential was held positive of the reaction potential.

Calibration curves from differential pulse (DP) polarograms and differential pulse cathodic stripping voltammograms (DPCSV) were constructed to find the linear dependence of peak current with concentration. The limit of detection for each mercaptan using DPP was $1x10^{-5}M$, and $1x10^{-7}M$ using DPCSV. Differentiation of the mercaptans in mixtures was also investigated. The peak current due to 2MP, at concentrations higher than $1x10^{-4}M$, was greater than that due to equimolar concentrations of the other three mercaptans. This seemed to indicate that the 2MP electrode reaction product was adsorbed in a more compact film at the electrode surface, than the products of the other three mercaptans. The different possible electrode mechanisms and their correlation with their current potential equations were examined.

A voltammetric procedure was then developed for the determination of 2-chloropyridine-N-oxide (2PCl-O) and the sodium salt of 2MP-O in an industrial process stream.

A. INTRODUCTION

1. Aim of Project

The main aim of this project was to develop a polarographic method for the determination of 2-mercaptopyridine-N-oxide (2MP-O) in process streams. This compound is an intermediate in the synthesis of Zinc Omadine, produced by Olin Chemical Company, Swords, Co Dublin.

Before adapting the method to process control of the plant mercaptisation reaction, it was considered worthwhile to study the polarographic behavour of 2 MP-O and three other mercaptans, which were similar in structure to the industrially produced mercaptan.

2. Polarographic Determination of Mercaptans

The four mercaptans studied in this project were 2-mercaptopyridine (2MP;I), 2-mercaptopyridine-N-oxide (2MP-O;II), 2-mercaptopyrimidine (2MPr;III), and 2-mercapto-4-methyl-pyrimidine.HCl (2MmPr;IV), shown in Fig. 1 . Each of these compounds contains a thiol group which makes them amenable to a polarographic method of analysis. Although the pyridine ring is not polarographically active, the pyrimidine ring can be reduced according to the mechanism put forward by Wrona [1] in the case of 2-mercaptopyrimidine. In this study, however, the reaction of the thiol group at the mercury electrode was investigated.

At a mercury electrode, thiols are not oxidized to disulphides. The polarographic behavour of mercaptans is generally believed to be due to the oxidation of mercury in the presence of the mercaptan [2]. The chemical reaction of the oxidized mercury with the mercaptan

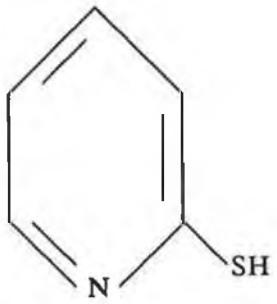

(I)

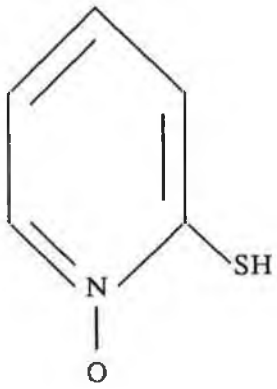

(II)

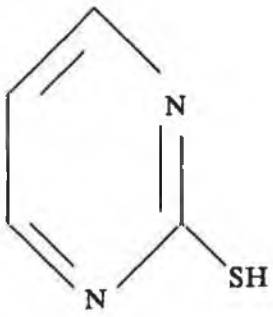

(III)

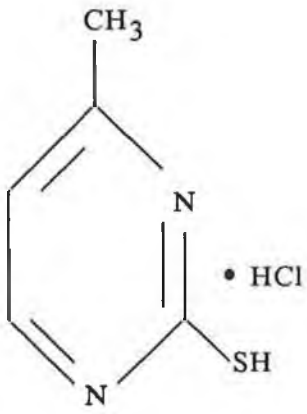

(IV)

Figure 1

Structure of mercaptans studied.

results in the formation of a mercury salt, which is adsorbed at the electrode surface. Elemental analysis of the oxidation product of 2MP-O by Krivis and Gazda [3] established the formula of the product as the mercury dimercaptide, ie: $Hg(SR)_2$. This would suggest that mercury was oxidized in a two electron reaction to Hg^{2+}. However, further coulometric and 'log plot' investigations indicated that a mercury (1) mercaptide, ie: HgRS, was probably formed . It is known that compounds of the type HgRS are unstable in aqueous solution and decompose to $Hg(RS)_2$ and Hg [4]. Therefore it is generally believed that a 1-electron charge transfer reaction is followed by a disproportionation reaction which results in an adsorbed $Hg(SR)_2$ salt [4,5,6]. This mercury (II) salt is adsorbed as a porous film at the electrode surface.

Theoretical treatment of adsorption has been carried out using cyclic voltammetry (CV) by Sluyters et al. [7] and Schiffrin [8]. According to Schiffrin, complete analysis of the voltammetric curve is difficult when electrodeposition of an insoluble product has occurred, because quantities such as peak potential separation cannot be used to obtain meaningful parameters. Also, the stripping peak current is strongly dependent of the morphology of the deposit.

The adsorption of mercury thiolate salts has been shown to occur at the electrode surface by electrocapillary curve measurements [9-11]. A variety of explanations are given for the occurrence of current spikes observed in cyclic voltammograms and cathodic stripping voltammograms (CSV). They are mainly believed to be due to compact film formation as a result of film rearrangement [5,12-16]. Casassas et al. [17] have stated that the current spike occurring

in CSV scans of 2-mercaptoethanol may be due to the presence of a disulphide in the surface film, produced during the anodic oxidation of the compound. Monolayer coverage (mol/cm^2) of some mercury mercaptide salts were calculated by Birke and Mazorra [5] and Stankovich and Bard [15]. These studies gave conclusive evidence that the limiting of peak current with increased depolarizer concentration was due to the completion of a monolayer of film at the electrode surface, and also that a new peak detected at slightly different potentials was due to multilayer formation of the mercury mercaptide salt.

Differential pulse polarography (DPP) and differential pulse cathodic stripping voltammetry (DPCSV) are both very sensitive methods used in the analysis of mercaptans. DPCSV is the more sensitive of the two methods, because the mercaptan is accumulated at the electrode surface in the form of a mercury mercaptide film before the current/potential scan is recorded. These techniques have been mainly employed in the study of mercaptans of biological importance, especially of the aminoacids cysteine and cystine [9,10,14,18,19], and protein disulphides [15,20]. Using DPP, Mairesse-Ducarmois et al. [9,10] determined cysteine and cystine down to concentrations of $1x10^{-5}M$, while Florence [14] determined them at concentrations as low as $1x10^{-8}M$ by CSV at a mercury pool working electrode. Chemicals of pharmaceutical importance have also been determined by DPCSV: e.g. thioamide drugs in plasma and urine at concentrations down to $2x10^{-8}M$ [21,22]; and penicillins at concentrations down to $2x10^{-10}M$ [23,24]. Sulphur-containing pesticides and fungicides have also been determined by DPP and DPCSV: e.g. derivatives

of thiourea [25], dithiocarbamates [26], and 2-mercaptopyridine-N-oxide [27]. Peter and Rosset [6] employed DPP in the determination of thiols in petrol at concentrations down to $1x10^{-8}$M. Therefore the usefulness of voltammetric techniques for both industrial and biological analysis of mercaptans is evident.

3. Production of Zinc Omadine

The industrial process which was examined in this study was part of the plant production of Zinc Omadice carried out in Olin Chemicals BV in Swords.

The Olin Chemical plant in Swords is a subsidary of the American-based Olin multinational company, which is mainly involved in chemical manufacture. The Swords factory manufactures Sodium Omadine (NaOm) products. Metal derivatives of NaOm are used in shampoos as active anti-dandruff agents. NaOm is also used in the preservation of paints and cutting fluids.

The first step in the production of sodium omadine is the oxidation of 2-chloropyridine (2PCl) to form 2-chloropyridine-N-oxide (2PCl-O), as shown in Step 1 of Fig. 2. Hydrogen peroxide (H_2O_2) is the oxidizing agent and sodium tungstate (Na_2WO_4) is the catalyst. Permalaic and peracetic acids were used in the past as catalysts in the reaction. Due to effluent problems, however, they were replaced by a non-acidic catalyst. At the end of Step 1 of the reaction , unreacted 2PCl is recovered by distillation and it can be reused in subsequent oxidations. The yields in this reaction are usually around 85%.

Step 1

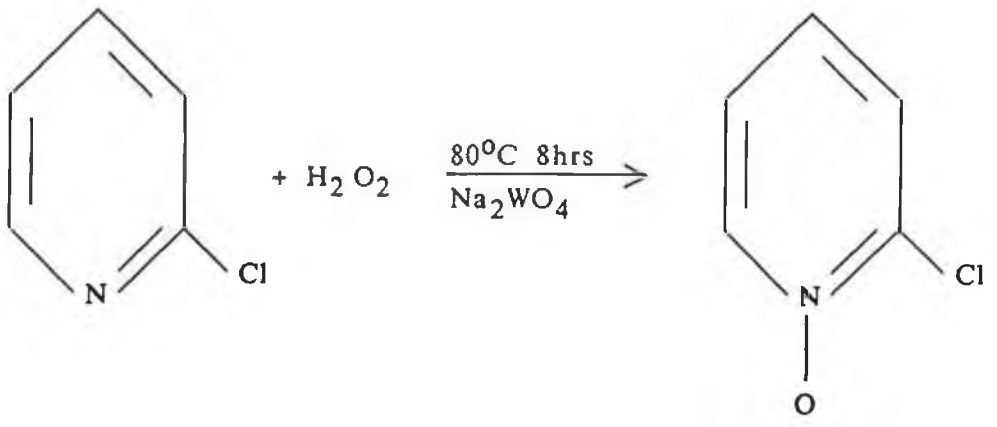

(2PCl) (2PCl-O)

Step 2

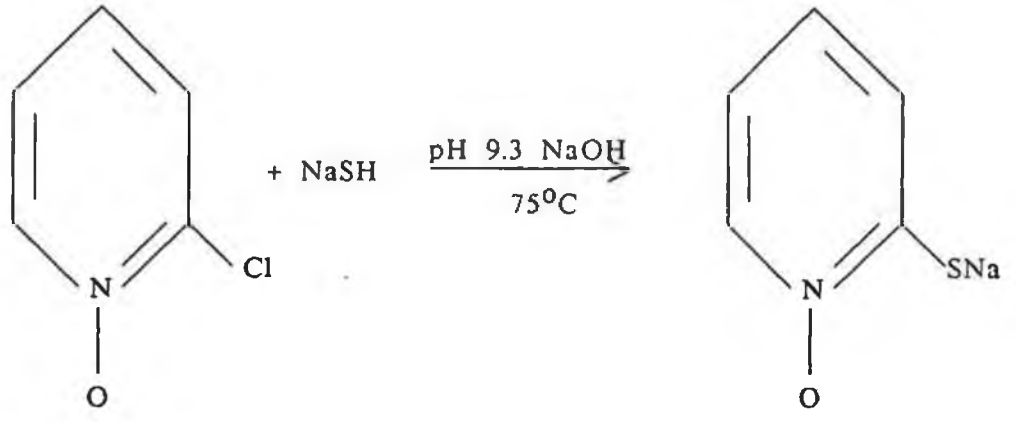

(2PCl-O) (NaOm)

Figure 2

Olin plant process: Step 1. Oxidation of 2-chloropyridine;
Step 2. Mercaptisation of 2-chloropyridine-N-oxide.

Zinc Omadine

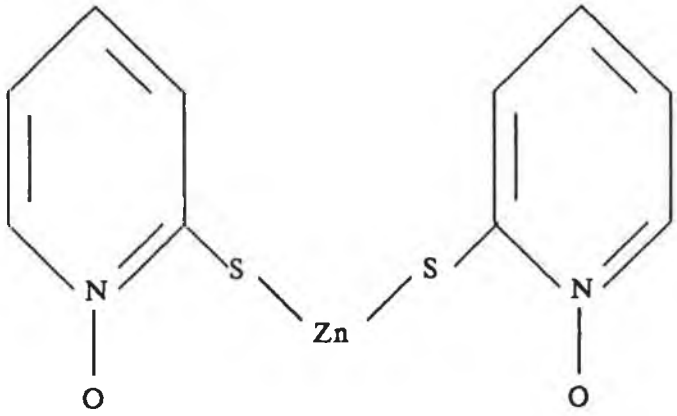

Magnesium Omadine

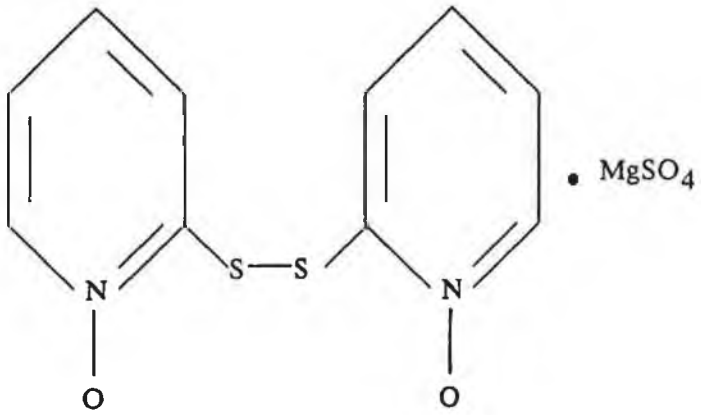

Sodium Omadine

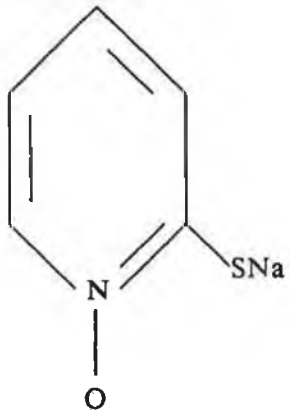

Figure 3

Products of the Olin plant process.

The second step in the production of NaOm is the mercaptisation of 2PCl-O. This occurs by nucleophillic replacement of the chlorine atom by sodium sulphahydride (NaSH), as shown in Step 2 in Fig.2. The pH is kept at 9.3, because a massive evolution of hydrogen sulphide (H_2S) would occur if the pH went below 8.0 . This step in the reaction takes over two hours to go to completion, and yields of 95% are achieved in the plant. At the end of the reaction, H_2S is removed from the NaOm solution by bringing the pH down to 6.5 with the addition of hydrochloric acid, and by purging with nitrogen.

The sodium omadine is then used to form a variety of products as shown in Fig. 3.

In this study, the mercaptisation reaction was monitored using polarography. Although the polarographic activity of mercaptans is well documented, the polarographic activity of 2PCl-O is not. Ochlai [8] has reported the reduction potentials of pyridine-N-oxide and other related compounds in a paper in which he gives comprehensive details of its chemical activity. The polarographic reduction of heterocyclic amine N-oxides has been studied by Kubuta and Miyazaki [29,30]. The application of pulse polarography to their determination was investigated by Vaneesorn and Smyth [31]. Krivis and Gazda [3] are the only authors who have reported on the polarographic reduction of 2PCl-O.

The polarographic activity of NaOm is due to oxidation of the sulphur atom, while its N-oxide group is not reducible. This is different to the behaviour of 2PCl-O, the N-oxide group of which is

reducible. It was therefore thought that mixtures of NaOm and 2PCl-O, which are present in the Olin mercaptisation reaction, could be analysed simultaneously by a voltammetric approach.

B. THEORY

1. Ultraviolet Spectroscopy

1.1. General Theory

An ultraviolet spectrum arrises from absorption of electromagnetic radiation as a result of an electronic rearrangement in atoms or molecules. The electronic energy levels in a molecule are shown below in order of their relative energy.

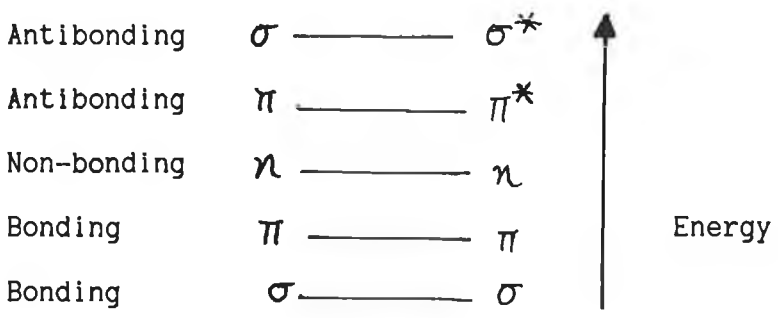

Transitions in the ultraviolet/visible (UV/Vis) region of the electromagnetic spectrum are usually due to $\pi - \pi^*$ and $n-\pi^*$ transitions. At low wavelengths, $n-\sigma^*$ transitions can also occur, however the higher energy gap reduces their intensity. The intensity of the $n-\pi^*$ transition is weak, because it is a forbidden transition under molecular orbital theory selection rules. Aromatics and unsaturated aliphatic molecules absorb in the UV/Vis spectrum. The UV spectra of pyridine and pyrimidine are similar to that of benzene, because the replacement of carbon with nitrogen has little effect on the $\pi-\pi^*$ absorption wavelength. Substituents cause shifts in both wavelengths of maximum absorption and their intensity by inductive, resonance and steric effects [32,33].

The intensity of absorption (A) is related to the molar concentration of the absorbing material (C), through the Beer-Lambert expression.

$$A=\log_{10}(I_o/I) = \varepsilon Cl \quad \ldots\ldots\ldots 1$$

where I_o = intensity of incident radiation .

I = intensity of transmitted radiation .

ε = extinction coefficient of the absorbing material at a given wavelength.

l = path length (cm)

1.2 Determination of pK_a Values

The absorption spectra of organic compounds with acidic or basic functional groups are usually dependent on the pH of the medium. The pK_a values of such compounds can be determined using spectrophotometric methods. The dissociation of an acid HB in water is an equilibrium process described by

$$HB + H_2O \leftrightharpoons H_3O^+ + B^-$$

where B^- is the conjugate base.

The equilibrium constant for dilute solutions is given by

$$K_a = [H_3O^+].[B^-]/[HB] \ldots\ldots\ldots 2$$

Taking the negative logarithm of the above equation gives

$$-\log_{10}K_a = -\log_{10}[H_3O^+] - \log_{10}([B^-]/[HB]) \quad \text{...2b}$$

$$pK_a = pH + \log_{10}([HB]/[B^-]) \quad \text{..... 2c}$$

$$\text{and} \quad pK_a = pH, \text{ when } [HB] = [B^-] \quad \text{..... 2d}$$

A plot of absorbance versus pH at a constant wavelength, results in a sigmoidal shaped curve when the equilibrium is rapidly established and when it is unaffected by other competing equilibrium processes. At values near the pK_a value, the absorbance changes rapidly corresponding to the changes in the concentration ratio $[HB]/[B^-]$ in equation 2c. At the midpoint of the curve, $pH=pK_a$ (i.e. when $[HB]=[B^-]$), and thus the pK_a value for the equilibrium can be determined.

2. Polarographic and Voltammetric Methods

2.1. Introduction

Polarography is an electroanalytical technique where current-voltage relationships are studied at a dropping mercury electrode (DME).

Modern polarographic measurments are carried out using a three electrode cell containing a DME as a mercury working electrode, a platinum counter electrode and a reference electrode. Current is measured between the working and counter electrodes as a function of the potential applied between the working and reference electrodes. Current flows through the system when a substance present in the solution undergoes reduction or oxidation at the working electrode at a given applied potential.

Motion of charge through the solution to the working electrode occurs in three ways: (i) migration; (ii) convection; and (iii) diffusion. In polarography, migration and convection can be effectively minimized by the use of a supporting electrolyte, and it is the rate of diffusion of electroactive species to the electrode which usually determines the resultant current. Diffusion occurs when a concentration gradient exists for the analyte of interest between the electrode and bulk solution.

In an electrolysis experiment, the current due to the transfer of electrons across the electrode solution interface is measured, i.e. the faradaic current (i_f). However, the measured current (i_t) also includes current resulting from non-faradaic processes (i_{nf}).

$$i_t = i_f + i_{nf} \quad \ldots\ldots\ldots \quad 3$$

It is desirable to minimise the contribution of the non-faradaic currents to the total current. Non-faradaic currents arise from charging the electrode/solution interface (which effectively acts as a capacitor), to the required potential. This is often called the capacitance current (i_c). Many modern polarographic techniques discriminate against this capacitance current in order to increase their sensitivity, or decrease their limit of detection (LOD).

2.2. Direct Current Polarography

2.2.1. General Theory

In direct current (DC) polarography, current is measured at a dropping mercury electrode continuously as a function of a linear potential ramp. A sampled DC current-potential curve or polarogram, where the current reading is obtained at the end of the life of each drop, is shown in Fig. 4. A steep rise in current is observed when a potential is reached where the electroactive species in solution reacts at the electrode. The rate of reaction increases with applied potential to a point where the molecules are reduced or oxidised as soon as they have reached the electrode surface. This corresponds to the current plateau which is called the limiting current (i_l). Another important feature is the half-wave potential ($E_{1/2}$), which is defined as the potential at which current is one-half the limiting value. Values of $E_{1/2}$ are independent of concentration, but are

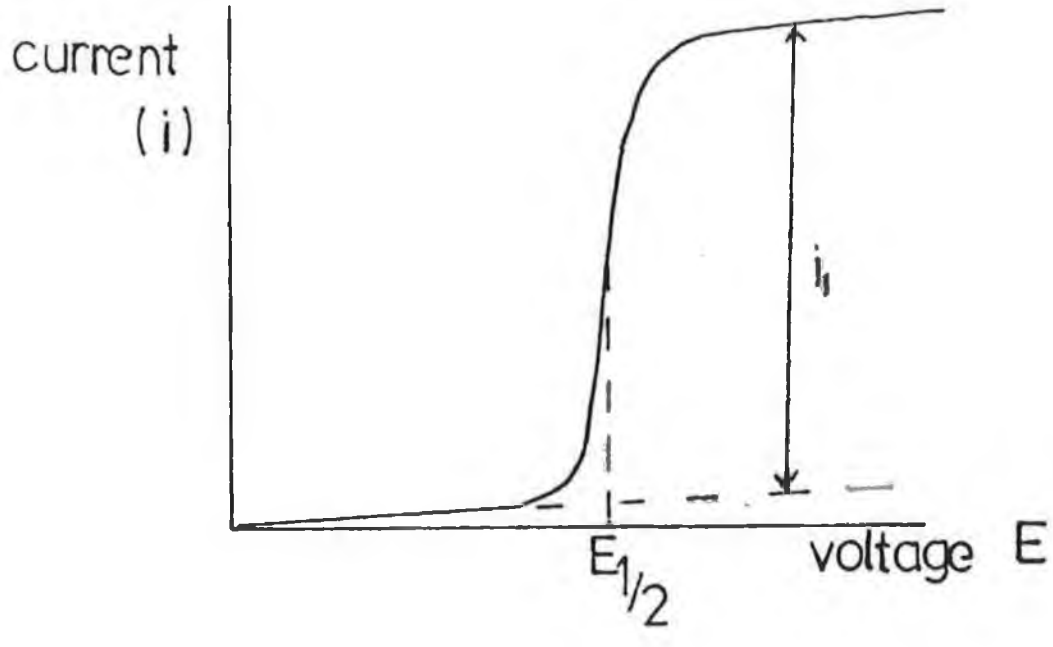

Fig. 4 A typical sampled DC polarogram.

dependent on the choice of supporting electrolyte, pH and solvent system. The $E_{1/2}$ value can be used for qualitative characterisation of electroactive substances.

2.2.2. Types of Limiting Current

A diffusion limited current is linearly dependent on the bulk concentration of the electroactive substance (C^b in mol/cm^3), as described by the Ilkovic equation [34].

$$i_d = 0.627nFC^bD^{1/2}m^{2/3}t^{1/6} \quad ..... \ 4$$

where n is the number of electrons consumed by the reaction of one molecule of the substance; F is Faraday's number (96,487 coulombs); D is the diffusion coefficient in cm^2/s; m is the rate of out-flow of mercury in g/s; and t is the drop time in seconds.

Since i_d is proportional to $m^{2/3}.t^{1/6}$ and the height of the mercury reservoir usually corrected for back pressure (h) is proportional to m and inversely proportional to t, i_d should therefore vary linearly with the square root of h. This fact can be used to determine whether the limiting current is diffusion controlled. If not, it may be controlled in one of the following ways: (i) kinetically; (ii) catalytically; or (iii) by adsorption.

(i) A kinetic current (i_k) can arise when an electroactive molecule is formed in a chemical reaction in the

neighbourhood of the electrode. The polarographic current is dependent on the rate of the chemical reaction. In this case i_k is independent of h, and dependent on pH and concentration.

(ii) A catalytic current may occur by chemical regeneration of the electroactive species, or through the presence of a catalyst in solution which shifts the reduction/oxidation (red/ox) potential of the substance of interest.

(iii) An adsorption current (i_a) is manifested by a separate wave at a different potential, either more positive or negative of the wave for the reduction or oxidation of the non-adsorbed compound. An adsorption-controlled current is proportional to the mercury reservoir height. The height of such waves also reach a limiting value, once the surface of the electrode is fully covered by the adsorbed species.

2.2.3. Investigation of the Reversibility of an Electrode Reaction

An electrode process is reversible if it obeys the Nernst equation:

$$E = E^{o} + \frac{RT.\ln[Ox]_o}{nF\ [Red]_o} \quad \ldots\ldots\ 5$$

where E^{o} is the standard electrode potential of the substance ofinterest; R is the universal gas constant; and $[Ox]_o$ and $[Red]_o$

are the concentrations of the oxidized and reduced species at the electrode surface at equilibrium and T is the absolute temperature.

Combining the Nernst and Ilkovic equations for a reversible oxidation reaction results in equation 6a:

$$E_{DME} = E_{1/2} + \frac{0.916RT}{nF} \ln \frac{i}{i_d - i} \quad \ldots\ldots\ldots \quad 6a$$

where i is the current at any point on the rising portion of the wave at a particular potential E_{DME}; 0.916 is a factor introduced when current is measured at the end of the drop life, which occurs in sampled DC polarography. In the case of an irreversible reaction, equation 6b results:

$$E_{DME} = E_{1/2} + \frac{0.916RT}{\alpha nF} \ln \frac{i}{i_d - i} \quad \ldots\ldots\ldots \quad 6b$$

where α is the transfer coefficient, and has a value less than 1.

A plot of E_{DME} vs $\ln[i/(i_d - i)]$ for a reversible, one electron reaction, will yield a line of slope 0.916RT/F . It is important to note that electrode reactions of different stoichiometry require different 'log plots' [35].

The slope of an $E_{1/2}$ vs pH plot is also indicative of the reversibility of an electrode reaction, according to equation 7.

$$\frac{dE_{1/2}}{dpH} = \frac{0.059p}{n} \quad \ldots\ldots\ldots \quad 7$$

where p is the number of protons per molecule participating in the reaction [36], and the temperature is 297K.

2.2.4. Determination of pK_a Values

When the acid/base equilibrium is established rapidly, as shown

$$RSH + H_2O \rightleftharpoons RS^- + H_3O^+$$

a single wave is observed on polarographic curves corresponding to the following electrode reaction.

$$Hg \rightleftharpoons Hg^+ + e^-$$

$$Hg^+ + RS^- \rightleftharpoons Hg(SR)$$

The half-wave potential ($E_{1/2}$) varies with pH according to equation 8

$$E_{1/2} = E^o + RT(-pH + pK_a)/F \quad \ldots\ldots \quad 8$$

Therefore as the pH rises, the $E_{1/2}$ value becomes more negative. However, when $K_a > H^+$, $E_{1/2}$ remains constant. In a graph of $E_{1/2}$ versus pH, there are two linear portions which intersect at a value corresponding to the pK_a value.

2.3. Cyclic Voltammetry

2.3.1. General Theory

In cyclic voltammetry (CV), the potential applied to a hanging mercury drop electrode (HMDE) is varied linearly with time, using scan rates ranging from 0.04 V/s to 1000 V/s. Cyclic voltammograms are recorded from an initial potential to a switching potential and back to the initial potential (Fig. 5a). Therefore both the oxidation and reduction portions of the electrode reaction can be recorded (Fig.5b).

The expression for peak current at a planar electrode is given by

$$(i_p)_{planar} = 2.69 \times 10^5 n^{2/3} A D^{1/2} v^{1/2} C^b \quad \ldots\ldots 9$$

where A is the area of the electrode; v is the scan rate and the rest of the symbols have the usual meaning.

Equation 9 is important because it shows that for a diffusion controlled process, the peak current is proportional to the square root of the scan rate and also proportional to bulk concentration of the electroactive species.

When a spherical stationary mercury drop is used as the electrode, the peak current equation has to be ammended for spherical diffusion, as in equation 10

$$(i_p)_{spher} = (i_p)_{planar} + 0.725 \times 10^5 n A D C^b / r \quad ..10$$

where r is the electrode radius in centimetres.

Fig. 5a

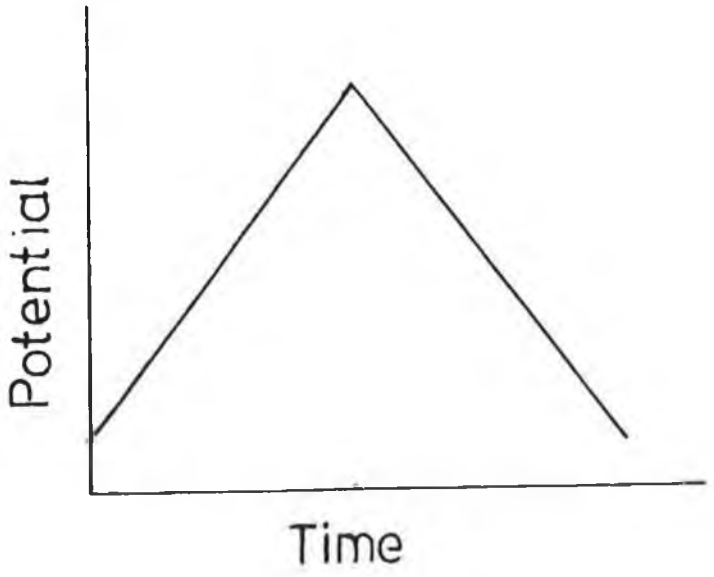

Fig. 5b

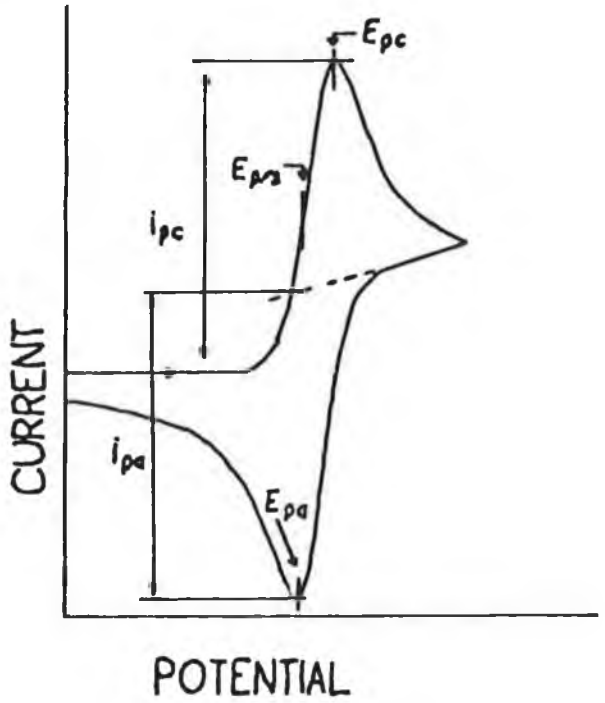

Fig. 5a Potential sweep in cyclic voltammetry.

Fig. 5b A typical cyclic voltammogram.

The charging current is given by equation 11

$$i_c = AC_{dl}v \quad \ldots\ldots\ldots 11$$

where C_{dl} is the capacitance of the double layer.

The peak current must always be measured from the charging current baseline, and since the charging current is scan rate dependent and the peak current is dependent on the square root of scan rate, this often puts a limit to the maximum scan rate that can be employed.

2.3.2. Studies of Reversibility

Two important parameters concerning the interpretation of cyclic voltammograms are (a) the ratio of the anodic peak current (i_{pa}) and peak cathodic current (i_{pc}); and (b) the peak separation $E_{pc}-E_{pa}$. For a reversible process the ratio of peak currents should equal unity and the peak separation should equal 59/n mV at 25C.

Reactions that show kinetic limitations to electron transfer are called quasi-reversible reactions. The peak separation in such cases is greater than 59/n mV and its value depends on the scan rate and the rate of electron transfer.

2.3.3. Adsorption

Distortion of cyclic voltammograms, and even the appearance of new peaks occur when there is adsorption of either the reactant or product [37].

When the product R in the following reaction

$$O + ne \rightleftharpoons R$$

is stongly adsorbed, there is a prepeak on the reduction wave in CV. This represents the reduction of dissolved reactant O to form a layer of adsorbed R. This wave occurs at potentials more positive than the diffusion-controlled wave, because the free energy of adsorption of R makes reduction of O to adsorbed R easier than to R in solution. The wave for reduction of dissolved O to dissolved R is slightly distorted due to the adsorption prepeak.

The prepeak separation from the the diffusion peak increases with strength of adsorption. The prepeak current $(i_p)_{ads}$ increases linearly with scan rate v, while the diffusion current $(i_p)_{diff}$ increases with $v^{1/2}$; so $(i_p)_{ads}/(i_p)_{diff}$ increases with increasing v, but it decreases with bulk concentration of O. At very low concentrations, only the prepeak is observed and as C^b increases, the surface coverage reaches a limiting value and the diffusion peak becomes the major peak.

When reactant is strongly adsorbed, a postpeak is observed following the diffusion controlled peak.

When adsorption is weak, the difference in energies between

reduction of adsorbed and dissolved species is small, therefore no pre- or post- peaks are observed. When reactant O is weakly adsorbed, there is an enhancement of i_{pc} with respect to i_{pa}; while when R is weakly adsorbed, the anodic current shows enhancement of current.

2.4. Differential Pulse Polarography

Differential pulse polarography (DPP) is a more sensitive technique than DC polarography, owing to effective discrimation against the capacitive current. In DPP, a linear potential ramp is applied to the electrode as in DC polarography. Near the end of the drop life, a small amplitude pulse (E< 100 mV) is superimposed on the ramp. The difference in the current measured before and after application of the pulse is outputted as the signal (Fig 6), resulting in a peak shaped curve. Since the faradaic current decays much slower than the charging current, measurement of the current near the end of the pulse provides substantial descrimination against the charging current.

The peak current i_{DPP} is proportional to the concentration of the electroactive species. The peak current also increases with increased pulse amplitude E, but this also results in broadening of the peak and decreases the resolution. The peak half width, $W_{1/2}$, defined as the width of the peak at half the maximum peak height, for a small pulse amplitude equals 90.4/n mV at 25°C. The peak potential and the DC half wave potentials only differ by half the pulse amplitude.

$$E_{DPP} = E_{1/2} - \Delta E/2 \quad \ldots\ldots\ldots\ 12$$

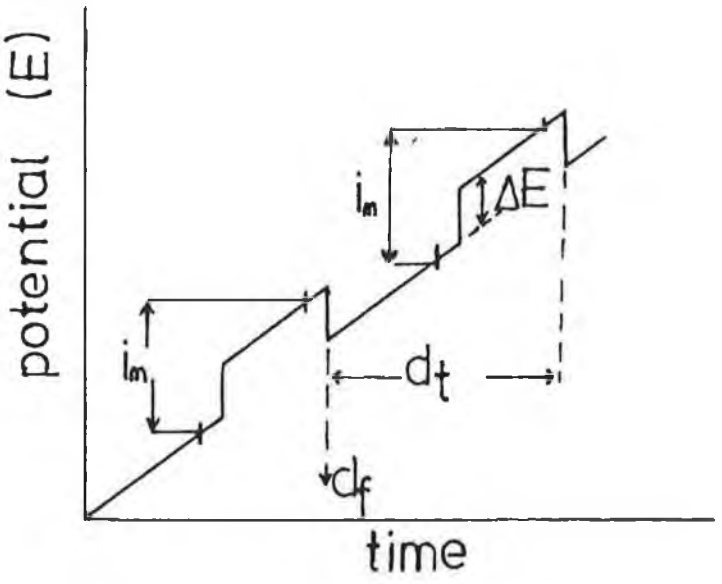

Fig. 6 Applied potential waveform in differential pulse polarography.

2.5. Cathodic Stripping Voltammetry

Cathodic stripping voltammetry (CSV) is the most sensitive of the polarographic techniques used. Its greater sensitivity results from increasing the faradaic current by applying a potential at which an adsorbed mercury salt is accumulated at the electrode surface. The adsorbed film is then "stripped" off the electrode on application of a cathodic scan, and the resultant current is recorded. The theory of stripping voltammetry is extremely complicated, because the measured current depends on both deposition and stripping steps. At slow (cathodic) scan rates, sphericity terms must be incorporated to allow for the effects of electrode curvature. This is especially the case in differential pulse cathodic stripping voltammetry where scan rates of 2-10 mV/s are commonly used. DPCSV is a more sensitive technique than linear sweep CSV, because the pulse technique discriminates against the capacitive current, as mentioned under 2.4.

In stripping voltammetry, calibration curves or standard addition methods are used to determine concentration.

The detection limit (LOD) in the formation of deposit at the electrode surface of composition $Hg_n(RS)_m$ is given by

$$C_{RS} > \frac{m+n}{m^{\frac{m}{m+n}} \cdot n^{\frac{n}{m+n}}} \cdot \left[K_S \cdot \frac{\delta}{\mu} \right]^{\frac{1}{m+n}} \quad \ldots\ldots \quad 13$$

where C_{RS} is the bulk concentration of the thiolate anion in solution, n and m are the numbers mercury atoms and thiolate anions respectively in the mercury thiolate molecule $Hg_n(RS)_m$, K_S is

the solubility product of the precipitate; δ is the diffusion layer thickness and μ the reaction layer thickness [38].

Optimisation of CSV sensitivity can be achieved by increasing deposition time, electrode area and varying deposition potential and rate of solution stirring.

2.6. Chronocoulometry

Chronocoulometry was developed by Anson to determine quantities of adsorbed reactants at an electrode surface [39].

Considering an electrode reaction where the reaction where the reactant O is adsorbed, and applying a potential step to the electrode as shown in Fig. 7a, at the initial potential E_i, insignificant electrolysis occurs in a homogeneous solution of species O. The potential is then switched to the final potential E_f at time t=0, where the electrode reaction occurs.

The chronocoulometric responce to the potential step is given by

$$Q = \frac{2nFAD^{1/2}C^{b}t^{1/2}}{\pi^{1/2}} + Q_{dl} + nFA\Gamma \quad \ldots\ldots \quad 14$$

where the first term on the right hand side of equation 14 corresponds to the charge resulting from diffusion of O to the electrode. Q_{dl} is the double layer capasitive charge and $nFA\Gamma$ quantifies the faradaic component due to the reduction of Γ mol/cm^2 of adsorbed O.

A plot of Q vs $t^{1/2}$ (Fig.7b) results in a straight line with an intercept given by Q_{dl} + nFAΓ. An approximate value for nFAΓ can be calculated by subtracting the intercept of the Q vs $t^{1/2}$ plot obtained for the supporting electrolyte, (yielding an approximate Q_{dl} value), from the intercept of the Q vs $t^{1/2}$ plot for the solution containing O. Anson, however, recommends the use of a 'drop extrusion' method for measuring Q_{dl}, where adsorption causes large changes in the charge on the electrode.

(a)

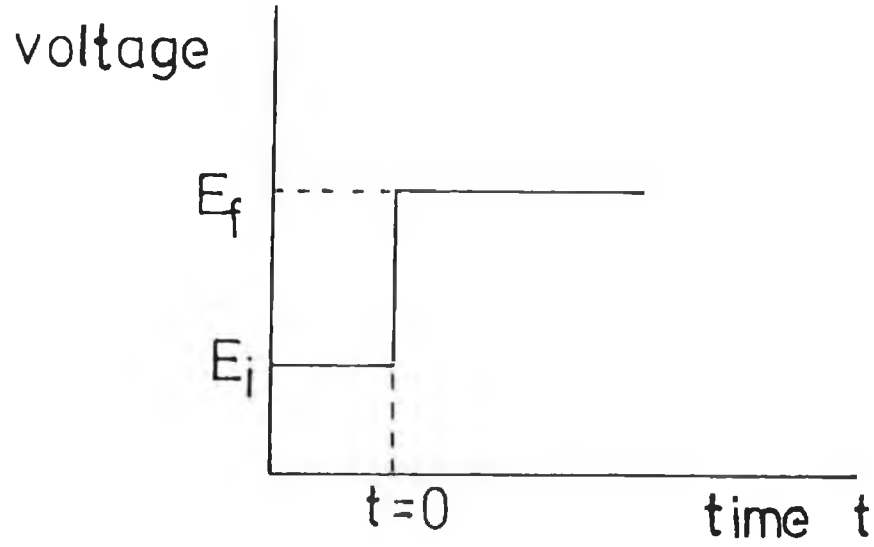

(b)

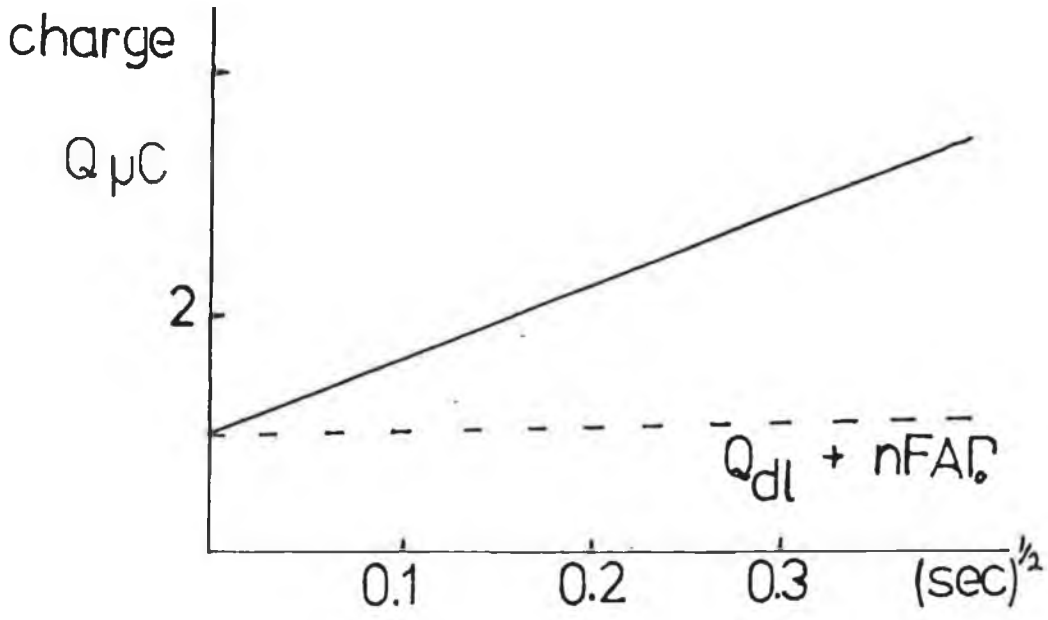

Fig. 7a Applied potential waveform in chronocoulometry.

Fig. 7b Plot of measured charge vs the square root of time, used to calculate the quantity of adsorbed reactant Γ .

2.7. Electrocapillary Curves

Electrocapillary curves are plots of surface tension against potential. Plots of time versus potential are drawn in practice, however, because drop time t is proportional to surface tension equation as in

$$t = 2.r\gamma/mg \quad \ldots\ldots 15$$

where γ = surface tension acting around the circumference the capillary

r = radius of the capillary

m = mass flow rate of mercury issuing from the capillary.

g = gravitational acceleration.

Electrocapillary curves have a maximum at a certain potential where there is no charge on the electrode, while either side of this maximum there is either a net positive or negative charge on the electrode depending on the applied potential. A charge on the electrode surface shortens the drop life, because like charges repel each other, therefore reducing the surface tension.

Adsorption deforms the electrocapillary curve. The drop time decreases at the potentials at which adsorption occurs because there is a charge build-up between the adsorbed layer and the mercury electrode.

C. EXPERIMENTAL

1. Apparatus and Materials

The chemicals studied were 2-mercaptopyridine (2MP), 2-mercaptopyridine-N-oxide (2MP-O), 2-mercapto-4-methylpyrimidine.HCl (2MmPr), which were obtained from Aldrich Chemical Co. and 2-mercaptopyrimidine (2MPr) which was obtained from Reidel-De-Haen AG. All chemicals were 99% pure. Sodium omadine (NaOm) and 2-chloropyridine-N-oxide (2PCl-O) were received from Olin Chemicals BV.

A stock Britton-Robinson (BR) buffer was made up from Analar quality acetic acid (0.04M), boric acid (0.04M) and o-phosphoric acid (0.04M) in deionised water. The BR buffer was adjusted to the required pH with 0.2M sodium hydroxide. Stock solutions of each compound were made up at the following concentrations: $1x10^{-2}$M 2MP and 2MP-O, $5x10^{-3}$M 2MPr and $1x10^{-3}$M 2MmPr in methanol. They were stored in a refrigerator and in darkness to prevent decomposition. Fresh solutions were made up every two months. Samples of the stock solutions were diluted in BR buffer to required concentrations, using Oxford micropipettes of 0-200 μl range, prior to analysis.

Since much of the work was carried out at analyte concentrations below $1x10^{-4}$M, care was taken that no contamination of the solution occurred. Glassware was washed in chromic acid before commencing any study. Chromic acid was prepared by adding 800 ml concentrated sulphuric acid to 92g sodium dichromate in 458 ml water and the glassware was soaked in it for twelve hours. After the acid wash, glassware was soaked in $3.6x10^{-2}$M ethylenediaminetetraacetic acid (EDTA) solution overnight and finally rinsed at least ten times

with Millipore-grade water. On a daily basis, glassware used was soaked in 2M nitric acid overnight, and washed with copious amounts of Millipore-grade water. The glass polarographic cell was soaked overnight in 6M nitric acid.

Sampled direct current (DC) polarography, differential pulse polarography (DPP) and differential pulse cathodic stripping voltammetry (DPCSV) were carried out using an EG+G Princeton Applied Research (PAR) Model 303 stationary mercury drop electrode (SMDE) in conjunction with an EG+G PAR Model 264 polarographic analyser and a Houston Instrument Model 2000 X-Y recorder. A stir bar and a PAR Model 305 stirrer were also used for DPCSV. For cyclic voltammetry (CV) the Model 303 SMDE was used in conjunction with the PAR Model 174A Potentiostat and the PAR Model 175 Universal Programmer. The cell was thermostated at 25^{o}C $\pm$1^{o}C. A Ag/AgCl reference electrode and a platinum wire counter electrode were used to complete the electronic circuit.

DC polarograms, for various mercury resevoir heights, and electrocapillary curves were recorded using a Metrohm Model 626 Polarecord with a Metrohm Model 505 polarography stand.

'Fast' cyclic voltammograms of scan rates from 200mVs^{-1}to 20Vs^{-1} were stored on a Philips PM 3311 0-60MHz cathodic ray oscilloscope (CRO), and outputted to a JJ instruments X-Y recorder.

Coulometry was carried out using an EG+G PAR Model 379 Coulometer in conjunction with an EG+G PAR Model 363 Potentiostat. A plastic 15 ml cell was used which contained a mercury pool working electrode, a platinum wire auxillary electrode and a standard calomel reference electrode (SCE).

Ultra-violet spectra were recorded on a Shimadzu UV-240 Recording Spectrophotometer with matching 1cm quartz cells. The pH readings were made on an Aquachem PTI-6 pH meter with an Orion glass electrode.

2. Techniques

2.1. Ultraviolet Spectral Investigations

Ultraviolet spectroscopy was used to determine the pK_a values of each compound. The pH of the BR buffer was adjusted by the dropwise addition of 0.2M sodium hydroxide and was increased in increments of 0.3 for 2MP , 0.4 for 2MP-O, 0.5 for 2MmPr and 1.0 for 2MPr. $1x10^{-4}$M concentrations of each compound were made up from their stock solutions in 10ml of the BR buffer at each pH before analysing. Matching quartz cells were used with the blank buffer solution in one cell and the compound of interest in the other. Scans were recorded from 420 nm to 200 nm. The spectrophotometer was allowed to warm up for 30 min before use. The values of absorbance (A) at a specific wavelength (λ) were noted and plots of absorbance versus pH drawn. The pK_a values could be read directly from the midpoint of the resulting sigmoidal curves (A vs pH).

2.2. Polarographic Investigations

Variation of half-wave potential $E_{1/2}$ with pH and the reversibility of the electrode reaction were studied using sampled DC polarography. Nitrogen was used as the purging gas and it was passed through a solution of vanadous chloride to remove any traces of oxygen present in the nitrogen, and then through deionised water, before entering the solution for analysis. The solution was purged with nitrogen for eight minutes, and the sampled DC polarograms were recorded between +0.3 V and -1.5 V using a "medium" sized drop, a drop time of 1 second, scan rate 2 mVs^{-1} and a sensitivity of 0.1 μA/in. The limiting current i_l and the half wave potential $E_{1/2}$ were measured as shown in Fig. 4. The reversibility of the reaction was investigated from these curves by plotting E_{DME} vs $\ln(i/i_d-i)$, as discussed in section B 2.2.3.

DC polarograms were recorded for a $1x10^{-4}$M concentration of 2MP. The height of the mercury resevoir was varied and the resultant limiting currents of the DC polarograms obtained plotted versus $h^{1/2}$ and h.

Electrocapillary (EC) curves were obatained by varing the potential in steps of 0.1 V or 0.2 V and recording the time taken for ten drops to flow through the capillary at fixed potentials. This was carried out first for a blank solution of BR buffer pH 6.0, and then when quantities of 2MP or 2MP-O were added to the buffer. EC curves of 2MP at concentrations of 0.5, 2.5 and $6.1x10^{-4}$M and 2MP-O at a concentration of $2.5x10^{-4}$M were recorded.

Differential pulse polarography (DPP) was also used to investigate the variation of E_p with pH using the same method of sample preparation as used in DC polarography. Variation of peak current i_{DPP} with concentration was studied using DPP. Various concentrations of each compound were made up to 10ml using BR buffer pH 6.0. The polarograms were recorded over the range +0.17V to -1.0V using a "large" sized drop, a drop time of 1 second and modulation amplitude of 50 mV. A concentration range of $1\text{-}50\text{x}10^{-5}$M and current range of 1-100 μA were used. Buffer background curves were recorded in all cases.

Differential pulse cathodic stripping voltammetry (DPCSV) was used to investigate the variation of stripping current with concentration. 10 ml of BR buffer (adjusted for pH) was first pipetted into a polarographic cell, and a scan of the buffer was taken after purging. The compound was then added to the cell via a porthole in the support block using a micropipette. The experimental conditions were: purge time = 14 min; deposition time = 300 sec; "medium" drop size.

Both DPP and DPCSV were used to investigate the differentiation of compounds in mixtures. A scan was first taken of the blank buffer solution and then the compounds were introduced into the buffer individually in various quantities via the porthole.

Coulometry was carried out on a $1\text{x}10^{-2}$M 2MP solution in BR buffer pH 6.1 . The potential was held at +0.16 V vs SCE for approximately one hour. Coulometric settings were: current scale 1mA; bipolar mode. Initially, 10 ml of buffer was electrolysed for half an hour, until a stable value of charge was achieved, then 50 μl of

$1x10^{-4}M$ 2MP was added to the buffer. The solution was purged with nitrogen during electrolysis and it was also stirred using a magnetic stirrer and stirring bar.

The 'drop extrusion' method used to measure the double layer charge was carried out on a Metrohm EA 290 hanging mercury drop electrode.

2.3. Cyclic Voltammetric Investigations

Cyclic voltammetry was used to examine the mechanism of the electrode reaction. Scan rate was varied between 20-200 mVs^{-1} for a constant $1x10^{-4}M$ concentration of each compound. The effect of changing concentration from $1-50x10^{-5}M$ for constant scan rates of 50 and $100mVs^{-1}$ was studied. In the examination of product adsorption, CV's were recorded, where the potential was held positive of the oxidation peak for fixed lengths of time, where accumulation of the reaction product occurred at the electrode. After the set holding time, the scan was allowed to continue and the reduction peak was recorded, where the product was 'stripped off' the electrode.

Cyclic voltammograms of scan rates >200 mVs^{-1} ('Fast' CV) were recorded as current versus time curves using a cathode ray storage oscilloscope (CRO). The starting, switching and final potentials were set on the PAR Model 175 Universal Programmer and scan rate on the PAR Model 174A Potentiostat. The CRO was triggered via a BNC cable from the 'cyc. sync.' junction on the Universal Programmer. The stored curves were outputted to an X-Y recorder. 'Fast' scan CV's

were taken of 2MP and 2MP-O. Scan rate was varied between 100 mVs^{-1} and 20 Vs^{-1}, for $1x10^{-4}M$ and $4x10^{-4}M$ solutions at pH's of 5.0 and 6.0 for both compounds.

2.4. Analysis of Plant Samples

Samples were taken from the plant mercaptisation reactor in a 250ml beaker, via a tap at the bottom of the reactor. Each sample was diluted (1:10 vol:vol) to 100 ml in distilled water, with aproximately 1 ml conc. HCl added to each to bring the pH to around 6.0 . This in effect quenched the reaction. The samples were then brought to the college laboratory, where they were diluted in BR buffer pH 6.0 (1:200 vol:vol) prior to DPP analysis.

D. RESULTS and DISCUSSION

1. Determination of pK_a values

The dissociation constants for all compounds were determined using both ultraviolet spectroscopy and sampled DC polarography.

1.1. Ultraviolet spectroscopy

The UV spectra were recorded for each compound over the pH range 2-12. A broad peak of low intensity at about 335-355 nm is present in the UV spectra of all the compounds studied. This is illustrated in the case of 2MmPr in Figure 8. This peak is not present however, in the UV spectra of pyridine [40], pyridine-N-oxide [41] or pyrimidine [32] at any pH. It is therefore concluded that this peak is due to the presence of the sulphur atom in this molecular structure, and is possibly a $n \rightarrow \pi^*$ transition of electrons from the non-bonding sulphur orbital to the anti-bonding π^* orbital of the aromatic ring. The absorption peak at approximately 270 nm, which is common to each of the compounds spectra, is probably due to the $\pi - \pi^*$ transition of the pyridine and the pyrimidine rings [33]. This $\pi - \pi^*$ transition usually occurs at about 250 nm for both pyridine and pyrimidine, but is now shifted to a higher wavelength due to the thiol group in the ortho position, increasing the energy of the π electrons. The spectrum of 2MP-O differs from that of 2MP and pyridine-N-oxide in having a peak at 240 nm. In addition, in acidic solution of pH<1.0, another absorption peak is found at 195 nm, which would seem to correspond to the peak at 205 nm for pyridine-N-oxide. It is not known, however, what transitions give rise to these peaks.

The peak at 195 nm may correspond to the protonated form of 2MP-O, ie: $2MP\text{-}OH^+$.

The four compounds exist in either thiol or thione tautomeric forms. 2-Mercaptopyridine and the 2-mercaptopyrimidines exist mainly in the cyclic thioamide form [32], and 2MP-O also exists mainly as 1-hydroxypyridine-2-thione. It is also known that the anionic form of 2MP-O predominately exists with the negative charge on the sulphur atom [3].

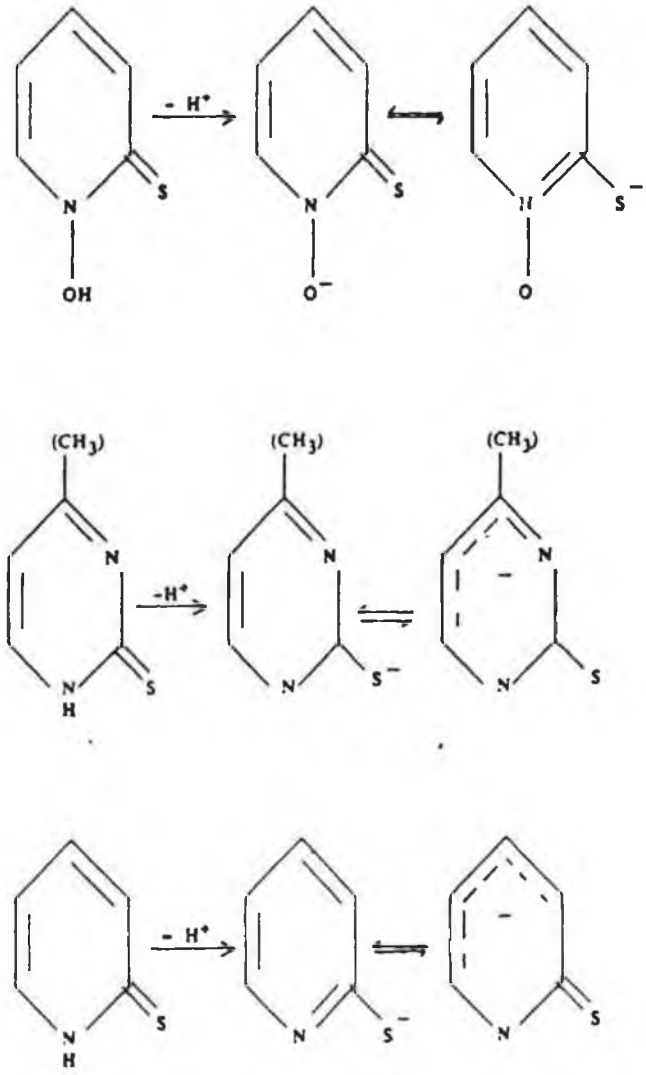

An attempt was made to discover the pK_a value for the association of a proton to 2MP-O by examining the UV spectra over the pH range 0-2. An isobestic point was found at 205 nm and a new peak resulted at 195 nm as the pH was reduced below pH 1.0. However its pK_a value was not determined. For the spectrophotometric determination of pK_a values in highly acidic regions ie: pH<1, an acidity function, H_o, should be used instead of the pH value [42]. Jones and Katritzky [43] determined the UV spectra of 2MP-O in its anionic form at pH 10, in its neutral form at pH 1.8 and in its cationic form in 20 N H_2SO_4. The H_o values of the sulphuric acid was used and the pK_a value was calculated at 299 nm from the three UV spectra.A pK_a value of -1.96 was reported. This pK_a value was outside the pH range studied here.

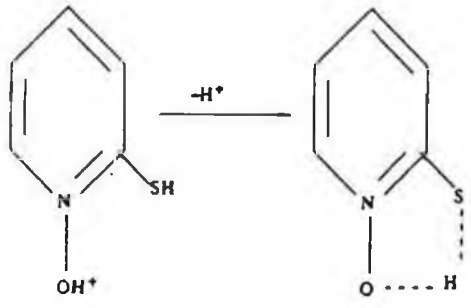

pK_a values for the mercaptan disociation were determined from the plots of absorbance vs pH at selected wavelengths. This is illustrated in the case of 2MmPr in Fig. 9. The results of this study are collected in Table I.

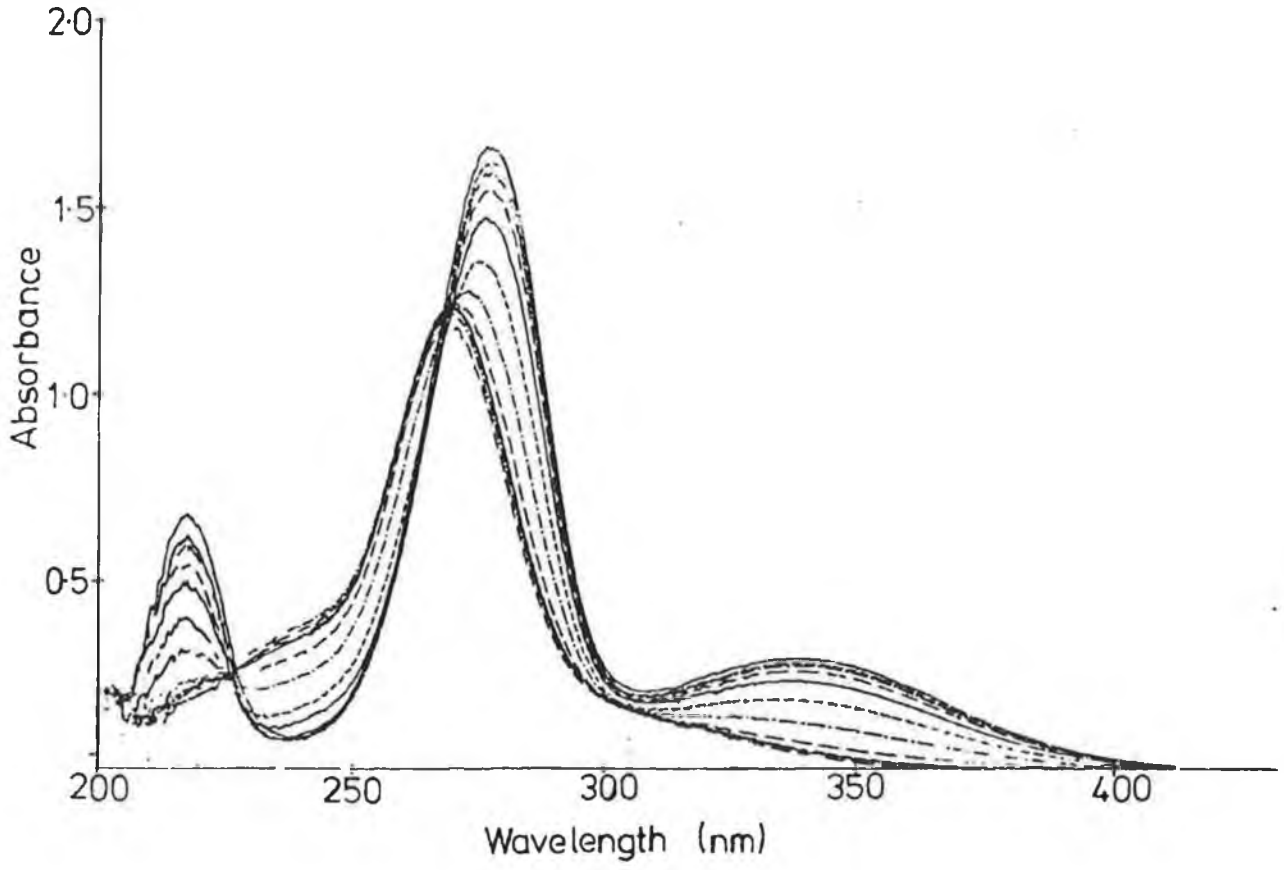

Fig. 8 UV spectra of 2MmPr over the pH range 5.0 to 10.0 .

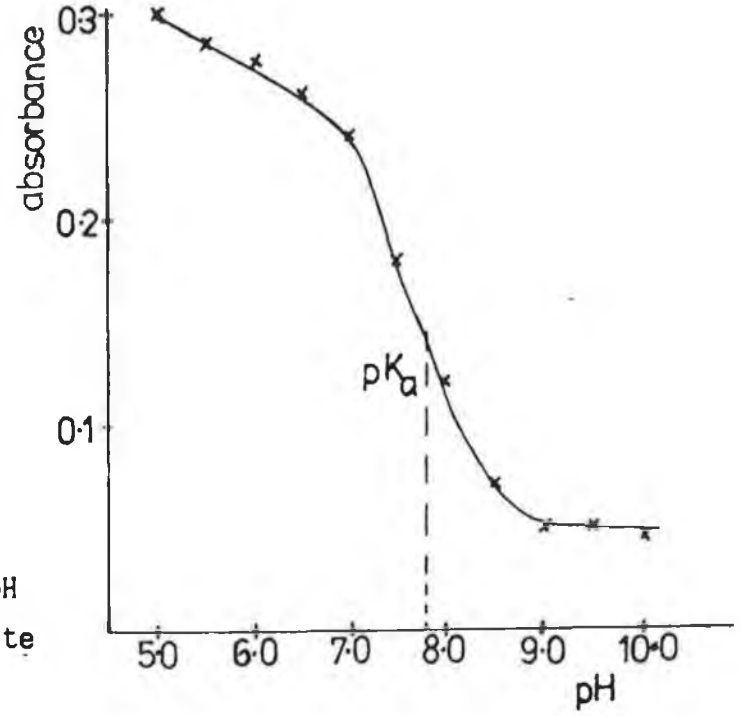

Fig. 9
Plot of absorbance vs pH @ 340 nm used to evaluate the pK_a value of 2MmPr.

1.2. Direct current Polarography

Sampled DC polarograms were recorded for each compound over the pH range 2-12. Typical sampled DC polarograms for 2MP are shown in Fig. 10. This study was undertaken to ascertain the pH dependance of parameters such as half-wave potential($E_{1/2}$) and wave height. The pK_a values were also determinable from plots of $E_{1/2}$ vs pH.

Each compound gave rise to a single, well-defined oxidation wave using sampled DC polarography. These waves are due to the catalytic oxidation of mercury in the presence of the mercaptan, and the formation of a mercuric thiolate film which is adsorbed at the electrode surface. The sampled DC polarographic behaviour of the compounds studied are limited by the rate of diffusion of the mercaptan to the electrode surface. The diffusion current for each compound remains almost constant for each of the examined compounds over the pH range studied. This is illustrated for 2MP in Figure 11. The current values were measured to an accuracy of $\pm$ 0.01μA.

According to Zuman, one single wave is observed on polarographic curves for a rapidly established acid-base equilibrium. The height of this wave corresponds to the number of electrons transferred and does not change with pH [36]. However, one exception arose for 2MP-O. The limiting current for 2MP-O was consistently higher at pH 4.0 than at any other pH. It was noted later, in the CV study, that there was stronger adsorption of 2MP-O mercuric salt at pH 4.0 compared with other pH's.

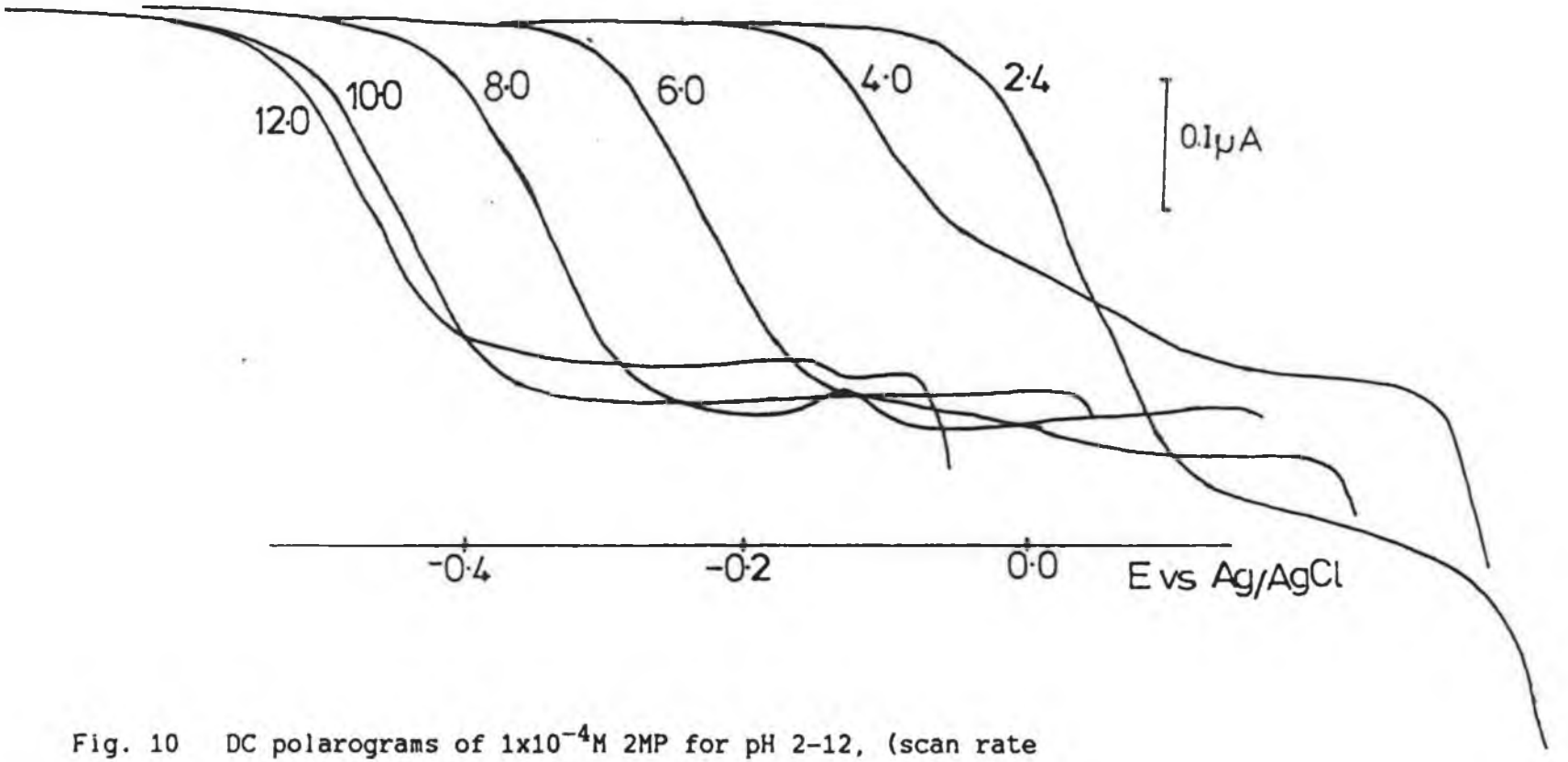

Fig. 10 DC polarograms of $1x10^{-4}$M 2MP for pH 2-12, (scan rate 2 mV/s, drop time 1 sec).

The electrochemical reaction at pH's below the pK_a value can be described by

$$Hg^+ + RSH \rightleftharpoons HgSR + H^+$$

and the $E_{1/2}$ value is dependent on pH.

For pH's above the pK_a value the thiolate anion is present in excess and the electrode reaction can be described by

$$Hg^+ + RS^- \rightleftharpoons HgSR$$

In this case, the $E_{1/2}$ value is independent of pH.

The plots of $E_{1/2}$ vs pH for each compound are illustrated in Fig. 12 and the pK_a values determined from these plots are given in Table I. The pK_a values determined by both UV spectroscopy and DC polarography can be seen therefore to be in good agreement.

The differences in the pK_a values of each compound are due to substituent effects. The pK_a value of 2MP-O is lower than that of other compounds because its hydrogen atom is less strongly bound to the sulphur atom due to hydrogen bonding with the oxygen atom.

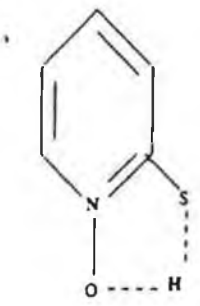

2MP-O is also more stable in its anionic form than the other compounds due to the electron withdrawing effect of the oxygen atom and the resonance stablisation of the negative charge on the sulphur atom .

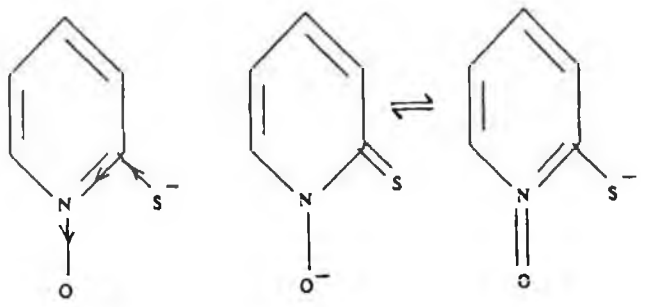

The pK_a values of the two pyrimidines are very similar . The methyl group is weakly electron donating and it is four bonds away from the sulphur/hydrogen bond of 2MmPr and so has little effect on its dissociation constant. It may cause a slight destabilisation of the anionic form so that the pK_a value of 2MmPr is slightly higher than that of 2MPr. The pK_a values of the pyrimidines are lower than that of 2MP because their anionic forms are probably stabilised by the extra nitrogen in the ring.

The differences in the half-wave potential values exhibited by each of the compounds (Fig.12) are also a result of substituent effects. $E_{1/2}$ values are linearly dependant on the lowest unoccupied molecular orbital (LUMO) energy. Therefore, differences in the $E_{1/2}$ values reflect the effect of substituent on the LUMO energy of the compound. In a solution of pH below 6.0, 2MP-O is oxidized at a lower potential than the other compounds due to the

S-H bond being weakened by hydrogen bonding with the oxygen atom . At pH's > 8.0 it is oxidised at higher potentials than the other compounds, probably due to the relative stabilisation of its anionic form by the oxygen atom. Similarly, 2MP, at pH's above its pK_a value, is oxidised at potentials lower than those of the other three compounds because its negative charge on the sulphur is less delocalized by substituents and so it forms a mercury salt more readily.

Compound	pK_a(a)	pK_a(b)
2-Mercaptopyridine	9.7 ±0.1	9.5 ±0.1
2-Mercaptopyridine-N-oxide	4.4 ±0.1	4.6 ±0.1
2-Mercaptopyrimidine	7.3 ±0.1	7.6 ±0.1
2-Mercapto-4-methylpyrimidine	7.8 ±0.1	8.0 ±0.1

Table I.

The pK_a values determined for mercapto compounds using (a) UV spectroscopy and (b) sampled DC polarography.

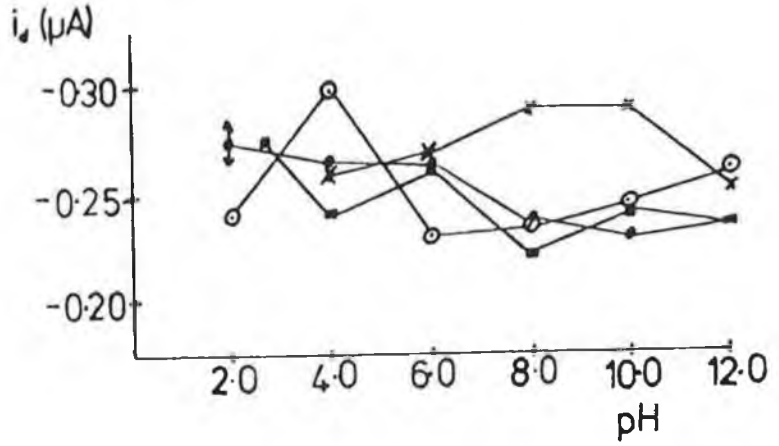

Fig. 11 Plots of diffusion current vs pH for each mercaptan studied; 2MP (x), 2MP-O (⊙), 2MPr (•), 2MmPr (▬).

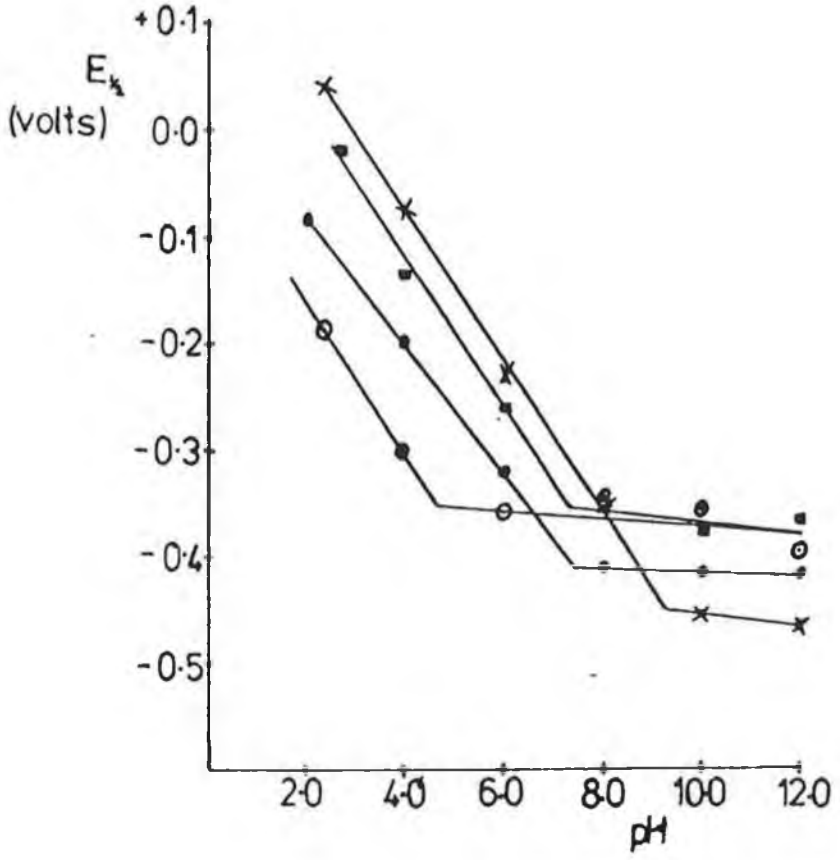

Fig. 12 Plots of half-wave potential ($E_{1/2}$) vs pH for each mercaptan studied; 2MP (×), 2MP-O (⊙), 2MPr (•), 2MmPr (▬).

2. Studies of the Electrode Process

2.1. Reversibility of the electrode process

The reversibility of the respective electrode processes was assessed from the sampled DC polarograms by plotting;

(i) $E_{1/2}$ vs pH (Fig.12), and

(ii) E_{DME} vs $\ln[i/(i_d-i)]$ for each compound (Fig.13)

2.1.1. $E_{1/2}$ vs pH plots

The $E_{1/2}$ values for each of the compounds were shifted in a negative potential direction with increasing pH when the pH was less than the corresponding pK_a value.

The slope of the graph, where $E_{1/2}$ is dependent on pH, for a reversible system depends on the number of electrons (n) and on the number of protons (p) transferred during the electrode process [36]. Assuming a 1-electron 1-proton reaction, a slope of 59 mV is expected for a reversible reaction. It can be seen from Table II that the slopes for three of the compounds correspond to a quasireversible electrode reaction. The slope for 2MPr, however, indicates that its electrode reaction was almost reversible.

2.1.2. Plots of E_{DME} vs $\ln(i/i_d-i)$

Plots of E_{DME} vs $\ln(i/i_d-i)$ curves were obtained for each compound from their sampled DC polarograms recorded at pH 6.0

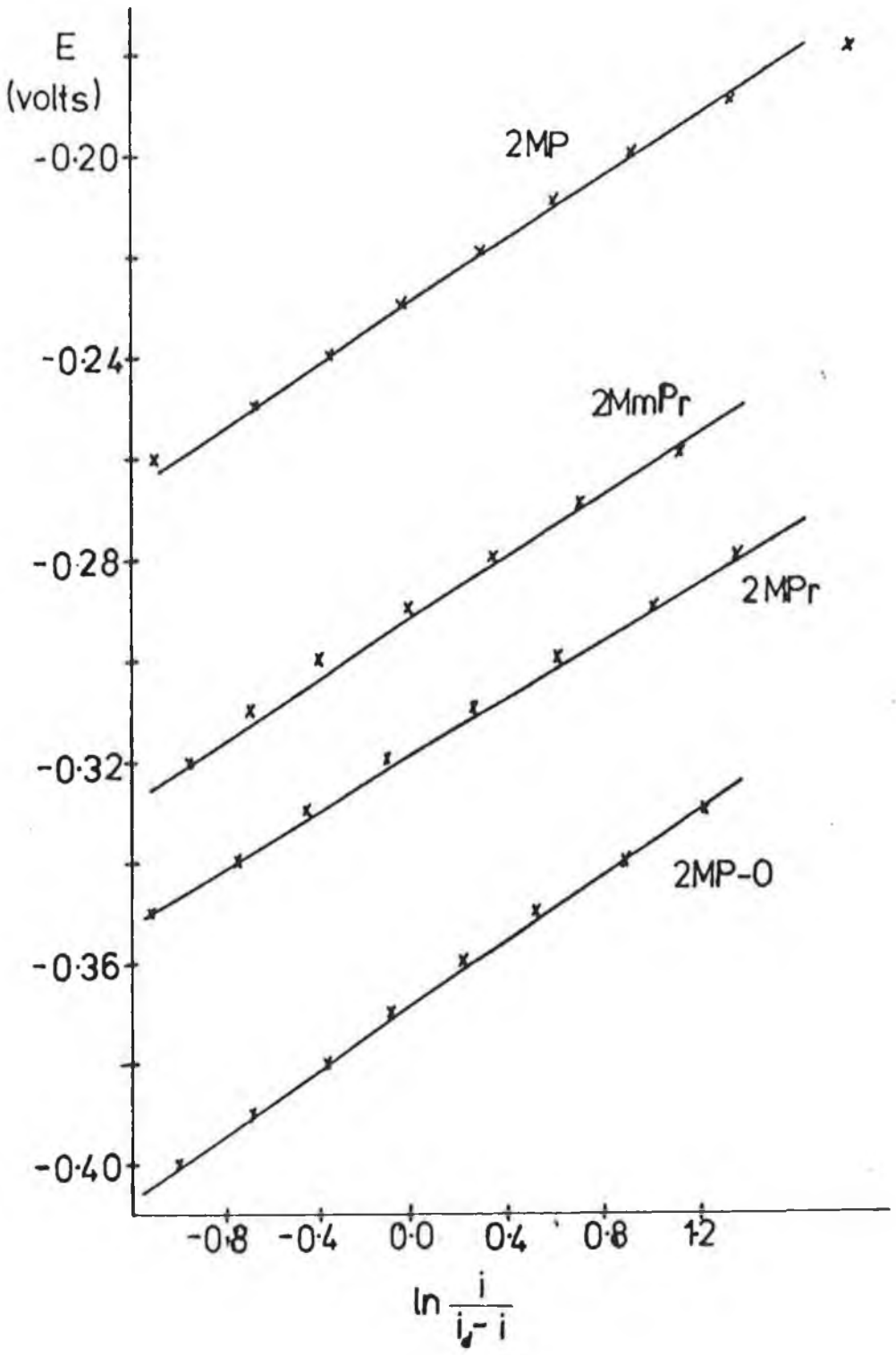

Fig. 13 Plots of E_{DME} vs $\ln[i/(i_d-i)]$ for each mercaptan at pH 6.0 .

Table II

Slope of $E_{1/2}$ vs pH curves.

Compound	slope (mV)
2-Mercaptopyridine	70.0
2-Mercaptopyridine-N-oxide	71.0
2-Mercaptopyrimidine	61.0
2-Mercapto-4-methylpyrimidine	71.0

Table III: Slopes obtained from the E_{DME} vs $\ln(i/i_d-i)$ plots.

Compound	Slope (mV)	r
2-Mercaptopyridine	32.0	0.9991
2-Mercaptopyridine-N-oxide	32.4	0.9995
2-Mercaptopyrimidine	28.6	0.9996
2-Mercapto-4-methyl-pyrimidine.HCl	30.2	0.9965

r is the regression coefficient.

(Fig.13). Points along the main sloping part of the curve were taken, while points near the base-line and the diffusion limiting current were considered to be less accurate [44]. The range plotted was approximately $0.015i_d$ to $0.85i_d$. The slope for a reversible reaction should equal 23.5 mV [35].

The reversibility of the reaction corresponds to the rate of electron transfer in the oxidation of the mercaptans. The reversibility in this case was measured with respect to the time domain of a sampled DC polarographic experiment, which was a drop time of 1 second. It can be seen from Table III that none of the compounds exhibit complete reversibility, their slopes being larger than that for a reversible reaction. The electrode reaction of 2MPr was the most reversible of the four compounds studied, which is in agreement with the results from the slope of the $E_{1/2}$ vs pH curves.

2.2. Electrocapillary Curves

Electrocapillary (EC) curves were recorded for 2-mercaptopyridine and 2-mercaptopyridine-N-oxide for various concentrations of each compound in BR buffer pH 6.0 . These curves were used to give some information about the adsorption of these compounds at mercury electrodes. The adsorption of other mercaptans has previously been demonstrated by other authors using EC curves [6,9,10,13].

Electrocapillary curves for $0.5x10^{-4}M$ and $6.1x10^{-4}M$ concentrations of 2MP are shown in Fig.14a. There is little difference between the curve due to the buffer and that due to 2MP at the $5x10^{-5}M$ concentration. At this low concentration very little 2MP diffused to the mercury drop surface during its lifetime of about 2 sec, to form an adsorbed film. However, as the bulk concentration of the mercaptan was increased to $6.1x10^{-4}M$, more of it diffused to the electrode surface and the amount of adsorption increased. This is evident from the electrocapillary curves in Fig.14a, where the the mercury drop time decreased over the electroactive region (-0.4 V to -0.2 V) as the concentration of 2MP was increased.

A comparison of the electrocapillary curves for equal concentrations of 2MP and 2MP-O is shown in Fig. 14b. Both compounds show appreciable adsorption at the electrode at potentials between +0.2 V and -0.4 V. However, since the drop time was shorter for the 2MP solution than the 2MP-O solution over the reaction potentials +0.20 V $\rightarrow$ -0.40 V, it is felt that either more 2MP mercuric salt was adsorbed at the electrode surface or that it formed a more compact film than the 2MP-O mercuric salt. A more uniform film formation for the 2MP salt is also evident later from the larger peak currents found for 2MP using DP and DPCSV analysis. The potential region where the drop time was reduced corresponds to the current-voltage waves exhibited on sampled to DC and DP polarograms. This potential region expanded at higher concentrations (cf: $6.1x10^{-4}M$), and this is reflected in the appearance of two peaks in the DPP scans run at this concentration. Both peaks were due to the formation of adsorbed mercury thiolate.

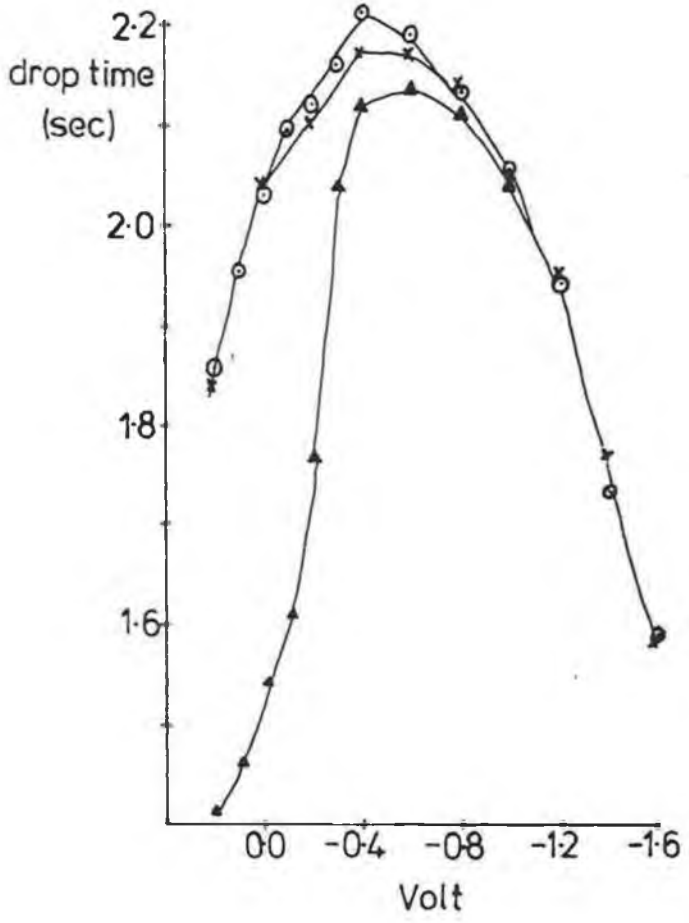

Fig. 14a Electrocapillary curves
(i) buffer pH 6.0 (×)
(ii) 0.5×10^{-4}M 2MP (⊙)
(iii) 6.1×10^{-4}M 2MP (▲)

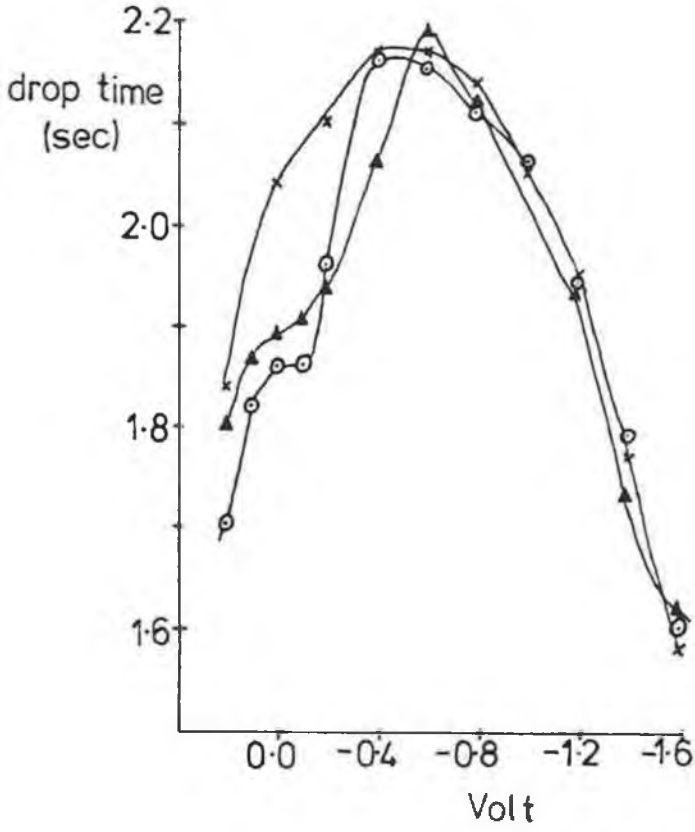

Fig. 14b Electrocapillary curves

(i) buffer pH 6.0 (x)

(ii) 2.5×10^{-4}M 2MP-O (⊙)

(iii) 2.5×10^{-4}M 2MP (▲)

The reduction in drop time was due to the effect of adsorption increasing the charge on the drop surface, resulting in a lowering of the drop's surface tension. Anson [39] reported that the charge on the electrode at +0.30 V was actually smaller than at -0.20 V due to the adsorption of $Hg(SCN)_2$, thus demonstrating the capacitive nature of the adsorbed film.

2.3 Plot of limiting current (i_l) vs reservoir height (h)

An attempt was made to determine whether the electrode reaction for $1x10^{-4}$M 2MP at the DME was either diffusion or adsorption controlled by plotting i_l vs h. A linear plot of i_l vs $h^{1/2}$ indicates diffusion control whereas a linear plot of i_l vs h indicates an adsorption controlled process. Neither plot gave conclusive evidence that the electrochemical reaction was adsorption or diffusion controlled, since each yielded a fairly linear curve ($r=0.9935$ for i vs h, and 0.9895 for i vs $h^{1/2}$).

Three possible reasons are given why the results were inconclusive ; (i) a calculated error of ($\pm$5nA) was mainly due to the shape of the limiting portion of the DC polarogram. This meant that all points on both graphs could be fitted onto a straight line within their error bars, (ii) the curvature of one of the i_l vs h plots may have been revealed if it had been possible to use a greater range of resevoir heights c.f. a small portion of a parabola often seems linear; (iii) neither adsorption nor diffusion may have had complete control over the electrode reaction. For current to be proportional to h, the drop surface is assumed to be fully covered as

soon as the drop is formed, which did not happen in this case. The electrocapillary curves show that adsorption of 2MP increases with concentration, and from the DP polarograms it can be seen that concentrations of $2.5x10^{-4}M$ are needed before peak splitting occurs due to multi-layer formation. So it was assumed that at this concentration the drop was not fully covered with adsorbed product during the drop's life, and so adsorption should not be the complete controlling factor.

3. Cyclic Voltammetry

Cyclic voltammetry (CV) is used for the study of both the anodic and cathodic steps in an electrochemical reaction. It is also possible to study electrode reactions at scan rates far in excess of those possible in DC polarography. The potential of a stationary electrode, such as a hanging mercury drop electrode (HMDE), is varied, and a peak rather than a sigmoidal wave results due to depletion occurring in the diffusion layer during mass transfer.

3.1. 2-Mercaptopyridine

2-Mercaptopyridine was studied in greater depth using cyclic voltammetry than the other three compounds because its behaviour was less complicated. The paramaters varied were (1) pH,(2) scan rate,(3) concentration, and (4) holding potential.

The peak separation between the oxidation and reduction peaks was not used as an indication of the compounds' reversibility, since the peak potentials shifted with concentration and scan rate, due to the formation of insoluble products.

3.1.1. Effect of pH

Cyclic voltammograms of $1x10^{-4}M$ 2MP were recorded in BR buffers of pH 2-12 (Fig. 15) at a scan rate of 100 mVs^{-1}. There was a shift in peak potential to more negative values as the pH was increased to pH 10, while the peaks obtained in solutions of pH 10

and 12 had the same peak potential. The dependence of peak potential on pH can be explained by the fact that since 2MP exists in its protonated form (RSH) below pH 10, hydrogen ions are involved in the electrode reaction; while above pH 10, no hydrogen ions are involved in the reaction since 2MP exists in its anionic form (RS^-). The reduction scans resulted in higher peak currents than the oxidation scans. This enhancement in reduction peak current was due to the reduction of the adsorbed mercury thiolate salt [$Hg(RS)_2$] [37].

As the pH was increased, more adsorption characteristics were seen, with the appearance of a 'pre-peak' on the oxidation scan and a 'post-peak' on the reduction scan. These pre- and post-peaks correspond to the greater thermodynamic stability of adsorbed oxidation product to non-adsorbed product [37]. Therefore oxidation of thiol to adsorbed product and reduction of adsorbed product occur at more negative potentials than the diffusion controlled redox couple. At pH 2.0 there was no pre-oxidation peak. However, as the pH was increased, this pre-peak appeared and the pre-peak potential separation from the main peak also increased. This was indicative of an increase in the relative stability of the adsorbed product with respect to the non-adsorbed product at higher pH's. This increased separation of the oxidation peaks with pH resulted in the decrease in the main peak's current due to the reduced overlap of the two peaks. However the reason for the overall decrease in peak current from pH 10 to 12 is not known; there is a similar decrease in diffusion current measured from DC polarograms at these pH's (Fig. 11). It may be due to the repulsion of the anion by the negatively charged electrode. At pH 12, 2MP exists mainly in its anionic form and the

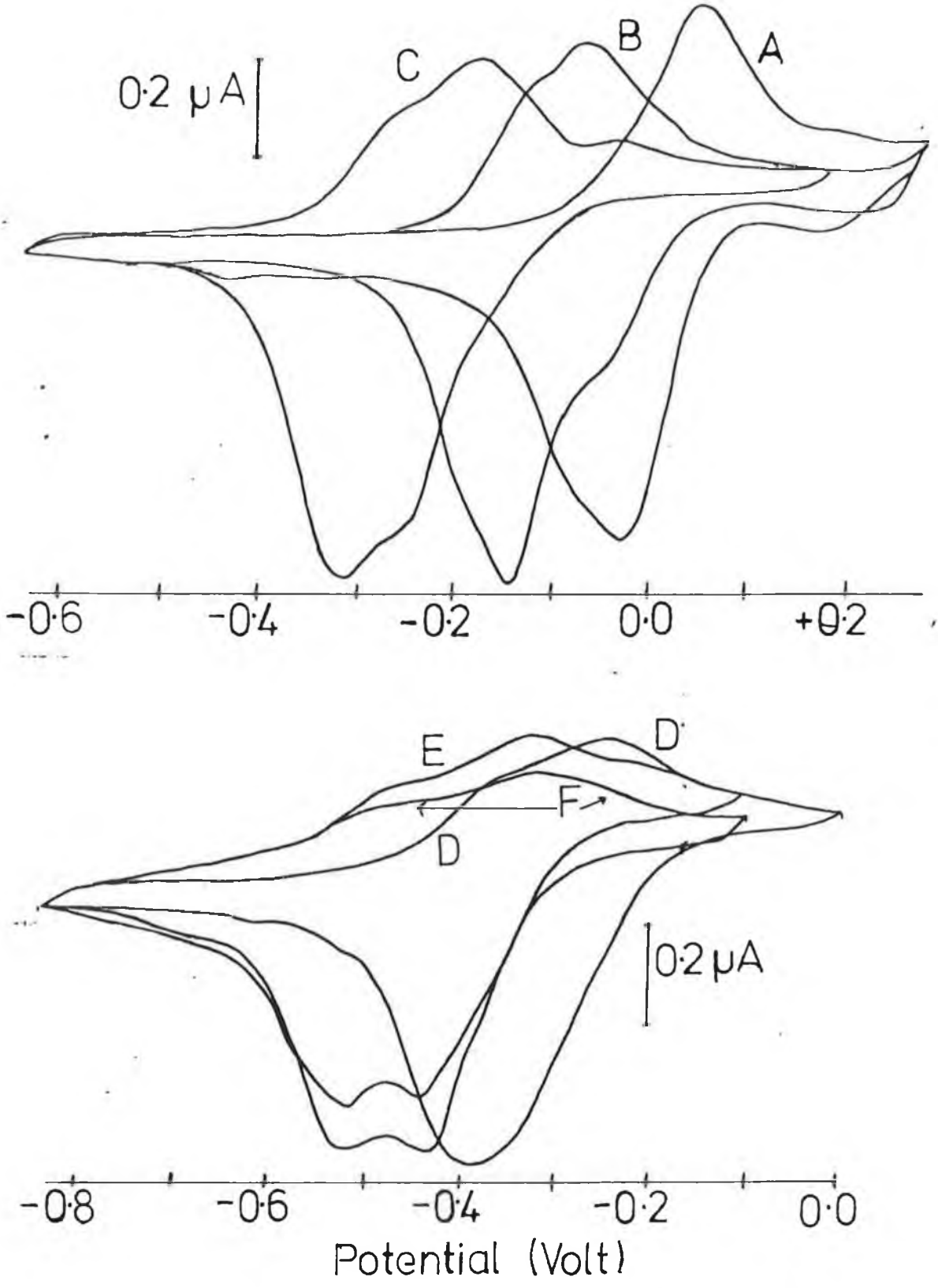

Fig. 15 Cyclic voltammograms of $1x10^{-4}$M 2MP over pH 2-12, scan rate 50 mV/s, pH: (A) 2.0, (B) 4.0, (C) 6.0, (D) 8.0, (E) 10.0, (F) 12.0

repulsion of anions from the electrode may reduce the overall current.

3.1.2. Effect of Scan Rate

The scan rate was varied in order to examine whether the peak current was diffusion or adsorption controlled. Under ideal conditions, diffusion-controlled peak current is proportional to the square root of scan rate, whereas an adsorption peak current is linearly dependent on scan rate [37]. Graphical analysis was carried out on the oxidation peaks, while analysis of the reduction peaks was not possible because of the variation in the background slope with scan rate.

Plots of current versus scan rate and the square root of scan rate were constructed for the oxidation peak for 2MP obtained from cyclic voltammograms. The peak current varied linearly with the square root of scan rate ($v^{1/2}$) for a $4x10^{-5}$M 2MP solution over the scan rate range of 20 mVs^{-1} to 200 mVs^{-1} (Fig 16). Therefore, over this scan rate range and concentration, the electrode reaction was predominantly diffusion controlled. A concentration of $4x10^{-5}$M was chosen because no pre-peaks appear on the oxidation peak at this low concentration. Variation of anodic peak current was examined over the scan rate range of 0.9 Vs^{-1} to 20 Vs^{-1} for $1x10^{-4}$M 2MP and 0.15 Vs^{-1} to 10 Vs^{-1} for $4x10^{-4}$M 2MP. For the $1x10^{-4}$M solution, both i_p vs $v^{1/2}$ and i_p vs v plots were found to reasonably linear (r=0.997 and r=0.990 respectively) for scan rates above 4.5 Vs^{-1}. The peak current for the $4x10^{-4}$M solution showed

a greater linear dependance with the square root of scan rate (r=0.996) than scan rate (r=0.974), over a 0.15 Vs^{-1} to 3.5 Vs^{-1} range (Fig.17). This is similar to the scan rate study from 20 mVs^{-1} to 200 mVs^{-1} shown in Fig.16, and it may be that the higher concentration compensates for the faster scan rates, keeping the reaction diffusion-controlled. At scan rates above 3.5 Vs^{-1} for the $4x10^{-4}M$ solution, the slope of the i_p vs $v^{1/2}$ curve changed. The i_p vs v curve was also fairly linear above 1 Vs^{-1}, (Fig.17); however, its intercept is far from zero and so the current cannot soley be due to adsorption of product. A cyclic voltammogram of 2MP recorded at 20 Vs^{-1} is shown in Fig.18 .

At these faster scan rates, one would have expected that there would be little time for diffusion of the substance to the electrode and that adsorption would be the peak current controlling factor. However, in order for peak current to be adsorption controlled and therefore proportional to scan rate, adsorption has to be the predominant factor. This occurs at fast scan rates when there is little time for diffusion to occur and adsorption is immediate, or when the adsorption peak occurs at a different potential to that due to diffusing species, as is the case with strong adsorption. The adsorption in this case was neither strong nor immediate. The product adsorption was also time-dependent, because as the scan rate was decreased, there was an enhancement of the reduction peak current. 'Weak' adsorption of an oxidation product is characterised by higher reduction peak current than oxidation peak current [37]. Since there was a increase in reduction peak current relative to the oxidation peak current as the scan rate was decreased (Table IV),

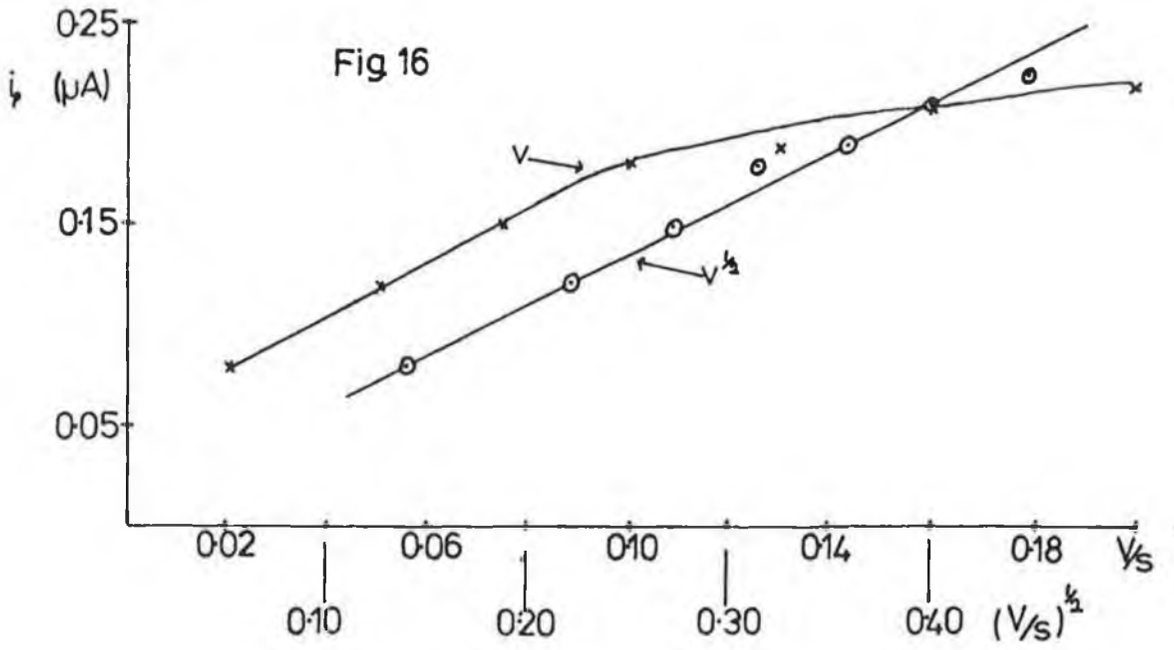

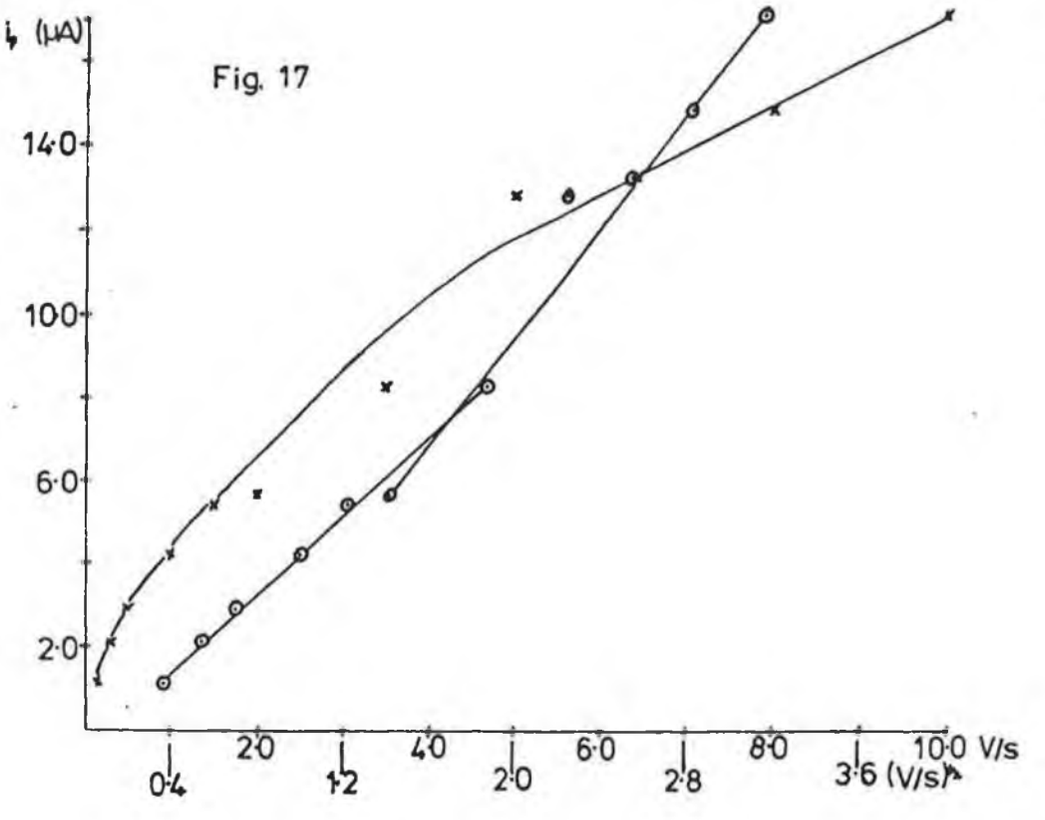

Plots of (a) peak current vs scan rate (×)
(b) peak current vs the square root of the scan rate (⊙)

Fig. 16 4×10^{-5}M 2MP over the range 0.02 V/s - 0.2 V/s.

Fig. 17 4×10^{-4}M 2MP over the range 0.2 V/s - 10 V/s.

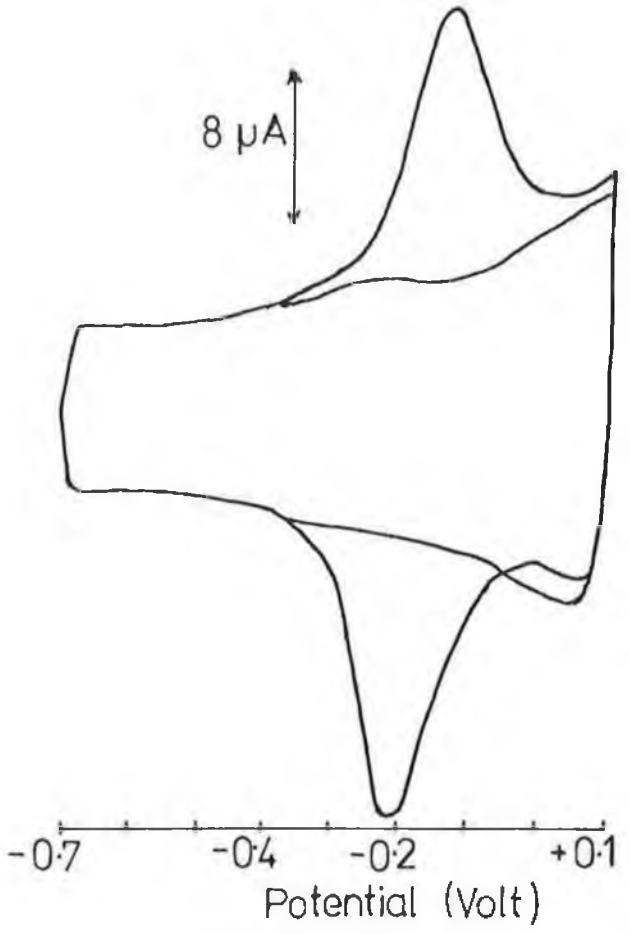

Fig. 18 Cyclic voltammogram of $1x10^{-4}$M 2MP, pH 5.0, scan rate 20 V/s.

Scan rate (Vs^{-1})	i_{pr}/i_{pa}
3.5	1.95
5.0	1.84
6.4	1.70
8.0	1.73
10.0	1.63

Table IV: Results showing that the ratio of reduction peak current to anodic peak current decreased with scan rate increase.

the 'weak' adsorption must also have been favoured by lower scan rates and adsorption in this case was therefore time dependent.

What can be deduced from the variation of scan rate is that diffusion seems to be the main controlling factor for the oxidation peak over the scan rate range of 20 mVs^{-1} to 10 Vs^{-1}, and that adsorption is also dependent on time for film formation.

3.1.3. Variation of Concentration

In measuring peaks obtained using CV a reproducible peak current is desired. So the 3^{rd} scan on each CV was taken because there was a slight increase in the oxidation peak current from the first to the third scan and the peak current then levelled off on further scanning, which was equivalent to recording the CVs when a steady state was reached [45].

Peak oxidation current varied linearly with concentration , from $1x10^{-5}M$ to $12x10^{-5}M$ concentration (Fig 19). The peak current then reached a limiting value, and another peak formed at more positive potentials. This levelling off of the peak height is interpreted as the completion of layer formation of product at the electrode surface, and the new peak corresponded to the commencement of the formation of a new layer (Fig. 20).

Oxidation peak current was limited by adsorption because it corresponds to the oxidation of dissolved 2MP diffusing to the electrode to form adsorbed mercurythiolate at the electrode surface. The oxidation of 2MP to form different film layers, which occurred as the concentration was increased, resulted in different peak

potentials, because the free energy of adsorption of the molecules in each film was not the same.

A shift in peak potential from -0.9 V to -0.6 V occurred when the concentration was increased from $5x10^{-5}M$ to $6x10^{-5}M$. This peak potential displacement may have been due to interaction between adsorbed molecules when the electrode was partially covered. This type of shift in peak potential occured for the adsorptive stripping analysis of folic acid at 40% coverage [46]. Therefore this peak potential shift was probably due to some interaction of the molecules in the film when it was being formed, which changed its free energy of adsorption.

At concentrations greater than $2x10^{-4}M$ the first and third scans on the same drop differ greatly with respect to their reduction peaks (Fig.'s 20 and 21). On the first scan, there was a sharp reduction peak characteristic of adsorption. These cathodic current spikes, as seen in Fig. 21, have been reported by several authors [5,14,15].

These 'spikes' are explained as being due to formation of a more compact structure of the adsorbed mercury salt. Stankovich and Bard [15] suggested that for cysteine, the tight packing may involve hydrogen bonding between the $-NH_2$ group on one molecule and the -COOH group of an adjacent molecule. However, as Birke and Mazorra [5] have pointed out, the same type of spike occurs in the CVs of other compounds, e.g. benzyl mercaptan, where hydrogen bonding could not occur. Muller [16] also stated that different molecular orientations occur for the adsorbed form of ferron and the more compact film which results, leads to an (anodic) adsorption spike.

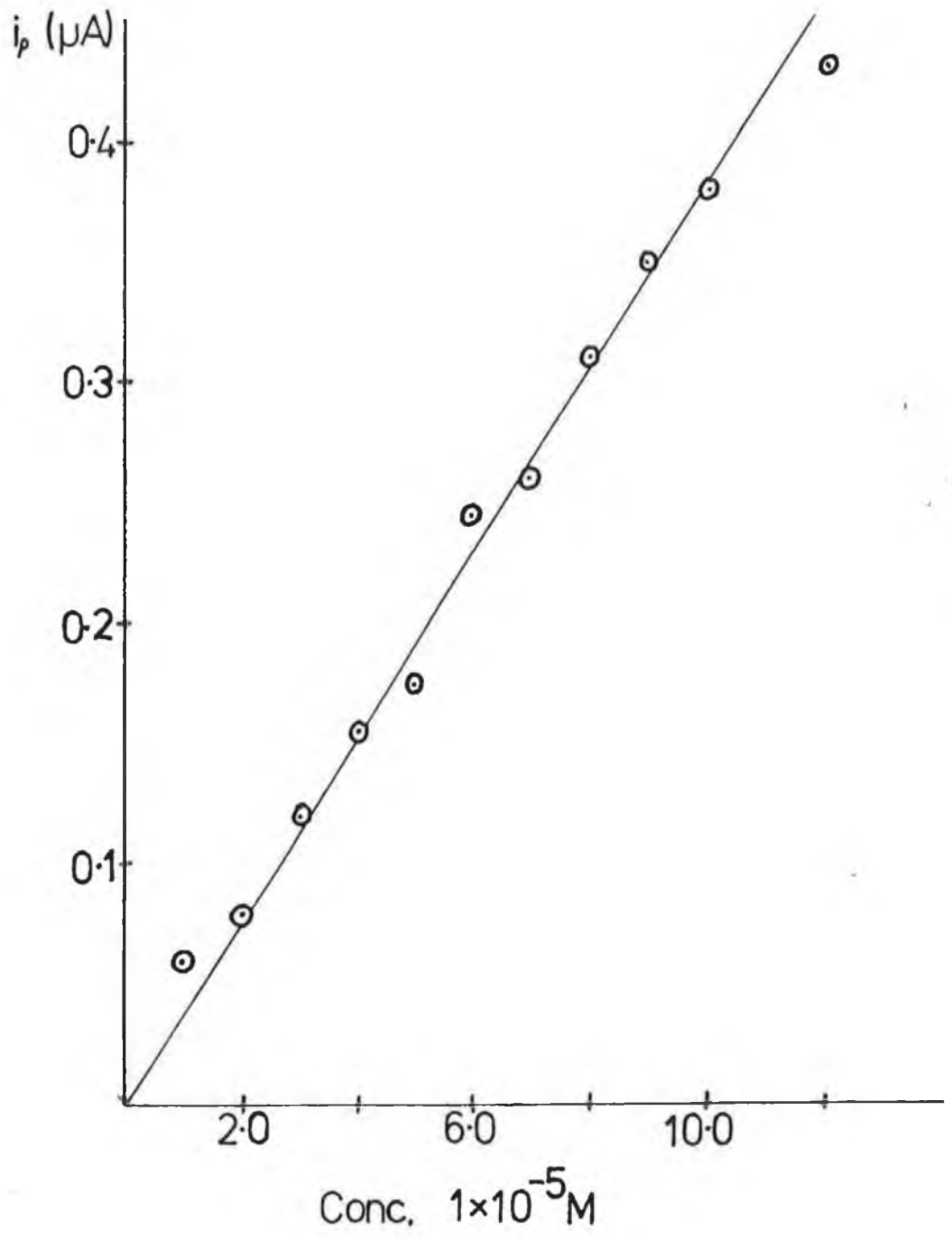

Fig. 19 Plot showing the linear dependence of peak current on 2MP concentration. CV scan rate was 100 mV/s.

Fig. 20

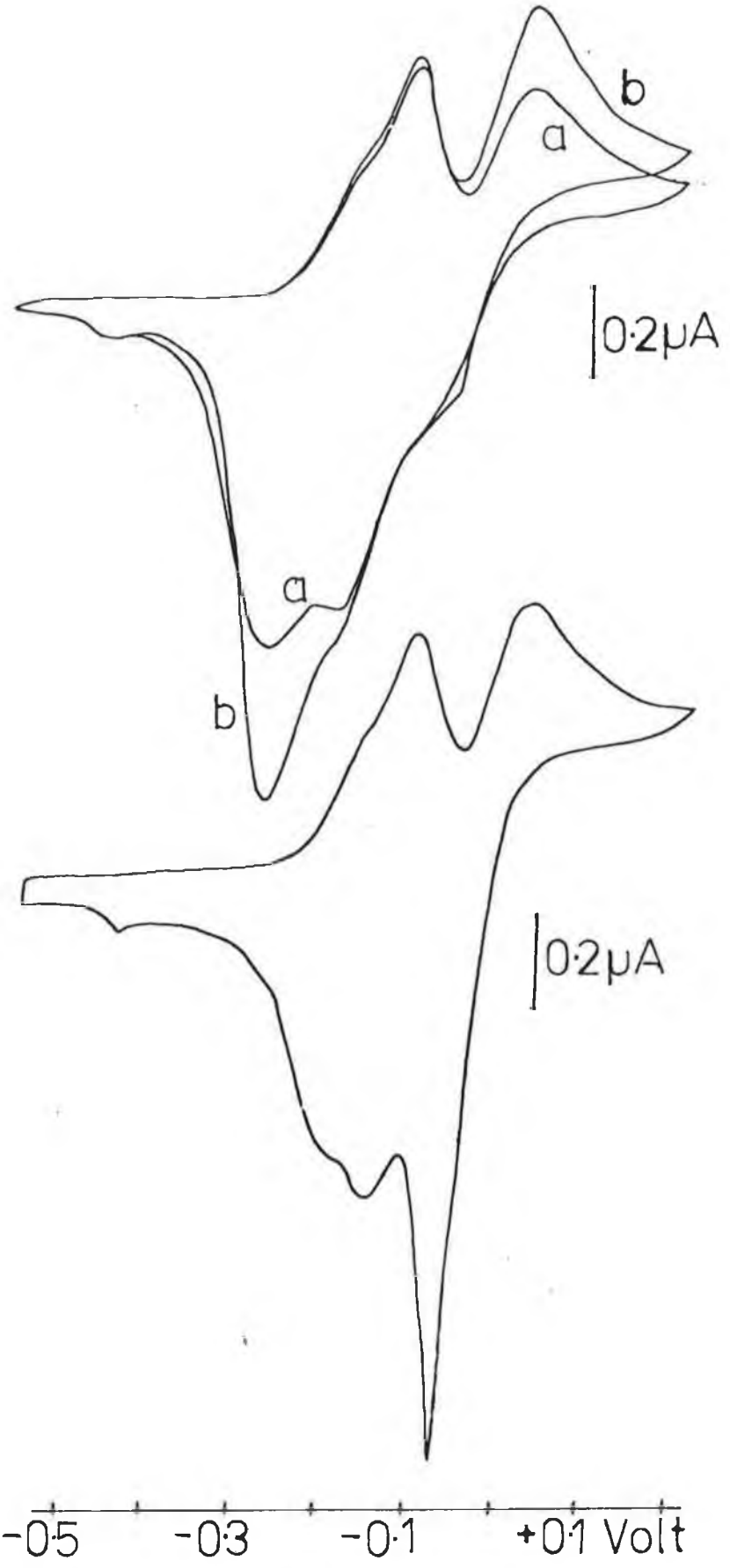

Fig. 21

Fig. 20 CV showing the adsorption limited oxidation peak @ -0.1 V The 3rd scan on the electrode was recorded, 2MP: (a) 2.0×10^{-4}M, (b) 2.5×10^{-4}M, scan rate 50 mV/s, pH 4.0

Fig. 21 Initial CV scan on the electrode was recorded of 2.5×10^{-4}M 2MP, pH 4.0, scan rate 50 mV/s.

So it would seem that there is agreement that the current spikes are due to compact film formation. The dissappearance of the spike by the third scan would indicate that the spike was dependent on the freshness of the drop surface. Under certain conditions, one can see the decay of the spike, and the resultant increase in the main reduction peak height with continuous scanning suggests that a change in morphology of the adsorbed film occurred.

3.1.4. Holding Potential

Cyclic voltammograms were recorded where the potential was held positive of the oxidation peak for different time intervals in order to further investigate the adsorption characteristics of the thiols, (Fig.22). The 2MP reduction peak shows a greater increase in peak height with holding time than the reduction peaks of the other compounds. It would appear, therefore, that more 2MP mercury salt was adsorbed at the surface, i.e. that its orientation towards the drop allows for a greater amount of salt to adsorb at the surface in a single layer compared to the other compounds. It may also be that there were stronger binding forces between 2MP and the mercury causing more of it to be adsorbed. After 45 s holding time, the current due to the reduction peak at more positive potential, did not increase further with longer hold times, indicating that a monolayer had been formed. However, on increasing the hold time further, another reduction peak was formed at a more negative potential and this peak current increased with longer hold times . The new peak was due to a new layer or a 3-dimensional multilayer of product being

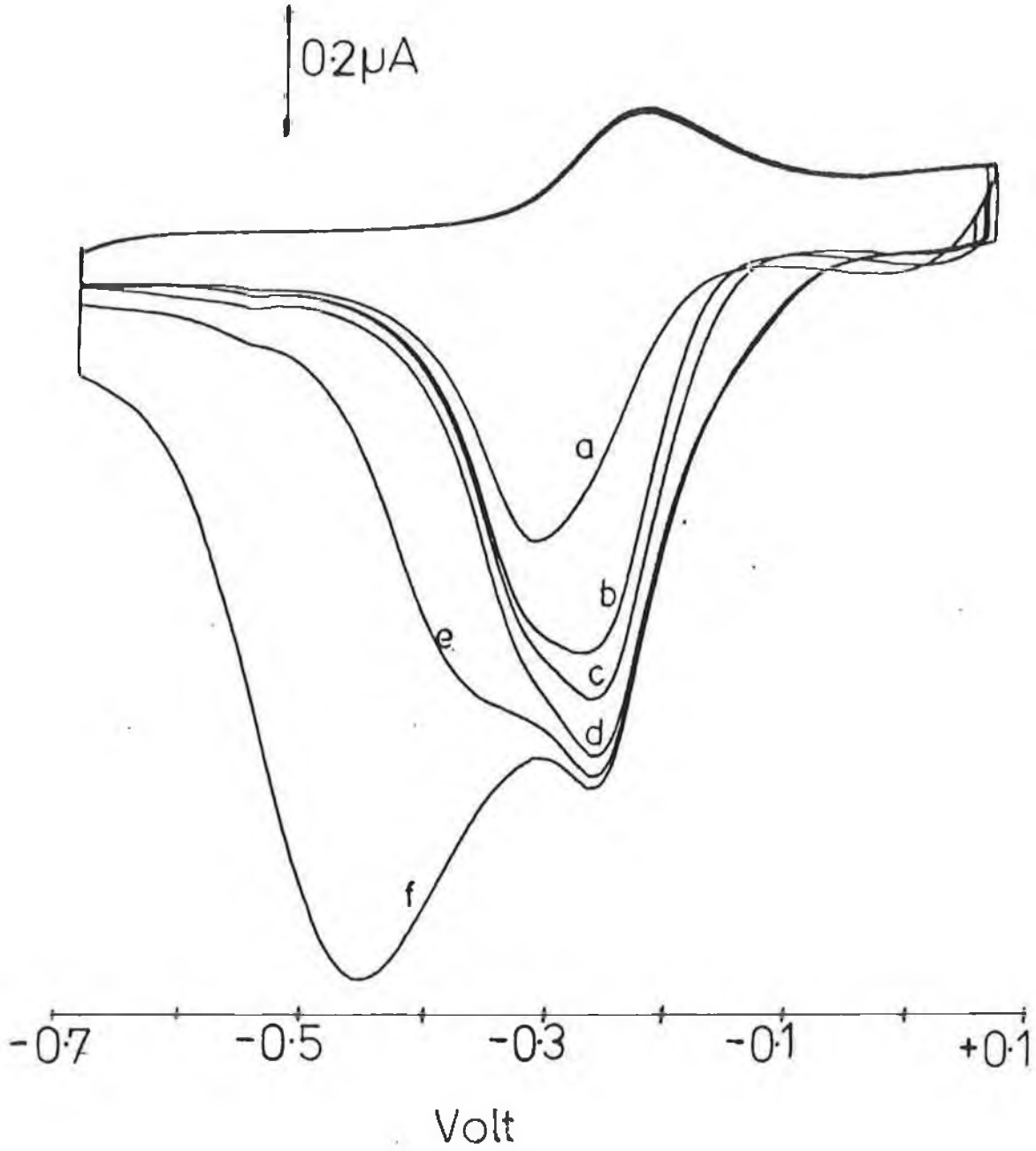

Fig. 22 CV of $4x10^{-5}$M 2MP pH 6.0, where the potential was held at +0.07 V for: (a) 0s, (b) 7s, (c) 10s, (d) 20s, (e) 45s, (f) 120s. Scan rate 100 mV/s

formed after the first layer was completed.

3.2. 2-Mercaptopyridine-N-oxide

3.2.1. Effect of pH

The peak potentials for 2MP-O were found to be pH dependent up to pH 4.0 which is approximately the pK_a value for 2MP-O. Above this pH, the E_p remains constant. The CV recorded at pH 4.0 had a redox couple at a more positive potential than the main redox couple. This redox couple was also seen at lower pH's (3.0 and 2.0) but with a reduced peak current, and it was not present in solution of pH 6.0 or greater. The enhanced size of the reduction peak of the redox couple would indicate that it was due to weak adsorption of product. However, it is not known why this feature predominates at pH 4.0, ie: near the pK_a value of 2MP-O.

3.2.2. Effect of Scan Rate and Concentration

A plot of peak current vs scan rate was found to be linear for the oxidation prepeak of a $3x10^{-4}M$ solution of 2MP-O (Fig.23), indicating an adsorption-controlled peak. It was not possible to plot current vs scan rate for the main peak because resolution between it and the prepeak decreased at faster scan rates. Qualitatively speaking, however, its peak height did not increase as much with scan rate as the prepeak, implying its square root dependence with scan

rate. The reduction peak potential varied with scan rate (0.1 V from 20 mVs^{-1}-200 mVs^{-1}) and this is indicative of reduction of a solid film on the drop surface [38].

Further evidence for the adsorption control of the prepeak was seen by varying the concentration of the 2MP-O (Fig.24). The oxidation prepeak current at -0.32 V ceased to increase after reaching a $2x10^{-4}M$ concentration limit, indicating adsorption control and probably the completion of a layer of film. The oxidation peak at -0.20 V was not limited by concentration and so is considered to have been due to the formation of a mercury thiolate multilayer at the electrode limited by the diffusion of 2MP-O to the electrode. The width of the reduction peak at half peak height was approximately 200 mV and this would seem to indicate that it was due to more than one peak. The broad reduction peak may be due to either (i) the reduction of both adsorbed and soluble mercuric thiolate salt, or (ii) the reduction of adsorbed film which is made up of layers at different adsorption energies. Both these possibilities would give rise to more than one peak, however since the energy difference between the different forms were so small, the resultant peaks appear as one wide peak.

Some cyclic voltammograms were recorded for 2MP-O at low concentrations ($2x10^{-5}M$) and slow scan rates (1-10 mVs^{-1}). It was felt that under these conditions, the CV behaviour would be less complicated. However, the CV behaviour proved to be even more complex due to the occurrence of an inverted peak on the scan in the oxidation direction (Fig. 25). 'Inverted' peaks are a characteristic of adsorption. They have been described as being due to tangential

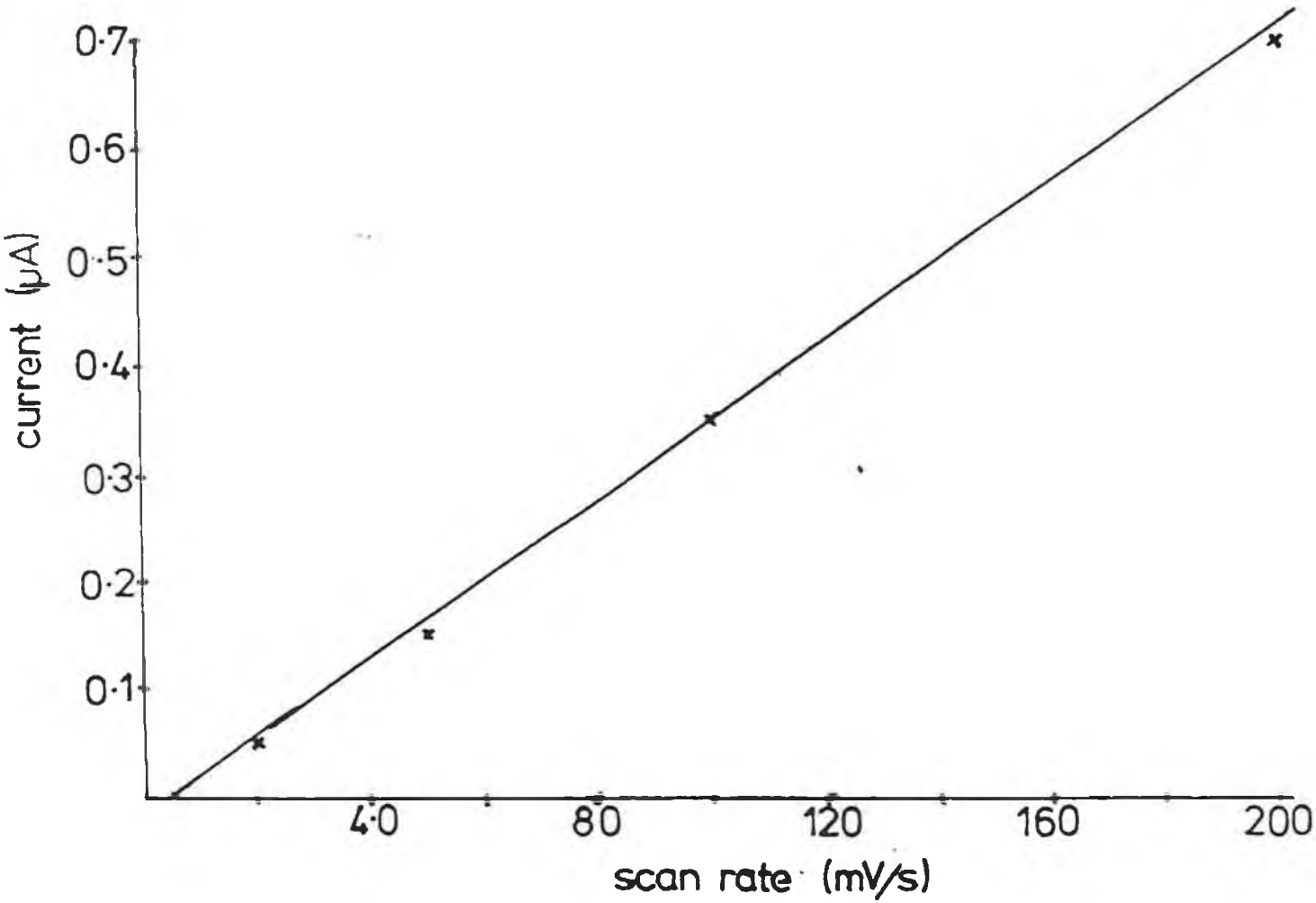

Fig. 23 Plot of peak current vs scan rate for the 2MP-O pre-oxidation peak, concentration 4×10^{-4}M.

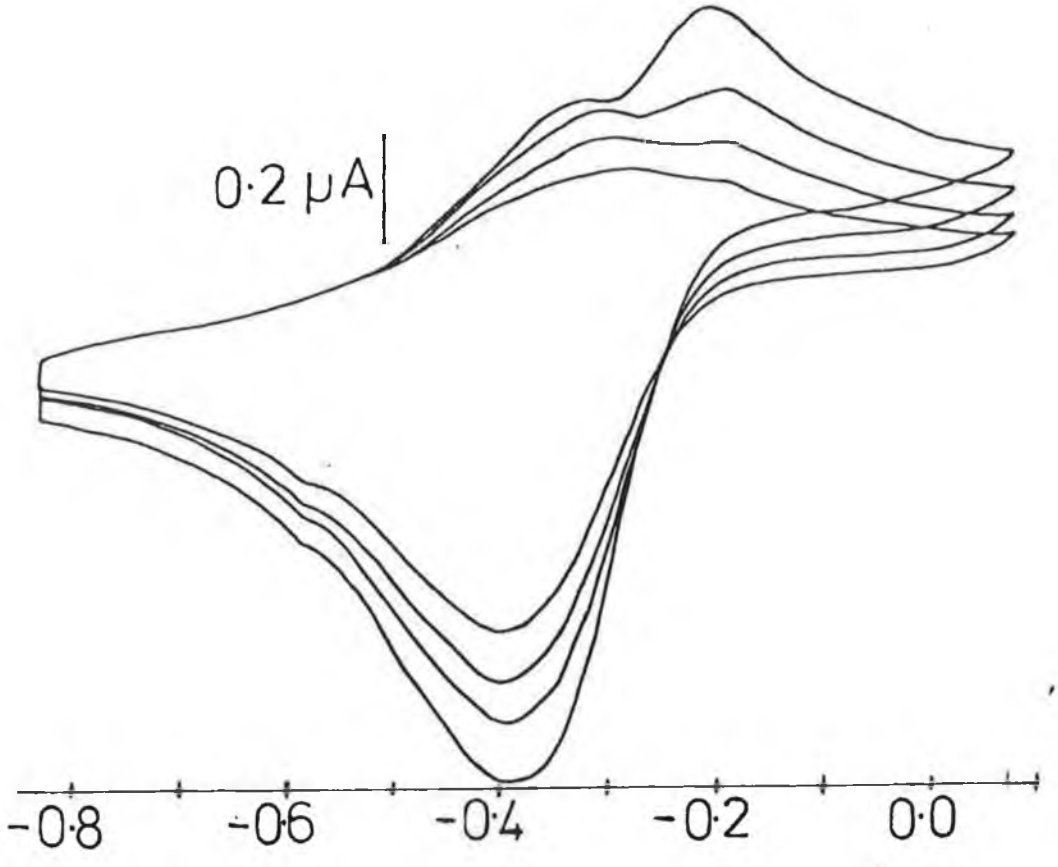

Fig. 24 Variation of concentration of 2MP-O; (a) 1.3×10^{-4}M (b) 1.6×10^{-4}M, (c) 2.0×10^{-4}M, (d) 2.5×10^{-4}M. Scan rate 100 mV/s, pH 6.9 .

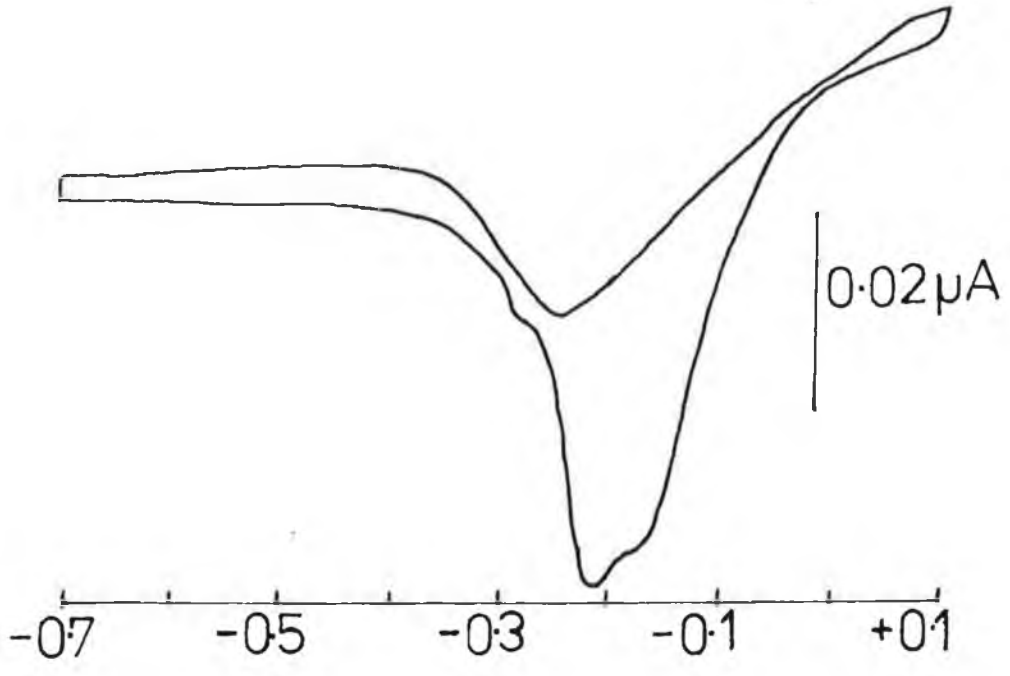

Fig. 25 CV of 1×10^{-5}M 2MP-O at 1 mV/s, pH 1.8.

movements of the mercury electrode surface [47] , which also results in maxima in DC polarography. Uneven adsorption of a compound onto the mercury drop results in differences in the surface tension of the drop. The resultant motion of the mercury along the drop surface stirs the solution so that more of the electroactive compound reaches the electrode and current maxima are formed. 'Inverted' CV peaks have been reported for other systems where mercury thiolate salts have been formed [45,13].

The inverted peak in this case would seem to be due to the reduction of adsorbed $Hg(RS)_2$, because of the similarity of the inverted peak potential and the reduction peak potential in the negative scan direction. The inverted peak is enhanced at lower concentrations because there is less competition from the oxidation of diffusing 2MP-O. It is not clear however, how $Hg(RS)_2$ was formed at such negative potentials. It is possible that the 2MP-O reacted chemically rather than electrochemically with the mercury forming this adsorbed $Hg(RS)_2$, which is reduced on the oxidation scan. Motion of the drops surface may have aided in bringing 2MP-O to the electrode surface where it could react. Florence [14] has reported the chemical reaction of thiols at low concentration with waste mercury in electrochemical cells.

3.2.3. Holding Potential

2-Mercaptopyridine-N-oxide also exhibits weak adsorption at most pH's, even for high concentrations and long hold times (Fig 26). The width and height of the major reduction peak increased as the

Fig. 26

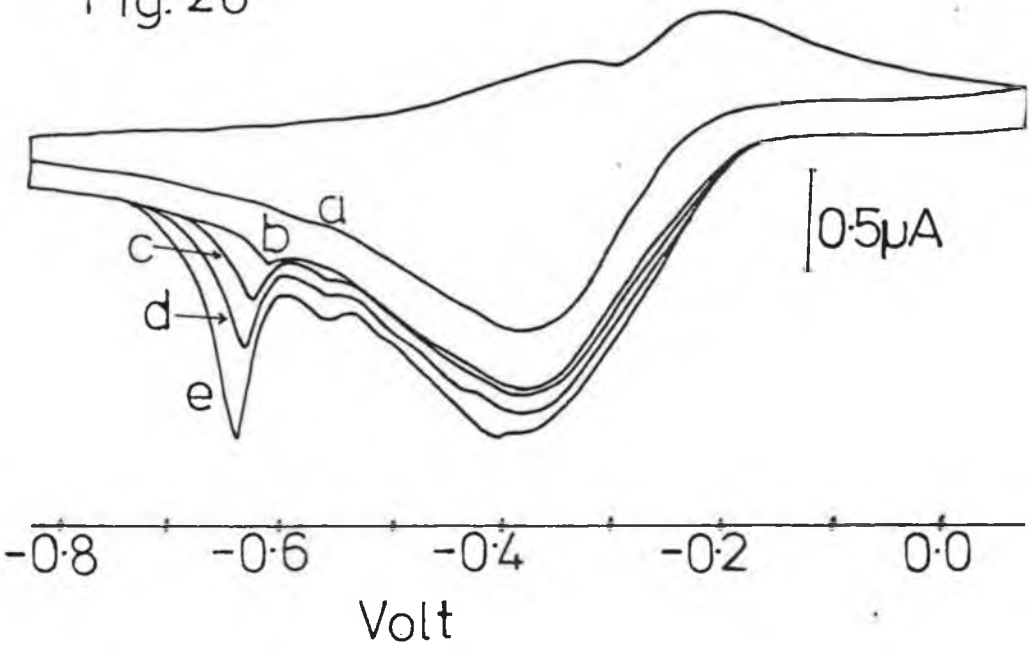

Fig. 26

Potential of $3x10^{-4}$M 2MP-O held @ +0.07 V for (a) 0s, (b) 1min, (c) 2.5min, (d) 4min, (e) 7min. pH=6.9

Fig.

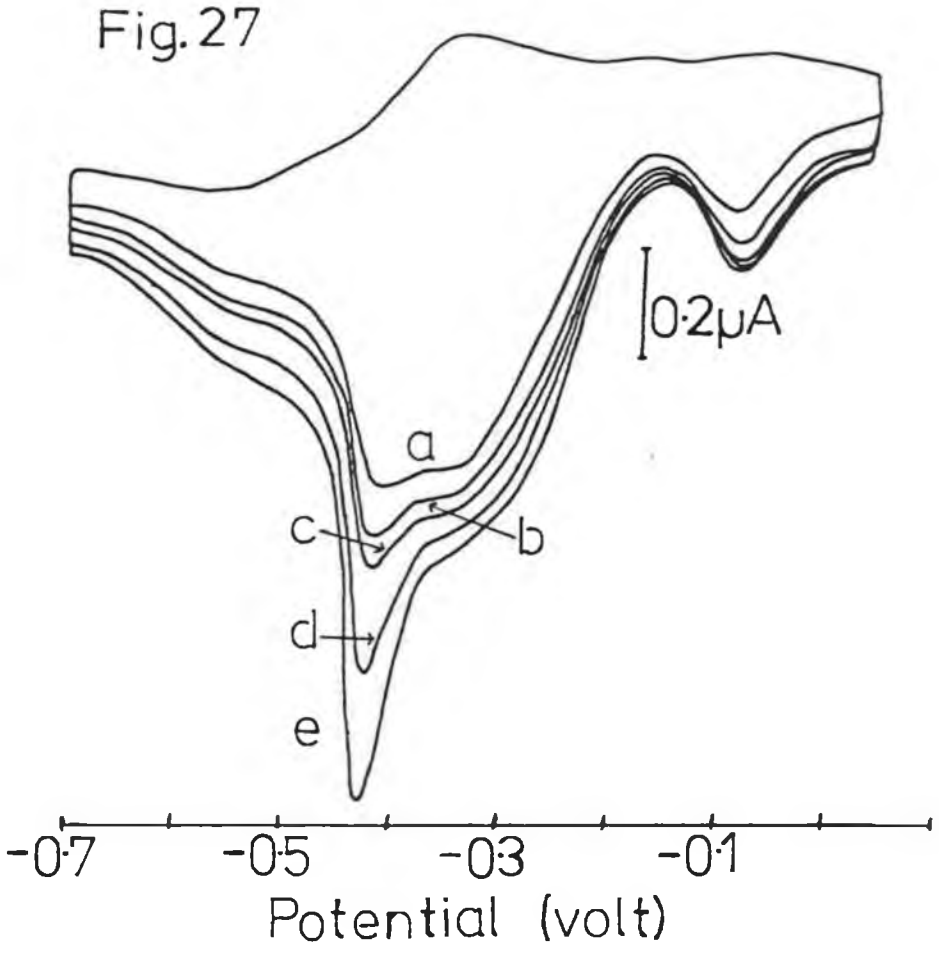

. 27 Potential of $1x10^{-4}$M 2MP-O, pH 4.0, held @ +0.05 V for (a) 0s, (b) 5s, (c) 10s, (d) 30s, (e) 60s.

potential was held for longer periods of time. However, the reduction peak height was not as large as that for 2MP, indicating that the adsorption of the 2MP-O mercury salt resulted in a less compact film than that of 2MP. A small sharp adsorption spike appears at more negative reduction potentials which is indicative of compact film formation.

At pH 4.0, 2MP-O exhibits greater adsorption than at other pH's. This can be seen in Figure 27, where a $1x10^{-4}$M 2MP-O solution resulted in a higher reduction current than a $3x10^{-4}$M solution at pH 6.9, (c.f. Fig.26). The reduction peak at -0.06 V is only present from pH 2.0 to 4.0 reaching its maximum height at pH 4.0 . This peak is clearly adsorption controlled, because of the enhanced reduction to oxidation peak current. It also reached a limiting peak current after 10 sec, while the current due to the reduction peak at -0.43 V increased with longer hold times.

3.3. 2-Mercaptopyrimidine and 2-Mercapto-4-methylpyrimidine.HCl

The effect of pH on the electrode reaction of 2MPr and 2MmPr was not investigated, since their pK_a values were known already, and changes in pH were not expected to cause any change on the electrode reaction, as seen from the DC polarograms recorded at different pH's. The CV behaviour of 2MPr and 2MmPr were almost identical, with only slight differences in peak potentials, showing how little the 4-methyl group affected the electrode reaction. At concentrations of about $2x10^{-4}$M, the prepeaks were not as well resolved from the

main peak compared with the pre- and postpeaks of 2MP, indicating that the adsorbed mercury thiolate films were not as strongly adsorbed. These pre-oxidation peaks gave rise to post-reduction peaks which were also badly resolved from the main reduction peak, but which could be seen more clearly when the potential was switched before the main oxidation peak. As with 2MP these pre-oxidation peaks and post-reduction peaks were due to the formation of different film layers. As the concentration was increased, the prepeak current leveled off indicating the completion of a layer. The main peak current continued to grow since it was due to the diffusion of the pyrimidine to the electrode surface, to form more mercury thiolate salt. The linear relationship between prepeak current and scan rate (Fig. 28), also suggests that the prepeak was adsorption controlled. At higher scan rates the peaks were badly resolved. The main peak current could not be measured accurately, because it was not known how much the prepeak current contributed to its current. However the main peak's current did not increase as much as the prepeak's current with faster scan rates, suggesting that it was dependent on the square root of scan rate and therefore diffusion-controlled. This is similar for each of the other compounds.

Another difference between the pyrimidines and 2MP was that a small redox couple was recorded for both pyrimidines at potentials positive of the main peak (Fig 29). This redox couple was symmetrical, especially at lower scan rates (20 mVs^{-1}), indicating that it was due to adsorption. This couple appeared at concentrations greater than $1x10^{-4}M$. However, it could also be seen for a $5x10^{-5}M$ concentration of 2MPr, when the potential was held at

-0.03 V for more than 5 seconds before recording the reduction scan. The peak reached its limiting current for a hold time of 30 sec. This limiting of its current with holding time confirmed its adsorption control. These type of sharp reduction peaks are said to be due to compact film formation [5,15,16]. When the potential for a $2.9x10^{-4}M$ solution of 2MmPr was held at +0.07 V, this spike dissappeared and some small similar reduction spikes were formed at more negative potentials than the main peak. This may be due to a change in structure of one compact film to form another compact film. For both compounds the reduction peak current did not increase as quickly with longer hold times as the reduction peak of 2MP. It is believed that the orientation of adsorbed 2MP mercury salt allows for its greater adsorption. It also forms a stronger adsorbed film on the electrode than any of the other compounds examined , indicated by the greater separation of prepeak and main peak. Like 2MP-O, the reduction peak of 2MPr broadened and grew in peak height, indicating the presence of more than one reduction peak. However, these peaks could not be resolved and may have been due to slightly different structures of adsorbed film, as well as reduction of solution species.

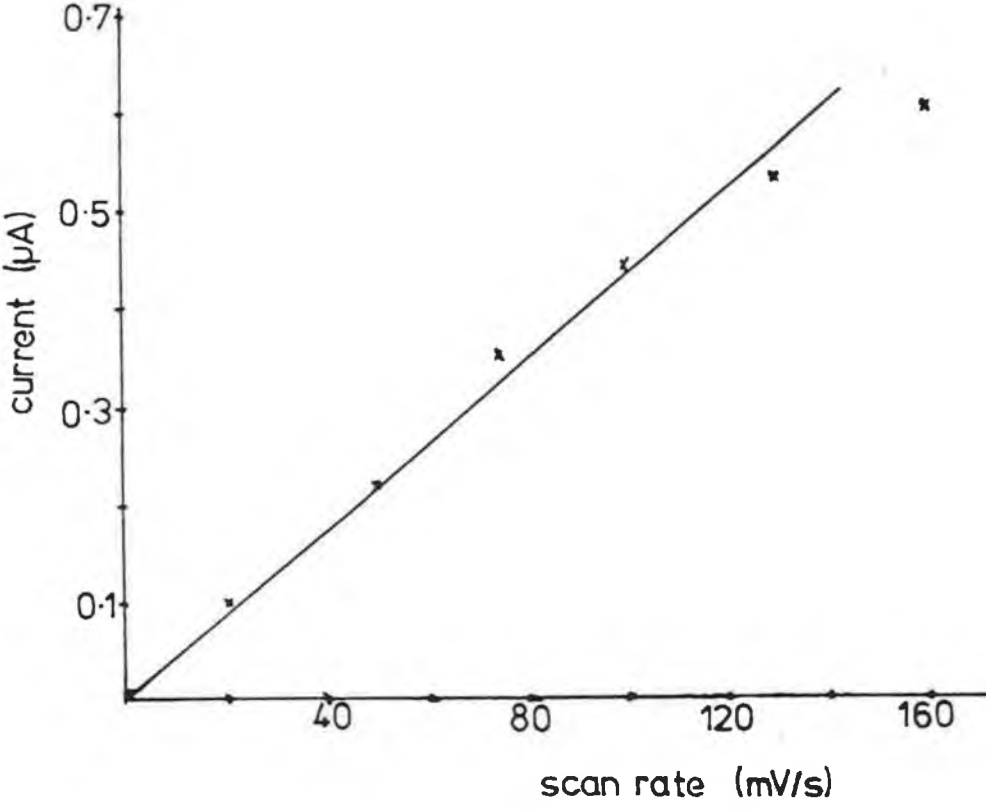

Fig. 28

Plot of peak current vs scan rate for the pre-oxidation 2MmPr peak, conc $3x10^{-4}$M.

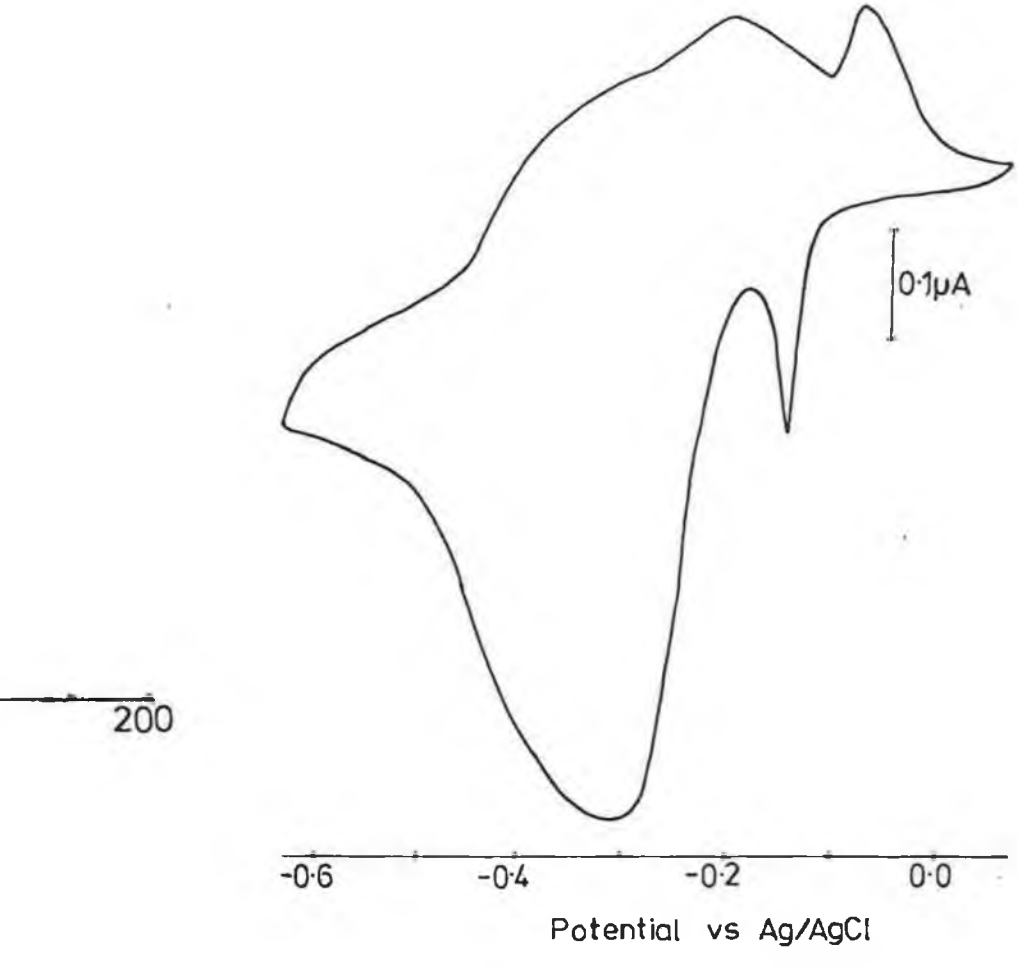

Fig. 29 CV of $3x10^{-4}$M 2MPr, 50 mV/s, pH 6.0.

4. Coulometry

A controlled potential coulometric experiment was carried out to verify that the reaction of mercaptans at a mercury electrode is a 1 electron, per molecule of mercury, reaction. It seemed possible that it could have been a two electron reaction, since the overall reaction equation given by several authors was

$$Hg^{2+} + 2RS^{-} \longleftrightarrow Hg(SR)_2$$

In this coulometric experiment, 10 ml of BR buffer pH 6.1 was electrolysed for a half an hour at +0.16 V vs SCE to determine a stable background charge. Then $5x10^{-5}$ moles of 2MP was added to the buffer and the charge due to its reaction at the mercury pool electrode was recorded. Electrolysis was stopped when the charge built-up had leveled off to the background level, i.e. after approximately 1 hour.

The expected charge for a one electron reaction is given by the number of moles of 2MP added to the cell, multiplied by Faraday's number. This was equal to $(5x10^{-7}M).(96487C)$, i.e. $4.824x10^{-2}$ coulombs.

Final charge	$4.055x10^{-2}C$
Background charge	$\underline{0.100x10^{-2}C}$
Total charge	$3.955x10^{-2}C$

No. of electrons $=4x10^{-2}/5x10^{-2} = 0.8 \simeq 1$

5. Chronocoulometry

Chonocoulometry was considered as a method of calculating the surface coverage of the mercuric salts of 2MP and 2MP-O. It was felt that a quantitative comparison of each compound's adsorption would lead to a more conclusive understanding of why greater i_p values were found for 2MP than 2MP-O. The design of an accurate chronocoulometric method proved too difficult. The examples of chronocoulometric experiments found in the literature dealt with reactant adsorption [39,48-51]. In this case it was intended to calculate the surface coverage of the reaction product. Therefore, when a pulse is applied, the initial potential E_i is in an electro-inactive region and the final potential E_f results in the formation of the adsorbed layer. A plot of charge versus the square root of time would not result in a straight line, with an intercept which corresponds to the charge due to the double layer charging and removal of film from the electrode, because adsorbed film is not being removed from the electrode.

It may however, be possible to apply the initial potential E_i at a value where the mercuric salt is formed and adsorbed onto the electrode, and at the final potential E_f the salt would be stripped off the electrode. In this case there would be no term due to the diffusion of $Hg(SR)_2$ to the electrode, because its bulk concentration would be zero.

It was noted by Anson that the double layer charge Q_{dl} should be measured by the 'drop extrusion' which Anson has described [39].

He reported that it was absolutely essential to correct for Q_{dl} by 'drop extrusion' for the chronocoulometric anodic oxidation of mercury in the presence of thiocyanate ion. The anodic oxidation of Hg in the presence of mercaptans is similar to the oxidation of thiocyanate. Attempts were made to measure Q_{dl} for a 2MP solution. However, results were not reproducible due to the continuous build up of charge when the potential was set at relatively positive values where the mercuric salt was adsorbed onto the electrode.

The quantity of adsorption of these mercuric thiolate salts is time dependent, as is seen from the CV 'potential holding' experiments. Therefore it would be necessary to set the potential at E_i for a certain length of time before applying a pulse. This would be similar to a fast scan cathodic stripping voltammogram, except that charge instead of current is being measured.

6. Reaction Mechanism

The mechanism of reaction of mercaptans at a mercury electrode has been reported by many authors [3,5,6,9-11,14,15,18]. It involves the catalytic oxidation of mercury in the presence of the mercaptan, followed by the formation of a mercury thiolate salt, which is adsorbed at the mercury electrode. It is widely believed that the reaction is a one electron, one proton process, according to mechanism 1.

Mechanism 1

$$Hg - e^- \rightleftharpoons Hg^+$$

$$RSH + Hg^+ \rightleftharpoons HgRS + H^+$$

This mechanism has the character attributed to a thiol anodic wave, even though the compounds studied exist mainly in their thione tautomeric form. The mechanism proposed for thiones such as thiourea (TU),(not capable of tautomerisation to thiols), is a two electron process as shown in mechanism 2

Mechanism 2

$$Hg \rightleftharpoons Hg^{2+} + 2e^-$$

$$Hg^{2+} + 2[TU] \rightleftharpoons Hg[TU]_2^{2+}$$

This two electron process written for the mercaptans studied here, would occur according to mechanism 3.

Mechanism 3

$$Hg \rightleftharpoons Hg^{2+} + 2e^-$$

$$Hg^{2+} + 2RSH \rightleftharpoons Hg(RS)_2 + 2H^+$$

The product in this case is a mercury (II) complex.

However, Birke and Mazorra [5] report that the one electron, one proton reaction forming the HgRS salt is probably followed by a disproportionation reaction

$$2HgSR \rightleftharpoons Hg + Hg(SR)_2$$

They say that the HgSR complex is soluble, whereas the $Hg(SR)_2$ complex is insoluble and adsorbed at the electrode surface. Krivis and Gazda [3] isolated and analysed the electrolysis product of 2MP-O and established its formula as the mercuric dimercaptide $Hg(SR)_2$. They also stated that compounds of the form HgSR are unstable in aqueous solution and decompose to $Hg(SR)_2$ and Hg. The one electron per molecule reaction they say, is supported by their controlled-potential electrolysis experiments. However, they do not mention whether it is one electron per molecule of 2MP or Hg. The controlled potential electrolysis experiment which was carried out here in the study of 2MP, showed that one electron per molecule of RSH was transferred in the electrode reaction . This is consistent with the mechanisms 1 and 3 shown above.

The slope of the $E_{1/2}$ vs pH curves (Fig.12) approximated to 0.059 V, which indicated that an equal number of protons and

electrons were involved in the electrode reaction. In investigating the reversibility of the mercaptan's electrode reaction, plots of E_{DME} vs $\ln[i/(i_d-i)]$ were drawn. This equation is deduced from the Nernst equation, assuming that mechanism (1) occurs, (see Appendix). It also follows that the slopes of these plots should equal RT/F for a reversible reaction and that $E_{1/2}$ is independant of the mercaptan concentration. If the reaction followed mechanism (3), (or if the product of mechanism 1 was insoluble), then a plot of E_{DME} vs $\ln(i-i_d)$ would be linear with a slope of RT/F , and $E_{1/2}$ would vary linearly with $\ln(1/[RS])$.

However , it has been suggested by Birke and Mazorra that the actual mercury (I) species may be the condensed ion Hg_2^{2+} and not Hg^+, for which there is little evidence in solution. If this is so, the mechanism would be:

Mechanism 4

$$2Hg \rightleftharpoons (Hg_2)^{2+} + 2e^-$$

$$(Hg_2)^{2+} + 2RSH \rightleftharpoons Hg_2(SR)_2 + 2H^+$$

followed by disproportionation

$$Hg_2(SR)_2 \rightleftharpoons Hg(SR)_2 + Hg$$

The dependence of potential on current, derived from the Nernst equation, is given by equation 16

$$E_{DME} = E^o + RT/2F\ln[-i/(i-i_d)^2].k \quad \ldots\ldots \quad 16$$

and the half wave potential varies with the log of the mercaptan concentration, as shown in equation 17;

$$E_{1/2} = E^{o} + RT/2F.\ln(k'/[RS]) \quad \ldots\ldots 17$$

where k and k' are constants.

The plots of E_{DME} vs $\ln(i/i_d - i)$ for each compound are linear, with slopes which approximate a reversible 1 electron mechanism, (Table III)

A plot of E_{DME} vs $\ln(i - i_d)$, which corresponds to mechanism (3), was constructed for 2MP at pH 6.0 and found to be curved. Its correlation coefficient equalled 0.9839. According to Bond [35], such a logarithmic plot which results in a curve may indicate a quasireversible reaction. However its limiting slope should be RT/F (ie: 25.7 mV), which was not the case for the above plot, where the limiting slope was 34.0 mV. It is therefore felt that mechanism (3) can be discounted as a possible mechanism. This can also be taken as an indication that the product of mechanism 1 is soluble, otherwise the E_{DME} vs $\ln(i - i_d)$ plot would be linear.

A plot of E_{DME} vs $\ln[-i/(i - i_d)^2]$ for 2MP was linear with a correlation coefficient of 0.9967. Its slope was equal to 18.9 mV, which is greater than 12.8 mV, (the slope of a two electron reversible reaction), and less than 25.7 mV, (the slope of a 1 electron reversible reaction). The linearity of this plot seems to indicate that mechanism (4) is possible. However, its slope may only be described as that due to a two electron irreversible reaction,

with a transfer coefficient α equal to 0.68.

The variation of E_p with concentration was also examined for 2MP over the concentration range $1\text{-}13\text{x}10^{-5}$M. There are large shifts in E_p at certain concentrations above $13\text{x}10^{-5}$M, however, these have been described previously in the CV study as being due to changes in the nature of the adsorbed film. Over the concentration range $3\text{-}13\text{x}10^{-5}$M there is little noticable shift in E_p, and so it would seem that mechanism (1) prevails. However, on calculating the expected E_p shift due to mechanism 4, it was found that only a 0.02 V shift was expected. This would seem to agree with the results for peak potential vs concentration reported in Table V , but the overall change of E_p is considered too small and difficult to measure accurately enough, to say for definite whether mechanism 1 or 4 prevails.

The potential/current relationships for each mechanism are derived in the appendix, having referred to both Bond [35] and Crow [55].

Table V: Variation of E_p with 2MP concentration.

Conc.x10^{-5}M	E_p Volt
1	-0.480
2	-0.490
3	-0.495
4	-0.510
5	-0.510
7	-0.525
8	-0.520
9	-0.520
10	-0.520
13	-0.515

7. Development of an Analytical Method

7.1 Differential Pulse Polarography

Calibration curves of current vs concentration were constructed for each compound using DPP. Calibration curves can be used to tell whether the electrode reaction is diffusion or adsorption controlled. A linear calibration curve is indicative of diffusion control. Adsorption controlled reactions can be recognised by the independence of the peak current with concentration after a certain concentration has been reached, which corresponds to a layer of product having been formed on the electrode surface.

The limit of detection (LOD) of the method was limited by the detection of impurities in the background, and for each compound concentrations of just under $1x10^{-5}M$ could be detected.

In the concentration range $1-10x10^{-5}M$ the DPP current due to each compound was roughly the same, each showing a linear dependence with concentration over most of the range (Fig.30a). The change which occured with further increase in concentration is shown in Figure 30b. Above concentrations of $1x10^{-4}M$ the slope of the current vs concentration curve due to 2MP was larger than that due to the other compounds. The reason why 2MP gives rise to a larger peak current than the other compounds at an equal concentration is not fully understood. It is felt, however, that it may be due to the more uniform orientation of the adsorbed 2MP mercuric salt than the electrode reaction products of the other three compounds studied. This would allow more 2MP mercuric salt to be adsorbed in a single

layer, which would give rise to a single peak. On examining the peak width at half the peak height ($W_{1/2}$), it was discovered that the $W_{1/2}$ value for 2MP was less than those due to the other compounds. For example, at $1x10^{-4}M$, $W_{1/2}$ for 2MP = 100 mV, while the $W_{1/2}$ values for the other three compounds were approximately 130 mV. The $W_{1/2}$ value for 2MP approximately equals 90 mV, the theoretical value for a reversible 1-electron reaction. The larger values of $W_{1/2}$ for the other mercaptans indicates that their DPP peaks were due to the occurence of more than one peak, which were not resolved. As seen from the CV study , adsorbed films of slightly different morphology can give rise to peaks at slightly different potentials, due to their differing free energy of adsorption. The overall charge transfered in the electrode reaction of equal quantities of each compound was probably the same. However, the more uniform adsorption of 2MP electrode reaction product results in a larger peak current.

There was a shift in the E_p values for 2MP ($1.4-1.6x10^{-4}M$ from -0.09 to -0.19 V at pH 6.8) which was followed by the formation of a second more positive peak at +0.07 V for concentrations above $3x10^{-4}M$. The initial peak current reached a limiting value and decreased with further increase in concentration (Fig.31). The levelling off in the peak current with increase in concentration corresponds to the completion of a layer being formed at the electrode surface. However, the decay of this peak's current on further increase in concentration indicates that there was a greater contribution to the diffusion controlled oxidation current at higher bulk concentrations of 2MP. The new peak increased linearly with concentration. The separation in the peak potentials of these two

Fig.
30a

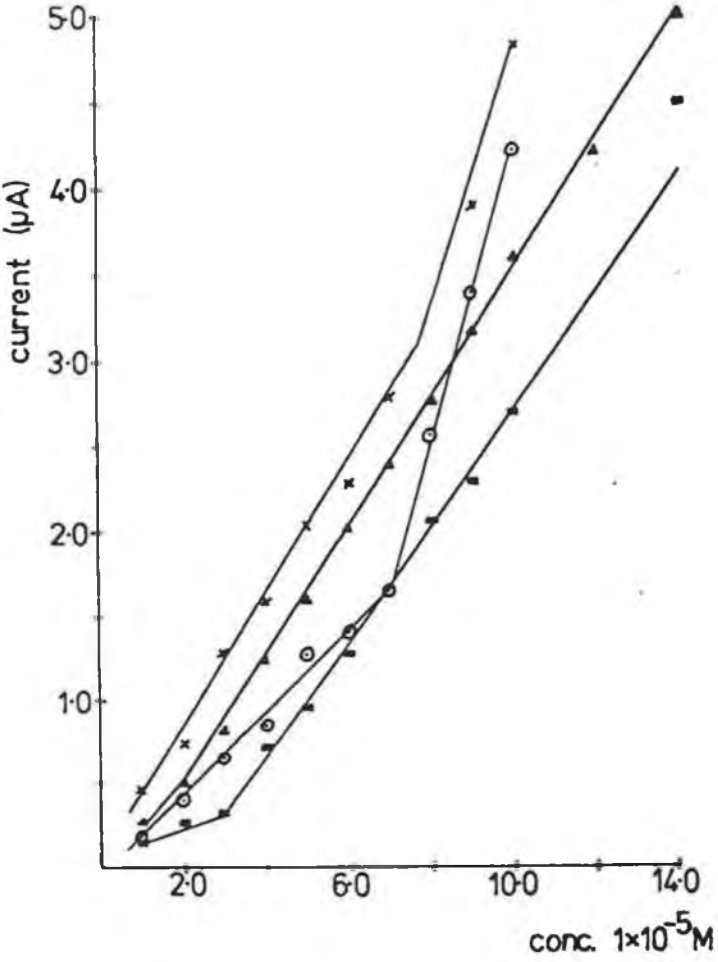

Fig. 30a and 30b

DPP calibration curves of each mercaptan; 2MP (⊙), 2MP-O (×), 2MmPr (■), 2MPr (▲).

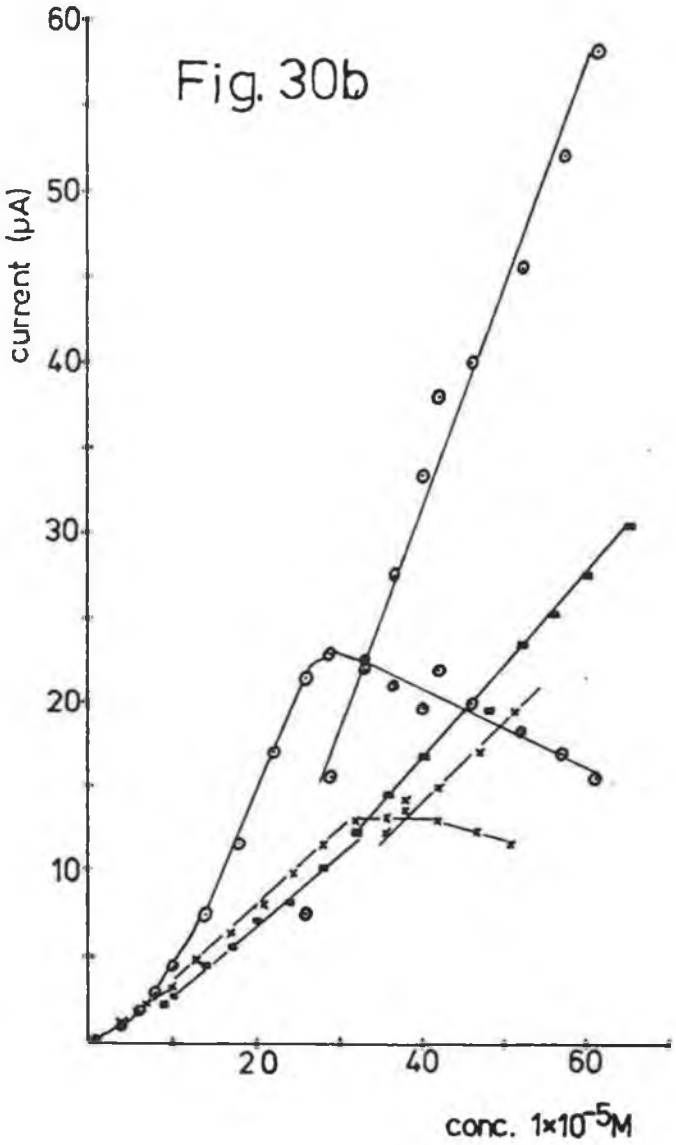
Fig. 30b
current (μA)
60
50
40
30
20
10
20
40
60
conc. 1×10⁻⁵M

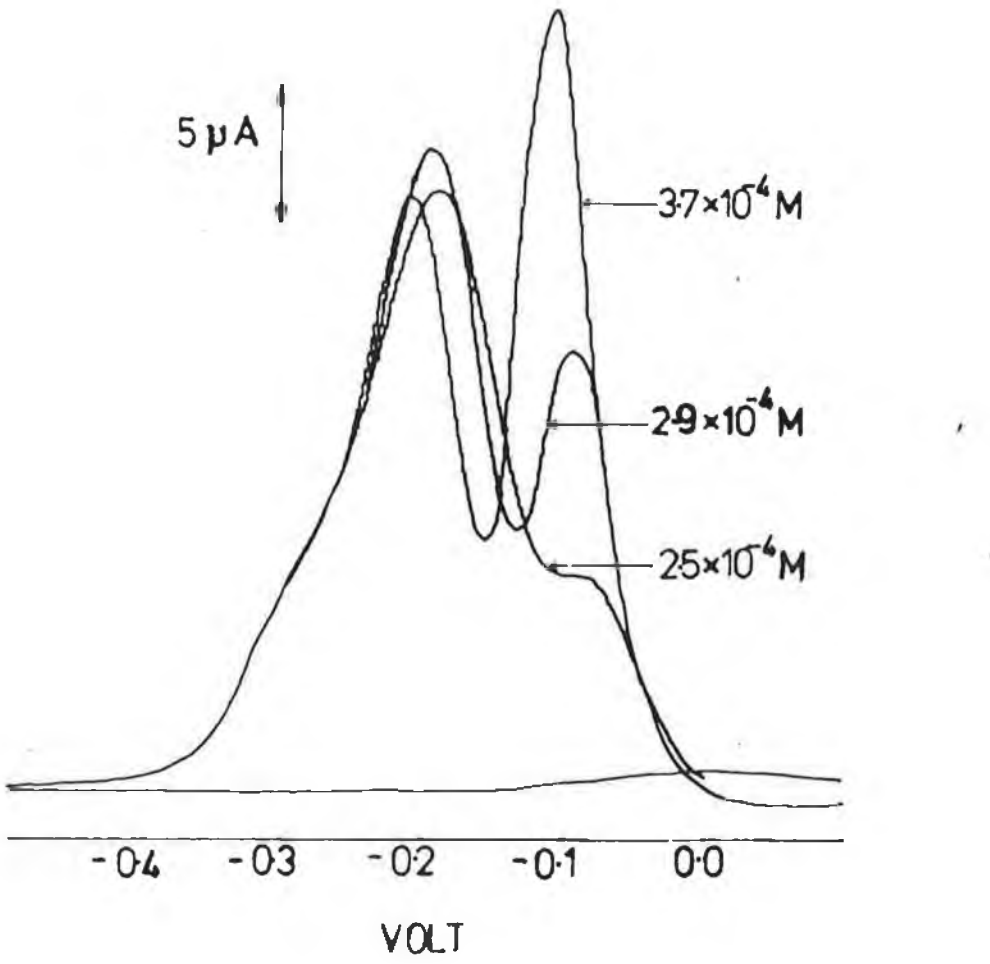

Fig. 31 Differential Pulse polarograms of 2-mercaptopyridine.

peaks is indicative of the difference in the free energy of adsorption of the different layers. The separation of the pre and main peak potentials was larger in the case of the two mercapto-pyridines studied than for the two mercaptopyrimidines. This corresponds to the 'prepeak separation' which occurred in the CV study. The greater the separation of the prepeak from the main diffusion controlled peak, the stronger the adsorption. The more positive peak was then assumed to be due to multilayer formation.

There was a similar splitting of peaks for 2MP-O. However, for 2MmPr there was a slight shift in slope of the calibration curve at $2.5x10^{-4}M$, which corresponded to a shift in peak potential at this concentration. The reason for this was, that the current due to the peak at -0.35 V, levelled off as the 2MmPr concentration was increased beyond $2.5x10^{-4}M$. A second peak was subsequently formed at a potential of -0.28 V, and this peak's current increased linearly with concentrations greater than $2.5x10^{-4}M$. However these two peaks were not completely resolved due to the proximity of their peak potentials. The formation of this second peak as the concentration was increased beyond $2x10^{-4}M$ yet again indicated multilayer formation.

7.2 Differential Pulse Cathodic Stripping Voltammetry

DPCSV is the most sensitive of the techniques used here for the analysis of mercaptans. It has also been used by other authors in the analysis of similar mercaptans [5,14,52,53], and other organic compounds of biological interest [19,21-26]. It involves holding the

electrode at a potential, where mercury thiolate is formed on the electrode. The solution is stirred while the electrode is held at this potential for a chosen length of time during which, there is a continuous accumulation of species at the electrode surface. When the accumulation time is completed, stirring is stopped and the mixture is allowed equilibrate for about 30 seconds. The potential is then swept cathodically and the film is 'stripped' off the electrode i.e. the film is reduced. The measured current is due to this reduction reaction, but the peak current height depends on the amount of film adsorbed onto the electrode.

The electrochemical reaction for the compounds studied is $Hg(SR)_2 \rightleftharpoons Hg^{2+} + 2RS^-$. The peak potential of the CSV wave is given by $E_p = (RT/2F).\ln[Hg^{2+}]$. Using the acid association constant $K_a = [RSH]/[H^+].[RS^-]$ and the solubility product $K_s = [Hg^{2+}].[RS^-]^2$, the equation for the peak potential can be written as:

$$E_p = E^o + 0.030(\log K_s + 2\log K - 2pH - 2\log[RS^-]) \quad ...18$$

The main feature of this equation is that the peak potential should become more negative with increasing pH.

Florence [14] states that the lower concentration limit for an anion $[RS^-]_{min}$ has been shown to be approximately given by $2(K_s)^{1/2}$. So the LOD for mercuric sulphide $[HS^-]$ at pH 9.2 should be equal to $10^{-22}M$. However, for $[HS^-]$ concentrations below $7x10^{-8}M$, no CSV wave was found. He explains the high LOD as being due to the presence of sulphide-binding heavy metals at

concentrations of 10^{-8}M - 10^{-7}M in the borate buffer used. Similarly an LOD of $1x10^{-7}$M was attained for DPCSV of the mercaptans studied here. This may also be explained to some extent, by the presence of sulphur-binding heavy metals in the buffer. However, interference resulting from the detection of some of these metal impurities in the buffer was another factor in raising the detection limit of these mercaptans.

Calibration curves were constructed for each of the compounds over a concentration range of $1-17x10^{-7}$M (Fig. 32). The current due to 2MP was greater than that due to the other three mercaptans. This is yet again due to the 2MP mercuric salt having formed a more uniform film, which was more strongly adsorbed onto the mercury drop than the mercuric salts of the other three mercaptans. On examining the peak widths at half peak height ($W_{1/2}$), it was discovered that the $W_{1/2}$ value for 2MP was less than the $W_{1/2}$'s of the other three compounds. For example, at a concentration of $6x10^{-7}$M, $W_{1/2}$ for 2MP was 115 mV, while for the other three mercaptans $W_{1/2}$ was approximately 140 mV. The peaks due to 2MP were almost symmetrical and their E_p values varied little with concentration. On the other hand, the other mercaptans' peaks often appeared like two unresolved peaks and their E_p values also shifted a few millivolts anodically at certain concentrations. It would seem therefore that the overall charge transferred during the reaction of each compounds at the electrode was probably equal, and that a more uniform 2MP mercuric salt results in the larger peak currents.

In order to optimize the DPCSV conditions, the deposition potential was varied for 2MP and 2MmPr. A deposition potential of +0.07 V resulted in the largest peak current (Table IV). The calibration curves for each compound were linear over the concentration range 1-6x10^{-7}M. At concentrations above 7x10^{-7}M the peak current levelled off. This limiting of DPCSV current has been reported by other authors. Florence [14] reported that it was apparently due to the fact that only the layer immediately adjacent to the mercury suface is reducible, even though multilayer formation can occur during deposition. He calculated the the limiting CSV current to be 50 $\mu C/cm^2$ for mercuric cysteinate, which corresponded to values for monolayer formation given by Stankovich and Bard [15]. Blanco et al. [46] reported that the folic acid stripping peak ceases to grow, becoming broader and distorted at a surface coverage close to 80%. In the present study, the current was either limited by layer completion, or by the kinetics of the film formation, i.e. that no more film could have been formed in that deposition time regardless of the bulk concentration.

The deposition time was varied for a 1x10^{-6}M concentration of 2MP using linear sweep CSV. The peak current increased with deposition time (t_{dep}), until t_{dep}=300sec, after which the peak current reached a limiting value. It is therefore probable that layer formation has occured after 300 sec deposition time for a bulk concentration of 1x10^{-6}M. According to the calibration curves, peak current also levelled off for concentrations above 1x10^{-6}M. It would also seem reasonable to conclude that the limiting of the peak current in DPCSV calibration curves, where t_{dep}=180 sec, was also due to completion of a layer of film on the drop surface.

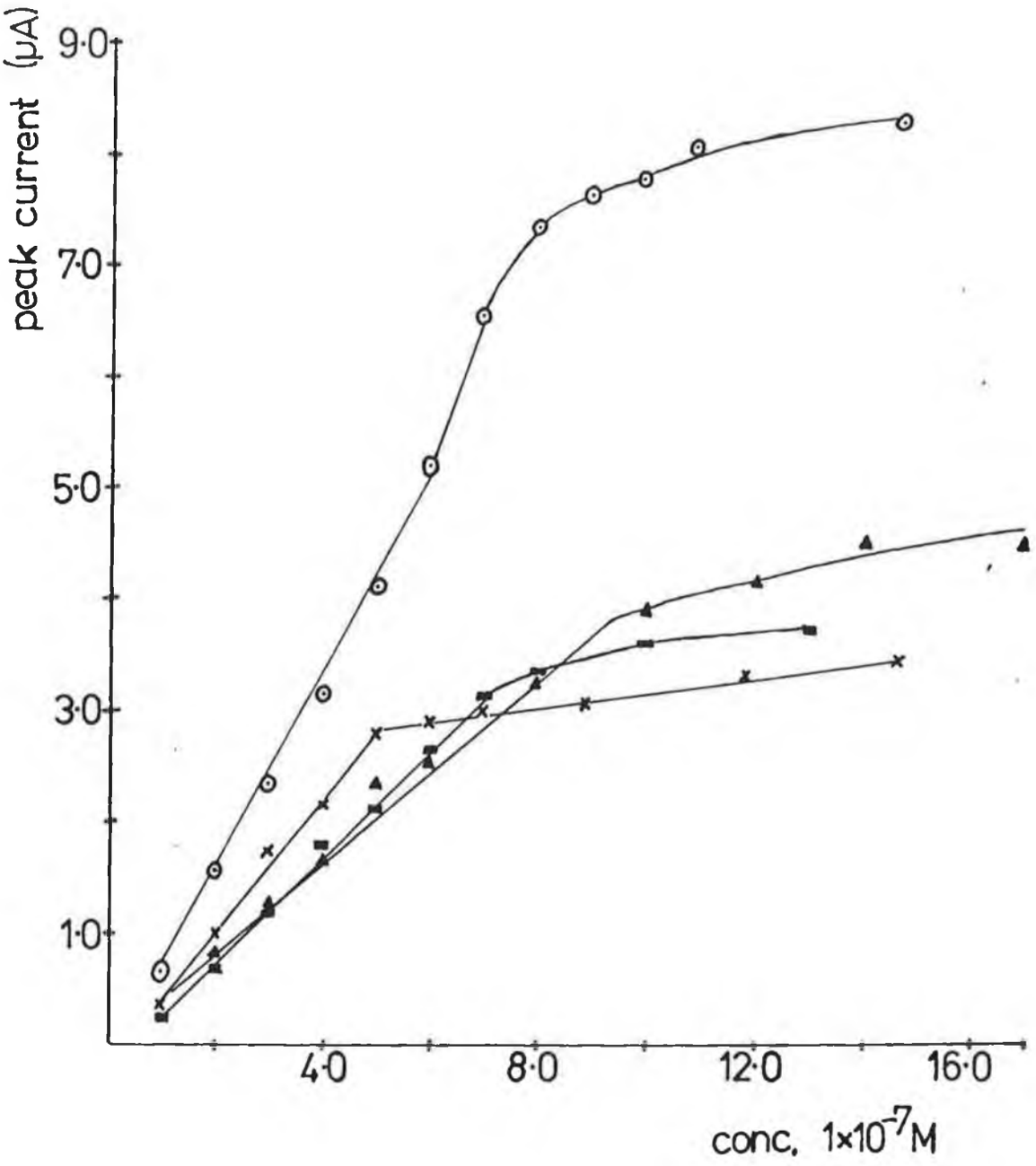

Fig. 32 DPCSV calibration curves determined for each mercaptan. Deposition potential 0.07 V, deposition time 180 s, scan rate 5 mV/s. 2MP (⊙), 2MP-O (×), 2MmPr (■), 2MPr (▲).

Table VI

Current resulting from the variation of deposition potential, E_{dep}, $1x10^{-6}$M 2MP, pH 6.0

E_{dep}	E_p	i_p nA
+0.22V	-0.30	275
+0.12V	-0.29	330
+0.07V	-0.29	365
+0.12V	-0.28	345

Table VII

Current resulting from the variation of deposition time for $1x10^{-6}$M 2MP in phosphate buffer pH 6.9. E_{dep} = +0.07V

t_{dep} (sec)	current (μA)
60	1.35
120	3.50
180	5.80
240	6.00
300	6.40
360	6.60
420	6.50

7.3 Resolution of Mixtures

From the graph of $E_{1/2}$ v's pH, (Fig.12), the best separation in the $E_{1/2}$ values of each of the compounds is in solutions of pH 2.0-4.0. DPCSV was used to separate a mixture of three of the four compounds. The two pyrimidines were not separable. Using a deposition potential of +0.17 V and a deposition time of 3 min ,a $2x10^{-7}M$ mixture of 2MP, 2MmPr, and 2MP-O at pH 4.0 gave separate peaks at -0.07 V, -0.17 V and -0.31 V respectively, (Figure 33a)

Using DPP, 2MP and 2MP-O can be separated satisfactorily, as seen in Figure 33b, where $1x10^{-4}M$ solution of 2MP and 2MP-O results in peaks at -0.12 V and -0.38 V respectively.

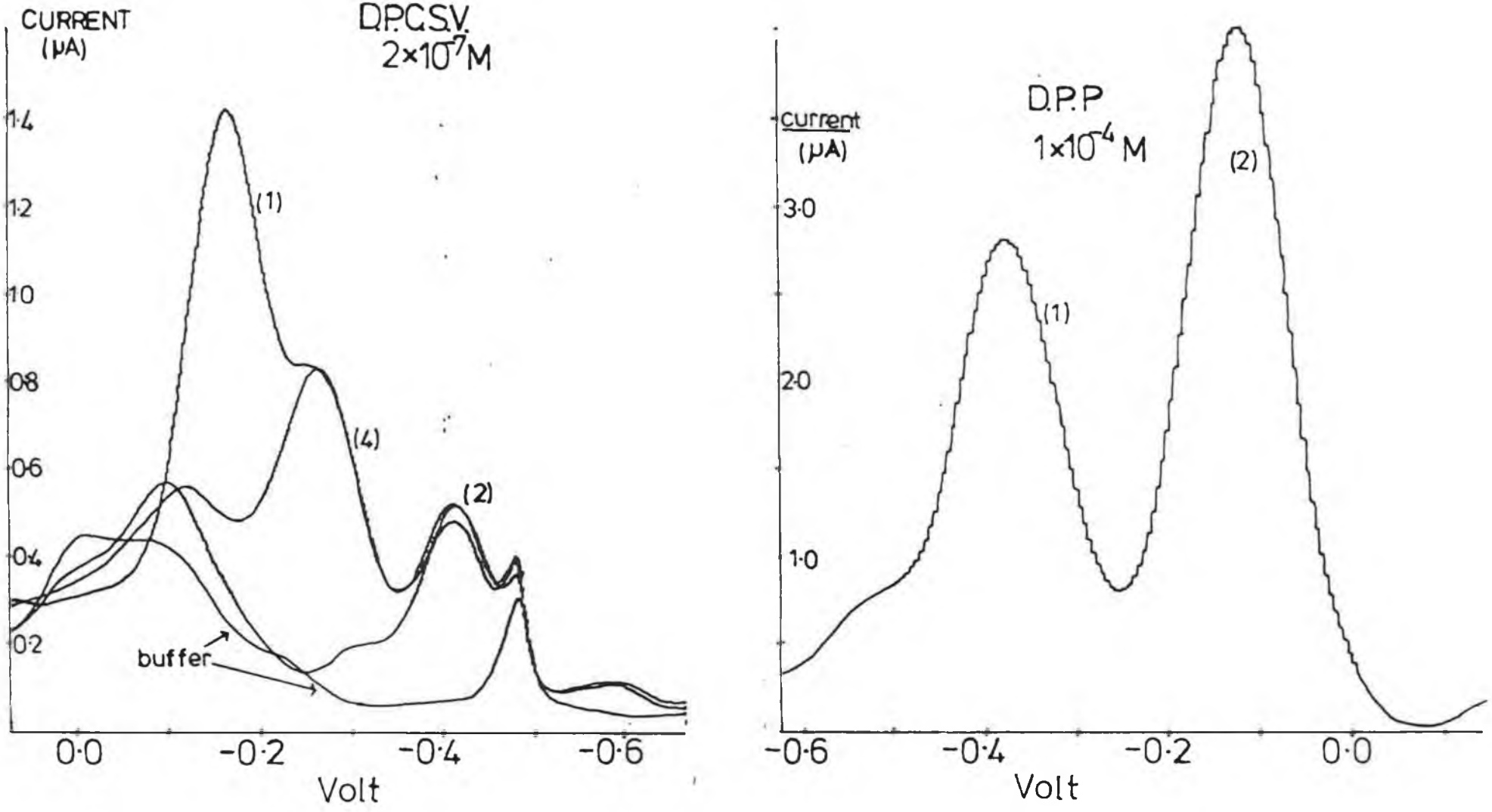

Fig. 33a, 33b

Determination of equi-molar mixtures of mercaptans using both DPCSV and DPP, (1) 2MP, (2) 2MP-O (4) 2MmPr.

8. Application of Polarography to the Olin Plant Process

8.1 DPP of NaOm and 2PCl-O at pH 2-12

Differential pulse polarograms of NaOm and 2PCl-O were recorded over the pH range 2-12 in order to ascertain the pH at which plant samples should be analysed. Plots of i_p and E_p versus pH have been constructed for both compounds (Fig. 34 and 35). The DP polarograms of NaOm at pH 4.0 resulted in a peak of increased current. This also occurred for 2MP-O at this pH. This was therefore investigated further using DC polarography and cyclic voltammetry. It was noted that for 2MP-O at pH 4.0, a prepeak maximum was present in the DC wave and CV showed that it adsorbed more strongly at this pH than at any other pH. The same mercury salt is formed from NaOm and 2MP-O; therefore increased adsorption at pH 4.0 is the reason for the increased current. The peak current due to NaOm was constant from pH 6.0-12.0. No cathodic wave attributable to an N-oxide reduction was found for NaOm at any pH level.

The DPP determination of 2PCl-O resulted in a reduction peak at negative potentials, slightly positive of the hydrogen evolution wave. This peak's current decreased with increase in pH and the E_p value shifted to more negative potentials. The peak was attributed to the reduction of the N-oxide. At pH 2.0 its peak height is approximately twice that due to a similar concentration of NaOm (at pH 6.0-12.0) . The NaOm reaction is a one electron per molecule of NaOm reaction, which suggests that the 2PCl-O reduction is a two electron reaction. The decrease in peak height with pH indicated

a need for protonation in order for the reaction to take place. The slope of the E_p vs pH curve for a reversible electrode reaction is given by -0.059.(p/n) where p and n are the number of protons and electrons involved in the reaction. The slope of the E_p vs pH curve for 2PCl-O is -0.106. This implies that 3-4 protons per molecules of 2PCl-O are involved in the reduction, assuming a two electron reaction. The mechanism for the reduction of pyridine-N-oxide reported by Baizer also seems to apply to 2PCl-O [54].

$$C_5H_5N\text{-}O \overset{+H^+}{\rightleftharpoons} C_5H_5N^+\text{-}OH \xrightarrow{2e^-+2H^+} C_5H_5N^+H + H_2O$$

He reports that it is the protonated N-oxide which is reduced. This is substantiated by the similarity of its reduction potential in acid solution, with that of the N-methoxy-pyridinium ion. This protonation step also accounts for the decrease in the electrode activity of 2PCl-O as the pH was increased. The above reaction is a 2 electron 3 proton reaction.

At pH's 10 and 12 there was another reduction peak due to 2PCl-O which also occurred at highly negative potentials (-1.65V). This peak also occurs at pH 8.0 and appears as a prepeak on the hydrogen evolution wave. The peak current and peak potential of this wave did not vary over the pH range 8-12, implying that hydrogen ions are not involved in the electrode reaction. The peak current of this peak is approximately equal to the peak current due to the reduction of the N-oxide function at pH 2.0, for equal quantities of the compound. This would suggest that the reaction was also a two electron

reaction. No peak was found for pyridine-N-oxide at pH 10-12. This would seem to indicate that the 2PCl-O peak is due to the chlorine reduction rather than the N-oxide reduction. This peak does not occur at lower pHs, because the N-oxide functional group is reduced first and the compound at the electrode surface is then 2PCl which is not polarographically active over the pH range 2-12. It may be possible that a two electron reduction of 2PCl-O occurs resulting in a chlorine ion and a pyridine-N-oxide radical anion.

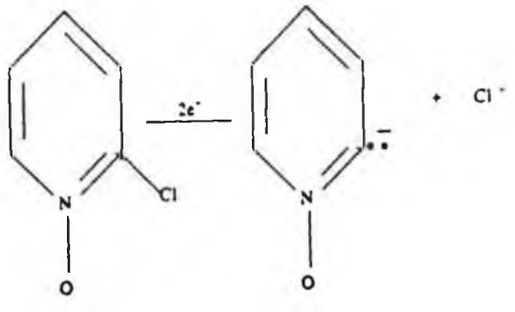

It was felt that a solution of pH 6.0 was the best pH for analysis of a mixture of both compounds. At this pH the peak current of NaOm was stable and the 2PCl-O peak current was still quite large. It was also possible to purge off any hydrogen sulphide H_2S present in the plant samples at this pH because the pK_a value due to the first dissociation of H_2S (ie: $H_2S \rightleftharpoons HS^- + H^+$), is approximately equal to 7.0 . The addition of 2PCl-O to a polarographic cell containing NaOm had no effect on the NaOm peak current when almost equal quantities of each compound were used. Similarly NaOm had no effect on the 2PCl-O peak current. The peak potentials of both compounds were separated by over 0.7 volts, therefore no interference occurred.

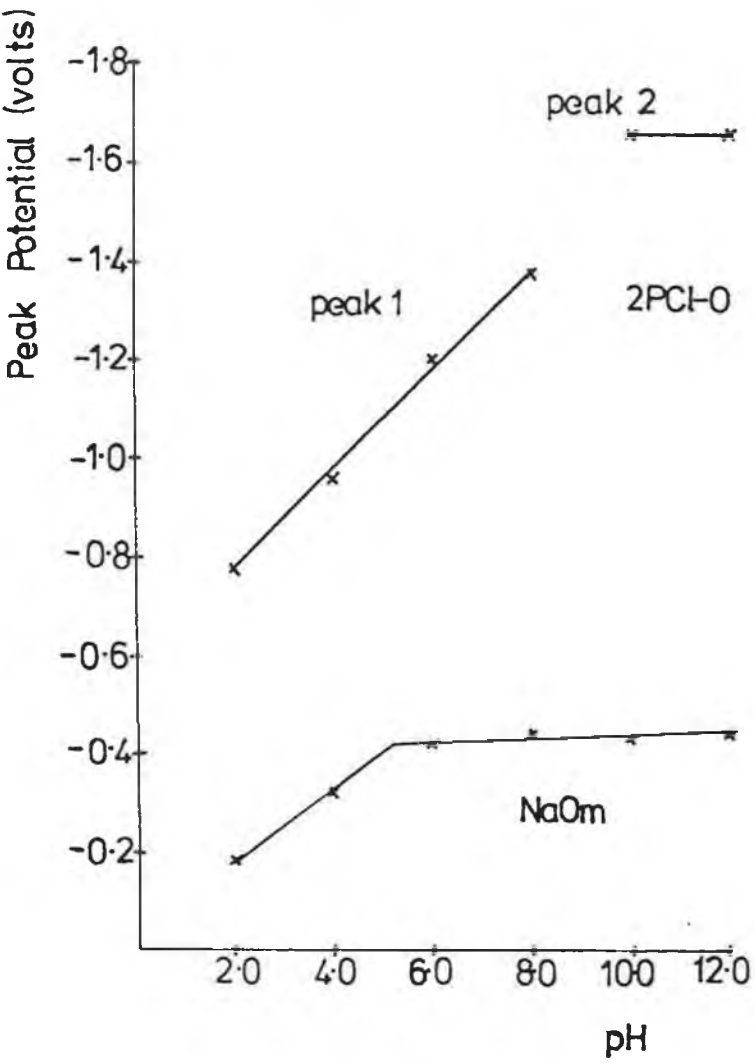

Fig. 34

Plot of peak potential vs pH for 2PCl-O and NaOm.

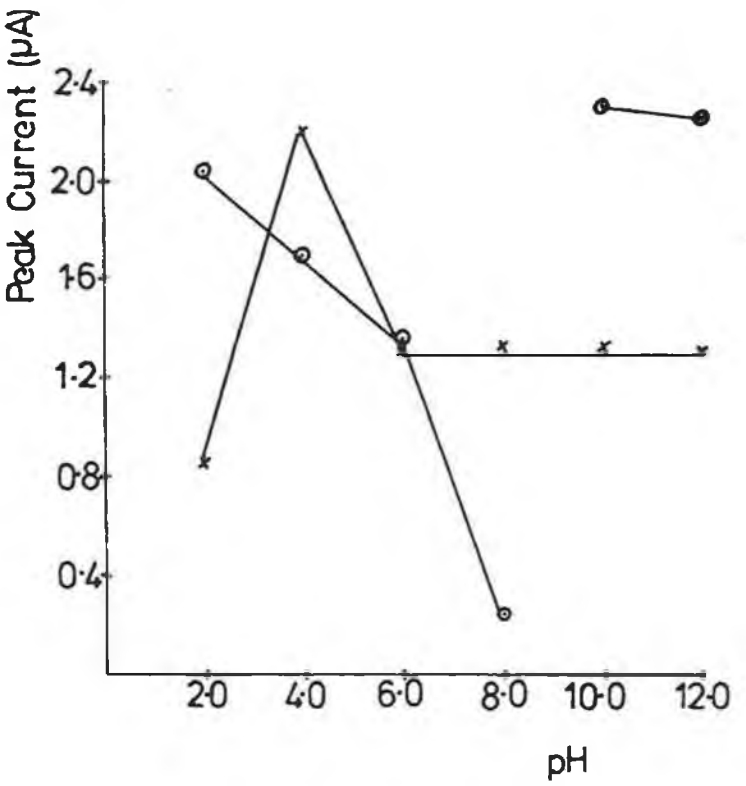

Fig. 35
Plot of peak current vs pH
for 2PCl-O (⊙) and NaOm (×).

8.2 Electrochemical Behaviour of Compounds Similar to 2PCl-O

The electrochemical behaviour of some compounds similar in structure to 2PCl-O was investigated over a 2-12 pH range to find out the similarities and differences of their reaction to that of 2PCl-O. It was found that neither the N-oxide of 2MP-O nor 2-hydroxypyridine-N-oxide were reducible. The alcohol and thiol groups must stabilise the N-oxide from being reduced. This stabilisation is not thought to be due to any inductive effect of the thiol or alcohol groups on the electrons of the N-oxide since chlorine is similarly electronegative. Resonance stabilization can also be ruled out since 2PCl-O and 2MP-O have the same resonance structures. It is felt however that the thiol and alcohol structures are stabilized by a 5 membered ring formation outside the pyridine ring due to hydrogen bonding between the hydrogen and the N-oxide. This is equivalent to the existence of tautomers.

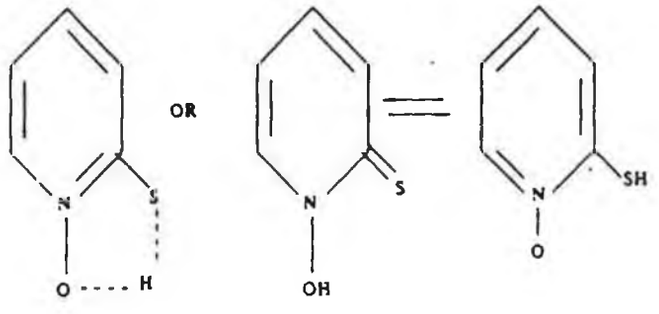

The reaction of pyridine-N-oxide at the electrode requires a pre-protonation step. This would seem to be fulfilled by the thiol and alcohol forms due to their existence as tautomers where the N-oxide is protonated. However, the differences between this protonated form and that of 2PCl-O is that the thiol and alcohol

forms are uncharged while the 2PCl-O form has a positive charge of the nitrogen atom facilitating reduction.

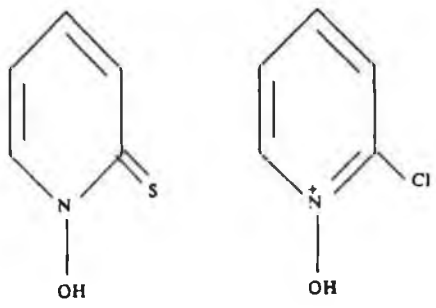

It was found that pyridine-N-oxide was electroactive over the pH range 2-8, thus differing from 2PCl-O which was reducible at pH 10 and 12. 2-hydroxypyridine was electroinactive over the pH range 2-12, while 2-chloropyridine was electroinactive over most of the pH range; it did however give rise to a sharp adsorption peak at pH 6.8 (E_p=-1.12V), and at pH 8.0 a rather broad peak at E_p=-1.6V very close to the $2H^+ \rightarrow H_2$ reduction wave.

8.3 Analysis of Plant Samples

Samples were taken from the plant mercaptization reaction at approximately 20 minute intervals, over the two hour reaction period. Each reaction sample was quenched, as indicated in the Experimental section. The DP polarograms were recorded in BR buffer pH 6.0. The qualitative decay of 2PCl-O and increase in NaOm can be seen from the DPP curves. The reaction was completed in less than an hour since no 2PCl-O was detected after that time; while in the factory, 2 hours is allowed for the reaction. It would be possible to stop the reaction earlier and thus speed up the plant process, if DPP was used as a

quick analytical technique to judge if all the 2PCl-O had fully reacted.

Analysis of sample 2 resulted in a third peak, apart from the NaOm and 2PCl-O peaks, which occured at -0.48V. It was thought that this peak was due to H_2S from the sample's foul odour and the fact that this peak decayed on purging. It was conclusively shown that this third peak was due to H_2S, by analysing a sample of H_2S produced from ferrous sulphate sticks and HCl. It had an E_p value of -0.53V in BR buffer pH 6.1, and when it was analysed along with NaOm its E_p shifted to -0.48V, the same potential as the third peak in sample 2. In the plant process it is necessary to get rid of all H_2S in the NaOm solution produced during mercaptization, before forming the NaOm metal derivatives. Polarography could also be used here as a highly sensitive analytical technique in the assurance that all H_2S was removed from the NaOm solution. In the plant, presence of H_2S in the reaction samples is detected either by moist lead acetate paper, which changes colour from white to black, or by a H_2S sensor.

It was not possible to quantify the amounts of NaOm and 2PCl-O present in the plant reactor during the reaction , because the volume of the reaction mixture was not known at each sample time, due to the continuous addition of NaOH to the reaction mixture to maintain a pH of 9.3 . Therefore if the concentration of both NaOm and 2PCl-O in a reaction sample were calculated via calibration curves of the mixture, it would still not be possible to relate this to the quantity of NaOm and 2PCl-O in the reactor when the sample was taken, because the volume of the reaction mixture at the sample time was

not known. A mass balance could be carried out, to find the yield of the reaction by sampling the 2PCl-O solution before mercaptization and the NaOm solution after the mercaptization. The total volume of each of these solutions can be measured. The concentration of each solution could be calculated from calibration curves of 2PCl-O and NaOm , and then the yield found. In the plant the yields are calculated using titration techniques, which would probably be more economical on time than the polarographic method , if it was found that calibration curves of 2PCl-O and NaOm had to be repeatedly run in order to get accurate results.

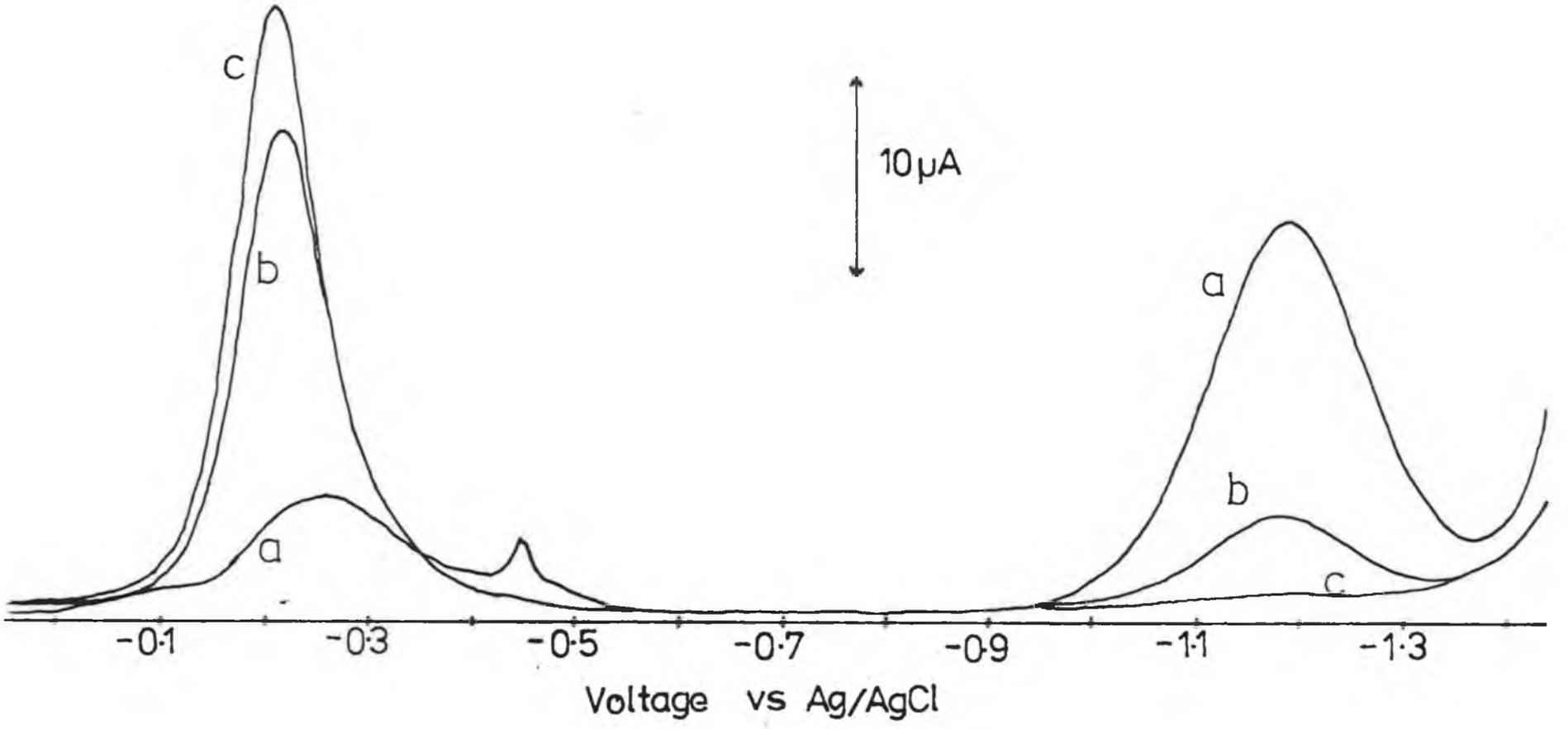

Fig. 36 DPP of samples taken from the Olin plant mercaptization reaction, (a) sample 2 (b) sample 3 (c) sample 4.

E. References

[1] Wrona, M., J. Electroanal. Chem., 104, (1979), 243-261.

[2] Kolthoff, I.M., Barnum, C., J. Amer. Chem. Soc., 63, (1941), 520.

[3] Krivis, A.F., Gazda, S.E., Anal. Chem., 41(1), (1969), 212-214.

[4] Kolthoff, I.M., Stricks, W., Anal. Chem., 74, (1952), 4646.

[5] Birke, R.L., Mazorra, M., Anal. Chim. Acta., 118, (1980),257-269.

[6] Peter, F., Rosset, R., Anal. Chim. Acta., 79,(1975),47-58.

[7] Sluyters-Rehbach, M., Wijnhorst, C.S., Sluyters, J.H., J. Electroanal. Chem., 74, (1976), 3-17.

[8] Schiffrin, D.J., J. Electroanal. Chem., 201, (1986), 199-203.

[9] Mairesse-Ducarmois, C.A., Patriarche, G.J., et Vandenbalck, J.L., Anal. Chim. Acta, 71 (1974), 165-174;

[10] ibid., 76, (1975), 299-308.

[11] Donahue, J.J., Olver, J.J., Anal. Chem., 41(6), (1969), 753-757.

[12] Hartley, A.M., Wilson, G.S., ibid, 38(6), (1966), 681-687.

[13] Lawton, R.S., Yacynych, A.M., Anal. Chem., 53, (1981), 1523-1528.

[14] Florence, T.M., J. Electroanal Chem., 168, (1984), 207-218.

[15] Stankovich, M.T., Bard, A.J., J. Electroanal. Chem., 75,(1977), 487.

[16] Muller, C., Valles, E., Vellve, P,. Gomez, E., J.Electroanal. Chem., 75, (1987), 237-251.

[17] Casassas, E., Arino, C., Esteban. M., Anal. Chim. Acta, 176,(1985), 113-119.

[18] Youssefi, M., Birke, R.L., Anal. Chem., 49(9),(1977),1380-6.

[19] Bond, A.M., Thomson, S.B., Tucker, D.J., Briggs, M.H., Anal. Chim. Acta, 156,(1984), 33-42.

[20] Florence, T.M., Biochem. J., 189, (1980), 507-520.

[21] Davidson, I.E., Smyth, W.F., Anal. Chem., 49(8),(1977), 1195-1198.

[22] ibid., Anal. Chim. Acta., 147,(1983),53-63.

[23] Forsman. U., Anal. Chim. Acta., 156,(1984),43-49.

[24] ibid., 146,(1983),71-86.

[25] Smyth, M.R., Osteryoung, J.G., Anal. Chem., 49(14),(1977), 2310.

[26] Brand, M.J.D., Fleet, B., Analyst, 93,(1968),498-506.

[27] Krivis, A.F., Gazda, E.S., Supp, G.R., Robinson, M.A., Anal. Chem., 35,(1963),966.

[28] Ochiai, E., J. Org. Chem., 18, (1953), 534-551.

[29] Kubota. T., Miyazaki. H., Bull. Chem. Soc. Jpn., 35, (1962), 1549-51

[30] ibid., 39, (1966), 2057-62

[31] Vaneesorn, Y., Smyth, W.F., in 'Electroanalysis in Hygiene, Environmental, Clinical and Pharmaceutical Chemistry', Smyth, W.F., Ed., Elsevier, Amsterdam, (1980), 299-308.

[32] Rao, C.R.N., in 'Ultra-Violet and Visible Spectroscopy', Butterworths (1975).

[33] Murrell, J.N., in 'The Theory of the Electronic Spectra of Organic Molecules', Chapman and Hall, (1971), 176-196.

[34] Heyrovsky, J., Zuman, P., in 'Practical Polarography', Academic Press, (1968).

[35] Bond, A.M., in 'Modern Polarographic Methods in Analytical Chemistry', Marcel Dekker, (1980)

[36] Zuman. P., Perrin, C.L., in 'Organic Polarography', Interscience, (1969)

[37] Bard, A.J., Faulkner, L.R., in ' Electrochemical Methods, Fundementals and Applications', Wiley, (1980), p520-532.

[38] Vydra,F., Stulik, K., Julakova, E., in 'Electrochemical Stripping Analysis', Wiley, (1976), p105.

[39] Anson, F.C., Anal. Chem., 38(1), (1966), 55-57.

[40] Brown, H.V., M^{c} Daniel, D.H., J. Am. Chem. Soc., 71,(1955), 3752-3755.

[41] Jaffe, H.H., J. Am. Chem. Soc., 77, (1955), 4451-4453.

[42] Albert, A., Serjeant, E.P., in 'The Determination of Ionization Constants', Chapman and Hall, 3rd ed., (1984).

[43] Jones, R.A., Katritzky, A.R.,J. Chem. Soc., 1960, 2937-2942.

[44] Oldham,K.B., J. Electroanal Chem., 167, (1984), 107-115.

[45] Schmidt, C.L., Swofford, H.S. Jr., Anal. Chem., 51(12), (1979)

[46] Fernandez Alvarez, J.M., Costa Garcia, A., Miranda Ordieres, A.J., Tunon Blanco, P., J. Electroanal. Chem., 255, (1987), 241-253.

[47] Ginzburg, G., Becker. J.Y., Lederman, E., Electrochimica Acta 26(7), (1981), 851-856.

[48] Gaus, E., Mas, F., Puy, J., Sanz, F., J. Electroanal. Chem., 224, (1987), 1-26.

[49] Souto, R.M., Gonzalez, S., Arevalo, A., J. Electroanal. Chem., 216 (1987) 273-282.

[50] Murray, R.W., Gross, D.J., Anal. Chem., 38(3),(1966),392-404.

[51] Parkinson, B.A., Anson, F.C., Anal. Chem., 50(13),(1978),1886-1891.

[52] Csejka, D.A., Nakos, S.T., DuBord, E.W., Anal. Chem., 47(2),(1975), 322-326.

[53] Stock, J.T., Larson, R.E., Anal. Chim. Acta., 138,(1982),371-374.

[54] 'Organic Electrochemistry an introduction and a guide', edited by M.M. Baizer and H. Lund; Marcel Dekker Inc., (1983).

[55] Crow, D.M., 'Polarograohy of Metal Complexes', Academic Press, (1969).

F. APPENDIX

Mechanism 1.

$$Hg^{+} + RS^{-} \rightleftharpoons HgSR$$

The potential at the DME for this reaction is given by

$$E = E^{0}_{Hg^{+}/Hg} + \frac{RT}{F}\ln[Hg^{+}]_{o} \qquad A1$$

The stability constant K_s, for the electrode reaction product is written as follows;

$$K_s = \frac{[HgSR]}{[Hg^{+}].[RS^{-}]} \qquad A2$$

Substituting for $[Hg^{+}]_o$ in equation A1 results in;

$$E = E^{0}_{Hg^{+}/Hg} + \frac{RT}{F}\ln\frac{[HgSR]_o}{K_s[RS^{-}]_o} \qquad A3$$

The anodic current flowing at the electrode is proportional to the diffusion of RS^{-} ions to the electrode and HgRS molecules from the electrode.

$$-i = k.([RS^{-}] - [RS^{-}]_o)$$

$$-i = -i_d - k[RS^{-}]_o \longrightarrow [RS^{-}]_o = \frac{i - i_d}{k} \qquad A4$$

also

$$-i = k'([HgSR]_o - [HgSR]) \longrightarrow [HgSR]_o = \frac{-i}{k'} \qquad A5$$

therefore

$$E = E^{0}_{Hg^{+}/Hg} + \frac{RT}{F}\left[\ln\frac{-i\,k}{(i-i_d).k'} + \ln\frac{1}{K_s}\right] \qquad A6$$

$E_{1/2}$ is constant , ie: independent of [RS]

Mechanism 2.

Mechanism 2 in section D.6. describes the polarographic reaction of thiourea. Its equivalent thiol reaction is outlined in mechanism 3.

Mechanism 3.

$$Hg^{2+} + 2RS^{-} \rightleftharpoons Hg(SR)_2$$

The potential at the DME for this reaction is given by

$$E = E^{o}_{Hg^{2+}/Hg} + \frac{RT}{2F}.\ln[Hg^{2+}]_o \qquad A7$$

$Hg(SR)_2$ is a solid salt adsorbed at the electrode. Its solubility product K is written as follows;

$$K = [Hg^{2+}].[RS^{-}]^2 \qquad A8$$

Substituting for $[Hg^{2+}]_o$ in equation A7 results in;

$$E = E^{o}_{Hg^{2+}/Hg} + \frac{RT}{2F}.\ln\frac{K}{[RS^{-}]^2_o} \qquad A9$$

The anodic current flowing at the electrode is proportional to the diffusion of RS^{-} ions to the electrode.

$$-i = k.([RS^{-}] - [RS^{-}]_o)$$

$$-i = -i_d - k[RS^{-}]_o \longrightarrow [RS^{-}]_o = \frac{i - i_d}{k} \qquad A10$$

By substitution of current into equation A9 , The potential at the electrode becomes;

$$E = E^{o}_{Hg^{2+}/Hg} + \frac{RT\ln K}{2F} - \frac{RT}{F}\ln\frac{i - i_d}{k} \qquad A11$$

$$E_{1/2} = E^{o}_{Hg^{2+}/Hg} + \frac{RT\ln K}{2F} - \frac{RT\ln}{F}\frac{-i_d}{2k} \qquad A12$$

Since $-i_d = k[RS^{-}]$, $E_{1/2}$ is proportional to $\ln[RS^{-}]$

Mechanism 4.

$$Hg_2^{2+} + 2RS^- \rightleftharpoons Hg_2(SR)_2$$

The potential at the dme for this reaction is given by

$$E = E^o_{Hg_2^{2+}/Hg} + RT\ln[Hg_2^{2+}]_o \qquad A13$$

$Hg_2(SR)_2$ is soluble, and its stability constant K_s is written as follows;

$$K_s = \frac{[Hg_2(SR)_2]}{[Hg_2^{2+}].[RS^-]^2} \qquad A14$$

Substituting for $[Hg_2^{2+}]_o$ in equation A13 results in;

$$E = E^o_{Hg_2^{2+}/Hg} + \frac{RT}{F}\ln\frac{[Hg_2(SR)_2]_o}{K_s[RS^-]_o^2} \qquad A15$$

The anodic current flowing at the electrode is proportional to the diffusion of RS^- ions to the electrode and $Hg_2(SR)_2$ molecules from the electrode.

$$-i = k.([RS^-] - [RS^-]_o)$$

$$-i = -i_d - k[RS^-]_o \longrightarrow [RS^-]_o = \frac{i - i_d}{k} \qquad A16$$

also

$$-i = k'([Hg_2(SR)_2]_o - [Hg_2(SR)_2]) \longrightarrow \frac{-i}{k'} = [Hg_2(SR)_2]_o \qquad A17$$

By substitution of current into equation A15, the electrode potential becomes;

$$E = E^o_{Hg_2^{2+}/Hg} + \frac{RT}{F}\ln\frac{-i.k^2}{k'.(i - i_d)^2 K_s} \qquad A18$$

$$E_{1/2} = E^o_{Hg_2^{2+}/Hg} + \frac{RT}{F}\ln\frac{2k^2}{k'.-i_d} \qquad A19$$

Since $-i_d = k[RS]$, $E_{1/2}$ is dependent on $\ln[RS^-]$